Improved density measurements of mesopelagic fish and the presence of physonect siphonophores in sound scattering layers, measured with multifrequency acoustics and a stereo camera mounted on a lowered probe

By

Kjetil Gjeitsund Thorvaldsen

Master of Science in Fisheries Biology and Management

University of Bergen

Department of biological sciences

2018

Improved density measurements of mesopelagic fish and the presence of physonect siphonophores in sound scattering layers, measured with multifrequency acoustics and a stereo camera mounted on a lowered probe

By

Kjetil Gjeitsund Thorvaldsen

A thesis submitted in partial fulfilment of the requirement for the degree of

Master of Science in Fisheries Biology and Management

University of Bergen

Department of Biology

2018

Acknowledgements

First and foremost, I want to express my deepest gratitude to Prof. Egil Ona, my supervisor, for his teachings and all interesting discussions we have had, both in biology and other topics. I would like to thank his patience with me, since I have a limited background in physics, and the learning curve have been steep. I also want to thank the comments on my drafts on my master thesis, they have been constructive and helpful, and I have learnt a lot about scientific writing in the process. I have always dreamt of studying deep sea organisms, and I am grateful I got the opportunity. I would also like to thank him for the opportunity to go on two surveys during the writing process. Both the CRISP-survey where all the data for this thesis were gathered, and he also gave me the opportunity to work for Sintef Ocean operating an echo sounder and using LSSS for 6 weeks during the survey with Br Birkeland, which gave me some real time experience trying to estimate mesopelagic fish abundance in the North Atlantic. I feel I have been able to gain a lot of practical experience in a very short time.

I would as well thank Dr. Rokas Kubilius for all his help both during surveys and afterwards, always patiently answering me the questions I was too embarrassed to ask anyone else, especially during the CRISP survey.

I thank Dr Rolf Korneliussen for applying me to the LSSS course, so I was able to do most of the post processing without problems. I would express my deepest gratitude to all employees both at the acoustic section and the catch section for the warm hospitality, including me in the IMR football team, and inviting me to non-work-related social events.

I thank Dr Aino Hosia for all the answers on my questions regarding siphonophores, and for her help with identifying siphonophores in the photo samples. I would also like to thank Dr Luis Felipe Martell Hernández for the visit at the Department of Natural history, showing me siphonophores with gas inclusions, and for sending me photos of siphonophores, which I could use in my thesis.

I would like to thank all the staff at G.O Sars which made the CRISP-survey an unforgettable one, and with all the help on lowering down the probe at each station.

I would like to thank Eduardo Grimaldo, and Leif Grismo of Sintef ocean together with the crew from Br Birkeland for giving me the possibility for a summer job of a lifetime. I feel privileged to be able to be a part of a 6-week survey and be able to observe the challenges of estimating mesopelagic fish first hand.

I would like to thank Dr Ingvar Huse for the 6 weeks days spent on Br Birkeland, with all the good advice on scientific writing and my master thesis. I would also like to thank you for all the good stories, and for all the good discussions.

I would like to thank my friends and family. Especially my domestic partner, for her patience with me staying at IMR late in the final writing process. I would also like to thank my dad for the advice on scientific writing.

I would express my deepest gratitude to my late mother, who always believed in me, and helped me with chemistry courses. Without your help, applying for a master's degree would probably not be possible.

Contents

Abstract

The mesopelagic layer is a massive layer of biomass which stretches from 200-1000 meters depth in almost all locations of the world oceans. These layers are inhabited by many groups of animals, from small zooplankton to larger fishes. While studied since the 1960s, the mesopelagic layer has gained recent scientific and industrial interest due to its potentially large unexploited biomass. These layers are populated by small fishes, which may be ensonified and detected by echo sounders, creating a layer of reverberation called the deep scattering layer. In Norwegian waters, two of the most abundant mesopelagic fishes are the Glacier Lanternfish (*Benthosema. Glaciale*), and the Muellers pearlside (*Maurolicus Muelleri*). Recent estimates using echo sounders, suggest that their potential biomass could be as high as 10 billion tonnes worldwide. There are however several challenges with respect to quantifying mesopelagic fishes in an accurate manner. Unwanted swimbladder resonance, other animals with similar echoes, and fishes without or changing swimbladder may potentially create large biases in these investigations. Very low catchability in modern trawls may also complicate the measurements. In this study mesopelagic fishes were measured both with traditional survey methods using vessel mounted transducers, and a lowered acoustic probe where the fishes were measured at short range at their natural depths. It was discovered that the biomass measured were lower with the lowered probe than with the traditional method, but in the same order of magnitude, from 0.01-0.09 fish/m^3. The difference was found was mainly due to the difference between target strength taken from literature, and the directly measured target strength from the probe. Camera observations of physonect siphonophores in the observation volume, may suggest that the biomass of fish measured is even lower. Observation and comparison of the difference in backscattering between 38 and 70 kHz, with higher backscattering at 70 kHz, may suggest that siphonophores are close to resonant at 70 kHz in our data. This gives hope for future classification of this group, especially if wideband are used. In this manner, this study shed light on some of these possible shortcomings and challenges for traditional ways to measure these fishes, but also suggest new methods for solving some of the more important questions.

Keywords: Mesopelagic fishes, Siphonophores, Acoustics, Target strength, Resonance, Swimbladders, Pneumatophores, vessel acoustics, Probe acoustics, Muellers pearlside, Glacier lanternfish

Nomenclature

Symbol	*name*	*Units*
f	Frequency	Hertz [Hz]
λ	Wave length	(m)
c	Sound speed	[Ms^{-1}]
ρ	Water density	kg/m^3
p	pressure	Pa
I	Sound intensity (W)	[w/m^2]
τ	Transmission pulse duration	S
P_t	P_t the power of the transmitted signal referred to the transducer terminal	W
G_0	the on-axis transducer gain	dB
P_R	Received signal power	W
r	Range from target	m
α	Absorption coefficient	bel m^{-1}
b	The beam pattern; function of direction describing the amplitude sensitivity	
θt	Split beam angle between the target and the along-ship directions	
φt	Split beam angle between the target and the athwart-ship directions	
$\eta\theta$	Split beam phase difference corresponding to θt	
$\eta\varphi$	Split beam phase difference corresponding to φt	
SNR	Signal to noise ratio	dB
ψ	The equivalent beam angle	sr
θ, φ	Angular coordinates of the scattering direction relative to the incident wave	
γ	Ratio for specific heats of gas	
$P0$	Ambient (undisturbed pressure)	Pa
σ_{sp}	Spherical backscattering cross section	m^2
σ_{bs}	Backscattering cross section	m^2
TS	Target strength	dB re 1 m^2

b	Constant in formulas relating target strength used to fish length	
s_v	Volume backscattering coefficient	$m^2\ m^{-3}$
s_a	Area backscattering coefficient	$m^2\ m^{-2}$
S_a	Area backscattering strength	dB re 1 ($m^2\ m^{-2}$)
s_A	Nautical area scattering coefficient (NASC)	$m^2\ nmi^{-2}$
S_v	Mean volume backscattering strength when sv is averaged over a finite volume	dB re 1 m^{-1}
S_A	Nautical area scattering strength	dB re 1 ($m^2\ nmi^{-2}$)
ρ_a	Area density	$^{m-2}$
ρ_A	Area density	Nmi^{-2}
ρ_v	Volume density	m^{-3}
$r(f)$	Relative frequency response	$S_V(f)/S_V(38kHz)$
ESR	Radius of a sphere having the same volume as the swimbladder	mm
L_{bubble}	Backscattering length of a gas bubble	
L_{tissue}	Part of backscattering length due to tissue	

Abbreviations	
SSL	Shallow scattering layer
DSL	Deep scattering layer
DVM	Diel vertical migration
IDVM	Inverse diel vertical migration
LSSS	Large scale survey system

1 Introduction

1.1 Fisheries acoustics

In fisheries science, acoustic methods are an efficient way to estimate abundance, size of fish, and with newer technology distinguish between species (Jennings et al., 2001; Simmonds & Maclennan, 2005). Echo sounders and sonars are electrical instruments that emits acoustic pulses into the water, receives backscattered sound and converts the sound into electrical signals. In fisheries science acoustic methods firstly were used for counting single echoes, but later more sophisticated ways of measure populations were invented. Sound is waves that moves through a medium. The curve between compression and expansion moves as a sine wave, and the relationship between the speed of sound is expressed as,

$$c = \lambda f \qquad (1)$$

Where c is the speed of sound, λ is the wave length, and f is the frequency. The wavelength is the distance between one wave top to another, while the frequency is the distance between each cycle. Sound speed can vary, depending on which medium it moves through, but in sea water it can vary between 1450-1550 ms^{-1}. The variation is due to differences in the water density, determined by salinity, temperature and pressure. The sound intensity diminishes with distance. Sound is lost due to geometrical spreading. The sound loses one half of its intensity for each doubling of distance. Some energy is also lost along the way, due to absorptions. Sound intensity is defined by,

$$I = \frac{p^2}{\rho c} \qquad (2)$$

Where p^2 is the pressure squared, ρ is the density of water and c is the sound speed. SI measures is used to describe sound pressure. The unit for sound pressure is pascal (Pa), but due to the high variation in pressure levels, sound is expressed in decibels (dB). Decibels are used to describe the difference in intensity from a reference value. This value is often one μPa. Decibel in fisheries acoustics is expressed as,

$$rdB = 10_{log}(\frac{I_2}{I_1}) \qquad (3)$$

Where I_2 is the measured intensity and I_1 is the reference value. Decibels are used in fisheries acoustics to measure targets reflectivity, where the reference value is the incident intensity, and the ratio is between the intensity and the targets reflection (Simmonds & Maclennan, 2005).

1.1.2 Transducers and beams

The transducer used in fisheries acoustics has a dual function. It converts energy to generate sound, and it converts backscattered sound into electrical energy. There are several types of sonars using this principle, but in this thesis the focus will be on Echo sounders. The echo sounder produces a burst of sound with a set frequency. The transducer transmits a sound which propagates through the water column. On the way the pulse reaches targets of different manner. These targets reflect the transmitted sound, and these echoes are converted by the transducer into electrical energy. The sonar equation for a single target is explained by,

$$I_r = I_o \sigma \left[\frac{10^{-2ar}}{r^4}\right] b^2(\theta, \varphi) \qquad (4)$$

Where I_r is the recorded intensity, I_o the transmitted intensity, σ is the backscattering cross section of the target. This parameter describes the ability of the target to reflect sound. $\left[\frac{10^{-2ar}}{r^4}\right]$, with geometric spreading, (r^4), absorption -2ar as the loss factors and $b^2(\theta, \varphi)$ the beam properties. A typical 38 kHz transducer used in fisheries acoustics, are made of piezo electric ceramic components, which creates voltage when an external pressure is applied, and creating sound pulses by contracting and expanding the ceramic elements. Usually transducers consist of matrix of individual elements. The number of elements varies together with the frequency applied. The beam pattern is determined by the different sound sources. They combine and make the acoustic beam lobe shaped. In (Fig.1.1), there are seven sound sources combined to create the beam. The pattern usually contains the main beam, and several side lobes.

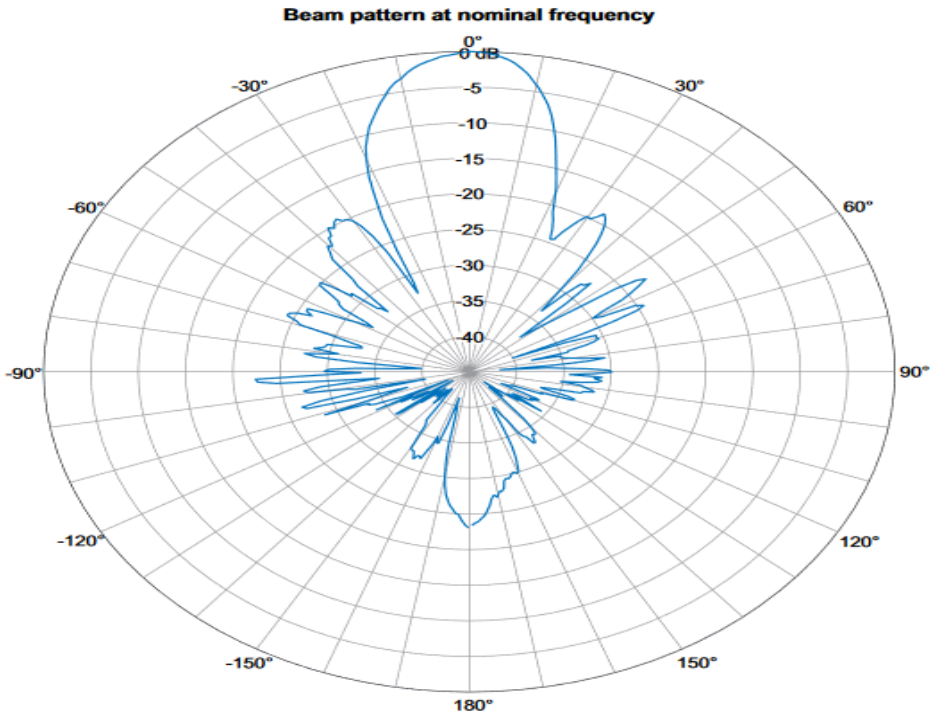

Figure 1.1. *Model describing the acoustic beam of a 38 kHz split beam transducer. The main lobe is showed in the middle, and side lobes at both sides. Taken from (www.simrad.com. 2018)*

The beam pattern is dependent on the frequency, and the opening angle of the beam which is defined as the area where the sound intensity is half the power of the acoustic axis. The effective area covered by echo integration is defined through the equivalent beam angle. Which is calculated as,

$$\psi = \iint b^2(\theta, \varphi) \qquad (5)$$

This angle is measured in steradian and describes the ideal beam where all targets distributed in space, would produce the same echo integral (Simmonds & Maclennan, 2005). The sonar used in this study is the SIMRAD EK60 split beam echo sounder. The beam produced by this transducer are split into four quadrants. The sound is emitted from the whole transducer surface, but the received echo is processed in each quadrant (Fig.1.1.2). Two angles are used to determine the direction which is respectively θt and φt, where θt is the along ship axis, and φt is the athwart ships axis. The phase difference between the four quadrants are computed to find where the target

location in the acoustic beam. If the quadrants are named a-d, the sum of a+c and b+d gives the $\eta\varphi$. While calculating a+b with c+d gives the angle $\eta\varphi$.

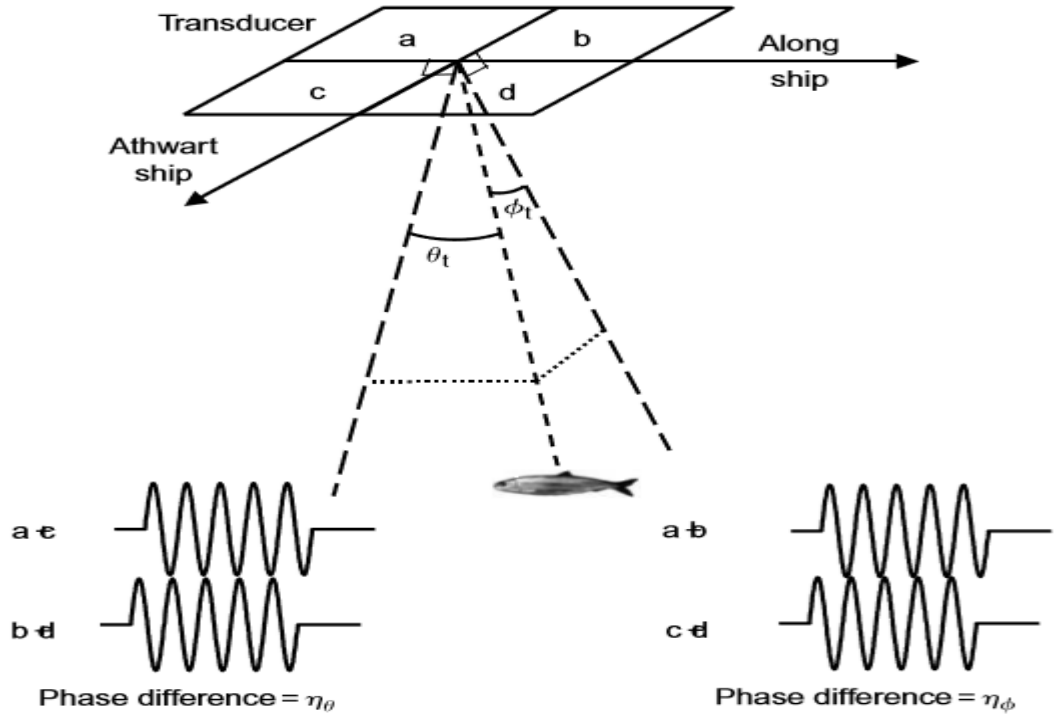

Figure 1.1.2. *Split beam echo sounder principle, taken from (Simmonds & Maclennan, 2005)*

1.1.3 Echo integration

When the target density is low, and all the targets are resolved, counting the targets can be done for density estimation, (Mitson, 1961). Fish and some organisms like krill and copepods, aggregate in dense layer, where the distance between targets is too small to separate. (Dragesund & Olsen, 1965) first invented the method called echo integration. The principle is to sum all the energy scattered from the water column, or within a specific depth layer over a certain distance. Echo integration is a widely used method for estimating populations of fish and is more applicable than echo counting since it doesn't have to rely on single echoes (Simmonds & Maclennan, 2005). When measuring several targets for echo integration, s_v is the parameter of interest. In modern echo sounders like the Simrad EK80 used in this study the sonar equation for volume scattering strength is,

$$S_v = 10\log(P_R) + 20\log(r) + 2ar - 10\log\left[\frac{p_t\lambda^2 c}{32\pi^2}\right] - 2G_0 - \left(10\log_{\tau_{nom}} + S_{a,corr}\right) - 10log\psi \quad (6)$$

Where P_R is the power of the received signal (W), r the range of the target from the transducer(m), a the absorption coefficient (bel m^{-1}), P_t the power of the transmitted signal referred to the transducer terminal(W), λ the wavelength (m), c the sound speed(m s^{-1}),G_0 the on axis transducer gain(dB), τ_{nom} the nominal pulse duration(s) ,and ψ the equivalent beam angle(sr) (Ona et al.,2009). As shown there are several parameters which need to be calculated for measuring the correct volume scattering strength. Many of them are however constant for a specific echo sounder and transducer. To correct for these parameters, the system is calibrated.

1.1.3.1 Calibration

For performing acoustic surveys with precise data, a calibration of the equipment is necessary. For estimating the abundance of a stock, a correct echo returned is required, or else a bias may occur. Before 1980 this was a major problem in fisheries acoustics. The calibration parameters can be found by measuring an object with a known acoustic property. This standard object is also used to find the acoustic axis. This is the point within the acoustic beam which it gives the strongest echo. This object is usually a metal sphere made of tungsten-carbide or copper. The transducers can be mounted differently, either on the hull of the vessel or a separate body outside the ship, but the principles for calibration are identical. The sphere is usually connected by three strategically placed nylon wires. The wires are as thin as possible to remove any noise from the recordings. The principle then is to move the sphere with these wires to find the acoustic axis, and to map the acoustic beam. The wires are usually moved by remote control. Before the calibration, a CTD is used to measure the temperature and salinity, between the transducer and the sphere. From the output of the CTD-measurements, the mean sound speed is measured and computed into the echo sounder. The equivalent beam angle for echo integration is assumed to be correctly estimated by the manufacturer.

The output of echo integration is the combined echo energy integrated over time a fixed depth. The formula for one echo integration is,

$$E_i = \int_{t_1}^{t_2} |v(t)|^2 \, dt \qquad (7)$$

Where E_i is the echo integral, t is time and v(t) is voltage created by the echo sounder at time t. This is calculated continuously, and for measurement of fish density, a mean calculation of many transmissions is applied (Simmonds & Maclennan, 2005). There is a pre-set range where echo energy is integrated. The integral is performed for a fixed time. Before converting echo energy into biomass estimates, knowledge of the average echo of one individual of the species of interest is needed.

1.1.3.2 Target strength

One of the important parameters needed for abundance estimation is the target strength of the species of interest. The target strength is described as the logarithmic measurement of the difference between the incident intensity which is returned by the target at a range of 1 m. This parameter describes the ability of the target to reflect sound. A fish has a stronger return of sound, than a single zooplankton. Having knowledge about different species target strengths there is a possibility to discriminate between different targets, and this value is an important parameter in abundance estimation. (Simmonds & Maclennon, 2005). The target strength is the parameter called backscattering cross section (σ_{bs}) defined as,

$$\sigma_{bs} = R^2 \frac{I_b}{I_i} \qquad (8)$$

Where R is the distance from the target, I_b the backscattered intensity, and I_i the incident intensity. In fisheries acoustics this measure is written on arithmetic form and is calculated as,

$$TS = 10log_{10}(\sigma_{bs}) \qquad (9)$$

The value needed for abundance estimation is the average TS, which also include the behaviour of the fish, especially its orientation. This is established either by experimental measurement (Nakken & Olsen, 1977), or by in situ direct measurement with a split beam echo sounder (Ona, 2003). There are three different approaches for studying target strength. Target strength can be measured on immobile fish, fish in cages or directly in situ, which means that the target strength is measured directly on free swimming fish in their normal environment. By using dead or stunned fish, target strength could be directly measured. The fish would be held still using nylon wires, and the only movement would be changing of the tilt angles (Simmonds &. Maclennan, 2005). Difference between sites and species could then be studied in detail (Nakken & Olsen, 1977). Target strength can also be measured using fish in cages. The fish is alive and swimming, but there is a significant difference between fish confined in cages, and fish in the wild. Often the TS must be extrapolated from the echo of many fish and must assume the behaviour is similar. The most accurate method is the measurement of target strength from wild fish. When surveying a fish stock, fish are measured in their natural habitat, and thus an average TS measured in situ will be most precise. The target strength has a linear relationship with the fish length. When estimating an accurate target strength to size relationship for a specific species, often both experimental data and in *situ* measurements are needed. This was done by (Foote, 1980). A formula was created, taking in to account the variability of the fish orientation in space together with the beam pattern and the geometric perspective. Gadoids like cod, saithe and pollack were measured and length ranges representing different life stages of the fish were used.

$$TS = m\log(L) - b \qquad (10)$$

Where m and b are parameters specific to the species of interest and l is the average fish length.
In acoustic surveys, the mean target strength to be used is extrapolated from the length distribution obtained by trawl sampling and the target strength to size relationship of the species.

1.1.3.3 Parameters needed for abundance estimation

With calibrated echo sounders, and some knowledge of target strength, the mean backscattered echo energy. First the echo from a specific volume, which is called the volume scattering coefficient, (s_v) and is calculated as,

$$s_v \frac{\Sigma \sigma_{bs}}{v} \quad (11)$$

Where (σ_{bs}) is the backscattering cross section and V is volume sampled by the acoustic beam. With this formula, the mean area backscattering coefficient is calculated. The area scattering coefficient is expressed as s_a, and is expressed as,

$$s_a = \int_{z_1}^{z_2} s_v \, dz \quad (12)$$

Which is the integral of volume density over range. Where z1 and z2 is the limit depth channel of interest. At sea, the nautical mile is used for measuring distance. 1 nautical mile=1852m. The backscattered energy for a depth layer is usually averaged over a distance, and the output normalized.

$$s_A = 4\pi(1852)^2 \int_{z_1}^{z_2} s_v \, dz \quad (13)$$

The mean area scattering coefficient, s_A, now has units $m^2nmi^{-2,}$ and is a direct measure of the fish density in the layer (Foote & Knudsen, 1994). According to the new definitions suggested by (Maclennan et al., 2002), they call this the nautical area scattering coefficient, or NASC for short. The output of the echo integration is the s_A-value, and this value are usually extracted from echo sounder, or a post processing system for abundance, or density estimation. Abundance estimation, the scattering properties of the target of interest is,

$$\rho_a = \frac{s_A}{4\pi(\sigma_{bs})} \quad (14)$$

Where target strength is converted to the backscattering cross section. With the correct data on length and target strength, the output will now be number of individuals [m^2nmi^{-2}]. During surveys, mean weight is calculated from trawl samples and multiplied by the ρ_a to get the gross tonnage for each nautical mile. Insight on the density distribution in schools and layers are often of interest, both for fishermen and scientists. The mean volume density within the layer of interest can now be found by dividing on the area density with volume average over 1 nmi^2, and layer thickness, z,

$$\rho_v = \frac{\rho_a}{1852^2} * \Delta \quad (15)$$

1.2 Biological targets

1.2.1 Fish as acoustic targets

The reflected acoustic energy from a target is very dependent of the properties of the target body. Gas filled cavities, oil, bone are good reflectors of acoustic sound, due to the sound speed contrast in sea water. In fisheries acoustic, teleost fishes have been frequently studied. Most fishes contain a swimbladder. It is an air-filled cavity with serves multiple purposes. It is used to control buoyancy, produce sound and receive sound. Since the bladder is filled by gas, the sound speed contrast to water is large, therefore it can contribute as much as 95% of the backscattered energy from a fish (Clay and Heist, 1984; Foote, 1985; Foote and Ona, 1985; Furusawa, 1988; Clay and Horne, 1994; Ye and Farmer, 1994; Jech et al., 1995; Simmonds and MacLennan, 2005). At neutral buoyancy, the pressure inside the swimbladder equals the pressure around the water. If it is exposed to an external force, for example an acoustic wave, the pressure will also change due to Boyle's law (Simmonds and MacLennan. 2005). The swimbladder have natural oscillations due to moving in and out of equilibrium. If the external force is at the same force as the swimbladder, it resonates. The formula for the resonating of a free bubble is,

$$\frac{1}{2\pi a}\sqrt{3\gamma\frac{P0}{\rho}} \qquad (16)$$

Where P0 is the ambient pressure, ρ the water density, γ is for gas properties and the bubble radius. Many fish undergo vertical migrations. Some fishes then adjust their gas volume in their swim bladders and their resonant frequency may not change, but for other fish the resonance frequency may change with depth (Hershey et al., 1961; Mozgovoy, 1986). Resonance frequencies for most commercial fishes are usually below 1000 Hz, but fish with small swimbladders resonate close to frequencies used in echo sounders. Resonance can give unproportioned strong echoes compared to the actual biomass, which can lead to a positive bias in abundance estimation (Holliday, 1972; Nero et al., 2004). In fisheries acoustics, important research has been made by modelling acoustic backscattering of swimbladders. (Foote, 1985) were the first to predict backscatter using the morphology of the swimbladder. Different approaches for modelling swimbladders were developed, from a simple sphere (Andreeva, 1964), a cylinder (Clay, 1992), or a prolate spheroid.

Swimbladder can either be extracted from the organisms or measured with x-ray. These models can be used to study how the swimbladder react to sound in different frequencies. Of the simple shapes, the prolate spheroid is the closest of representing a true swimbladder. The length of the radius is shorter than the main axis (Simmonds and Maclennan, 2005). Knowing the fish's relation to their swimbladders is crucial to understand their acoustic properties.

1.2.2 Zooplankton

Most targets in the ocean do not contain a swimbladder. The ocean ecosystem is diverse, and some other groups can also be observed acoustically. Zooplankton is low in the food chain and has an important ecological role but can also be potential economical important in future fisheries (Simmonds & Maclennan, 2005). These organisms usually do not contain a gas inclusion and scatter sound in a different manner. Classification of large fish targets has been possible for decades by ensonifying the target with several frequencies (Korneliussen and Ona, 2003). (Stanton et al., 1996) claimed that it was possible to separate zooplankton into three acoustic groups. They divided zooplankton into, fluid like, elastic shell and gas bearing. Even though the species composition of zooplankton is highly diverse, most species fall under one of these categories. As zooplankton usually are weak targets, high frequencies must be applied. High frequencies give an improved spatial resolution, but the range limitations at high frequencies inhibits research at greater depths (Simmonds and Maclennan, 2005).

1.3 The deep scattering layer

The deep scattering layer first described by (Duvall & Christensen, 1946), is an aggregation of organisms which resembles a layer or a false bottom in the water column. The layer usually consists of zooplankton, fish larvae, larger invertebrates and some species of fish. The species composition can vary regarding to where it is located. These layers are found in all world oceans, but the species composition can vary (Tont, 1976). Even in the arctic ecosystem, weak deep scattering layers can be observed (Gjøsæter et al, 2017). The organisms in the mesopelagic layers may play an important role in carbon cycling. Phytoplankton fixates the inorganic carbon during photosynthesis and is consumed by zooplankton. The mesopelagic fishes migrate from depths during night, feeds on zooplankton, and migrates back to the deep, and hence transfers carbon to greater depths (Tréguer et al., 2003; Christensen et al., 2009). An important contributor to the deep scattering layers is mesopelagic fishes. A mesopelagic fish is a fish that lives within the mesopelagic layer during day, and usually perform dial vertical migration (DVM) towards the surface during night. Their day depth distribution during day usually fluctuates between 200-1000 meters but can spatially vary due to biotic and abiotic factors (Kawaguchi & Gjøsæter, 1980). The study on mesopelagic fishes started with the discovery of the deep scattering layer (Duvall & Christensen, 1946), and the organisms were first described by (Marshall, 1951). They are usually short lived and small, even though at higher latitudes some grow older and larger (Salvanes & Kristoffersen, 2001).

1.3.1 Previous biomass estimates on mesopelagic fish

With use of midwater trawl samples, the global population of mesopelagic fishes were estimated to be about 1 billion tonnes (Kawaguchi & Gjøsæter, 1980; Lam V & Pauly D, 2005. When trawling for mesopelagic fish (Kaartvedt et al., 2012) discovered that the fishes actively and efficiently avoided the trawl, leaving a void where the trawl had traversed with an open cod end (figure 1.3.1). Their acoustic estimates were higher than the catches indicated.

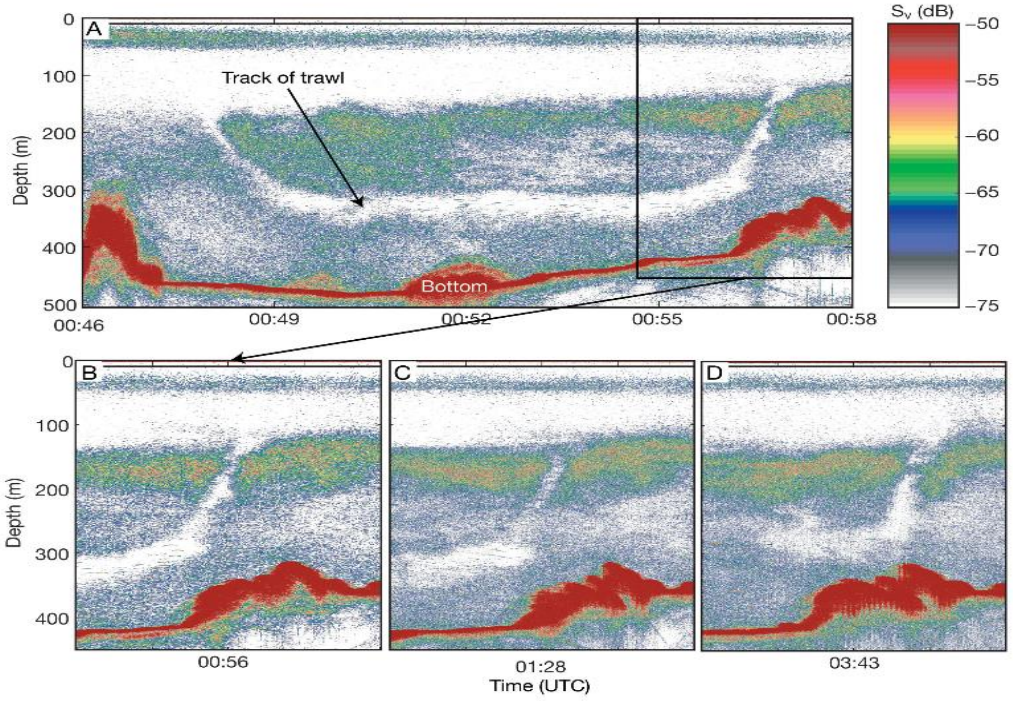

Figure 1.3.1 *Echogram of mesopelagic fishes leaving a void where the trawl has traversed. Taken from (Kaartvedt et al., 2012)*

Higher acoustic density estimates, compared with midwater trawl samples have also been observed in previous studies (Koslow et al., 1997; Kloser et al., 2009; Pakhomov & Yamamura 2010). More recent studies propose that the world biomass is higher than first estimated. By using acoustic data collected at 38 kHz, the biomass was calculated to be 10 billion tonnes (Irigoien et al., 2014). This has sparked a commercial interest in these species, due to the high unexploited biomass. It could potentially be an important fishery with respect to oils, food, and food for aquaculture (Gjøsæter & Kawaguchi, 1980). When harvesting mesopelagic fishes and other organisms, there is a concern of changing the carbon cycle and furthermore change the climate (St John et al., 2016). With unprecise biomass estimates, there is also a possibility for overfishing. Therefore, correct estimates of biomass in important (St John et al., 2016). In the study by (Gjøsaether & Kawaguchi, 1980) it was estimated that around 100 families of mesopelagic fish occurred in the samples. In the northern Atlantic, two species usually dominate the scattering layers. *Benthosema Glaciale* (Reinhardt, 1837), and *Maurolicus Muelleri* (Gmelin, 1789). In this study, the focus will be on these two locally abundant species of mesopelagic fish.

1.3.2. *Maurolicus muelleri*

Maurolicus Muelleri (Gmelin, 1789) commonly known as The Mueller's pearlside, is widely distributed, and probably the most abundant mesopelagic fish in Norwegian fjords (Gjøsæter, 1981). In this study it is referred to as pearlside. This fish is both small and short lived. The average body length is around 4-5 cm, while some specimens have grown to around 8 cm. The lifespan is short, and the natural mortality increases during summer when they are 2-3 years old. The fishes grow rapidly in the early life stages, while it plateaus after the first spawning. Pearlsides is most common near continental slopes, sea mounts, fjords, and rarer in the open ocean (Okiyama, 1971; Banon et al., 2016).

1.3.2.1 Behaviour

Pearlsides usually feeds on zooplankton like copepods and krill. While the younger specimen feeds mostly on copepods (Gjøsæter, 1981). The fishes perform dial vertical migration to shallower waters to feed at night. Pearlsides have a preferred light intensity, where there has been reported a relationship between the logarithmic light levels, and the presence of the fish (Staby & Aksnes, 2011). This intensity changes during day and night and the fishes follow these light levels. This is an evolutionary adaptation for being able to visually feed on prey, while they are still hidden for predators. Different life stages of pearlsides have been observed to live in different parts of the water column, the youngest larvae at 50 meters, older larvae at 75 meters (Folkvord et al., 2016). In some circumstances the fishes may also alter their anti-predation behaviour. When there is midnight sun north of the polar circle, the light regime is different for the fishes. They can't migrate to the shallows without exposing themselves for light. But some, probably as an anti-predator strategy, forms dense schools when feeding for plankton in the shallow waters (Kaartvedt et al., 1998). This behaviour has also been observed close to the equator, where the process of dusk and dawn is quicker (Alverson, 1961; Marchal & Le- Bourges, 1996). Pearlsides has a long spawning season between March and October. There is no suggestion that they perform horizontal migration to spawn (Gjøsaether, 1981). This can create separate stocks, especially in the fjord environments, whereas stock distribution in oceanic environments is less known (Gjøsæter, 1981).

1.3.2.2 Vertical distribution of pearlsides

In the mesopelagic layer, pearlsides usually distributes in a layer above the main deep scattering layer (Giske et al., 1990). Light is not the only determining factor with respects to the diel vertical migration, there are ontonogetic factors as well. In a long-term study done by (Staby, 2010) many different migrating patterns were observed. Adult pearlsides performed normal DVM during the productive months of the season, feeding on zooplankton. During fall (September- October) the fishes were observed migrating in the morning rather in the night. This can maybe be explained by a dense layer of zooplankton in the deep scattering layer, hence the migration can possibly be hunger-motivated. Some fishes have also been observed performing reverse DVM (Levy 1990a; Neilson and Perry, 1990; Kaartvedt et al., 2009; Staby et al.,2011), where they migrated only 20-30 meters during the middle of the day, while they migrated down during night. This migration improves the vision for the fish, which will increase the encounter rate with possible prey, but also increases the risk of predation (Rosland & Giske, 1997; Staby et al., 2011).

1.3.2.3 Acoustic properties of Pearlsides

Pearlsides belongs to the family *sternopyctidae*. These fishes are all described as fishes with well developed, thin walled swimbladders (Marshall, 1960; Brooks, 1977). As with all other fish, the bladder contributes to the major echo, and makes them visible at low frequencies. The relationship between length, and swimbladder size of the fishes usually follows a linear pattern (Foote, 1979; MacLennan and Simmonds, 1992). Both (Kleckner & Gibbs, 1972) and (Scoulding et al., 2015) have studied this relationship in these two fishes, as well as their target strength.

Table 1.3.2*. Target strength measured in situ in (Scoulding et al., 2015) at 4 different frequencies.*

	18 kHz	38 kHz	120 kHz	200 kHz
Large *M. muelleri*	−53.6 (31)	−60.8 (16)	−62.9 (16)	−66.4 (19)
Small *M. muelleri*	−57.1 (6)	−60.3 (8)	−62.0 (7)	−65.0 (9)

Notably both size groups have a much stronger TS at low frequencies (18 kHz) than higher frequencies. This is because the swimbladder is close to resonance at the lowest frequency, but probably not at the actual peak resonance.

1.3.3 *Bentosema Glaciale*

Benthosema Glaciale (Reinhardt, 1837) commonly known as glacier lanternfish, is distributed across the North Atlantic Ocean and Mediterranean. Glacier lanternfish belongs to the myctophids, which are the most abundant mesopelagic family globally (Gjøsaether & Kawaguchi, 1980). This fish is presumed to be the most abundant myctophid latitude of 35 degrees north (Mazhirina, 1988). This species grows to approximately 7 cm and have a life span around 4 years. The spawning season in Norwegian waters is around spring and summer but have been observed spawning at all months of the year in the Mediterranean (Gjøsaether, 1981b). The glacier lanternfish is a planktivory fish feeding on mostly crustaceans like copepods, but also other types of zooplankton.(Gjösæter, 1973; Kinzer, 1977; Kawaguchi & Mauchline, 1982; Roe & Badcock, 1984; Dypvik et al., 2012) They are mostly feeding at night, even though feeding at daytime have been observed (Gjøsæter, 1973; Kinzer, 1977; Roe & Badcock, 1984; Sameoto, 1988, 1989).

1.3.3.1 Vertical distribution

This fish usually distributes below the layers of pearlsides (Giske et al., 1990). Like pearlsides, there is a seasonal pattern where the fishes perform different migrations during different times of year. In a study done by (Dypvik et al., 2012) the fishes displayed three different migrating behaviors. The most prominent migration during spring and summer where the normal diel vertical migration where the fishes swam from the daytime depths towards the surface during the night. Inverse dial migration where fish ascended 20-30 meters during daytime and descended back during night were most prominent during the winter months. Some fishes never perform DVM and stay at deep waters all year round. The largest individuals usually stayed in deep waters. It's been suggested that this is the fish's adaption to cope with more dark waters (Warrant & Lockett., 2004), the fish have also been observed consuming larger prey as krill and shrimps (Kaartvedt et al., 1988; Baliño & Aksnes, 1993; Kaartvedt et al., 2009; Dypvik et al., 2012).

1.3.3.2 Acoustic properties of glacier lanternfish

Myctophids like the glacier lanternfish have swimbladders that can be filled with gas, lipids or completely inflated (Butler and Pearcy, 1972). Usually the fishes first have gas filled swimbladder, but the gas is replaced by lipids or inflate during maturity (Neighbors and Nafpakitus, 1982). Found in the study by (Scoulding et al., 2015), the myctophids have a negative linear relationship between length and swimbladder size. This will complicate the biomass estimation using acoustic data. Some Myctophids also have their swimbladder inflated (Marshall, 1960; Butler & Pearcy, 1972; Neighbors & Nafpakitus, 1982; Yasuma et al., 2003; Yasuma et al., 2010). Even though the glacier lanternfish is a larger fish than the pearlside, the swimbladder and mean target strength is usually smaller (Scoulding et al., 2015). The resonance peak is also at a higher frequency than pearlsides.

Table 1.3.2*. Mean Target strength of B. Glaciale on 4 frequencies*

	18 kHz	38 kHz	120 kHz	200 kHz
B. glaciale	−54.2 (84)	−62.1 (60)	−65.6 (33)	−67.6 (35)

1.3.4 Assessment of scattering layers and mesopelagic fishes

1.3.4.1 Errors in biomass estimation

There are two major issues, which have not been addressed in many of the previous biomass estimates. These problems are the probability of resonating swimbladders (Kloser et al., 2002; Godø et al., 2009), and the presence of gelatinous zooplankton with gas inclusions (Barham, 1963; Robison et al., 1998). As in previous acoustic studies of mesopelagic fish, low frequencies, mainly 38 kHz, have been applied. The range and absorption limit the possibility of using higher frequencies than 18 and 38 kHz at DSL depths. The resonance peaks of pearlsides, and lanternfish have been studied theoretically (Scoulding et al., 2015). Pearlsides had higher resonance peaks at lower frequencies (18 kHz), while glacier lanternfish had lower peaks at higher frequencies. When the fishes perform DVM, the resonance frequency changes (Hershey et al., 1961). Especially was this the case for pearlsides (Godø et al., 2009). It is suggested that the volume gas in the swimbladders is exchanged with lipids due to performing DVM (Yasuma et al., 2010). This makes

it difficult to standardize the target strength-relationships, especially for Myctophids (McClatchie et al., 2003). Resonance frequency is proportional to the volume of the swimbladder, but if it inflated or filled with lipids, the resonance frequency may change. When calculating target strength with the standard equation, the 20log(l)-relationship between length and swimbladder size is presumed. If this relationship does not exist, a bias will occur. This may complicate normal procedures used in acoustic surveying, where the size distribution from the catch is used to calculate the mean target strength. Validation of this methods seems highly relevant or establishing other means for measuring density must be developed.

1.3.4.2 Gelatinous zooplankton

There are challenges in measuring the scattering layers acoustically, because the species composition can be diverse, and morphological features can vary between species, and within species. This means the acoustic properties can vary as well (Stanton et al., 1994). Studies have shown that different gas bearing zooplankton as salps, siphonophores, and different kinds of medusae can produce significant backscatter at low frequencies, such as at 18 and 38 kHz (Toyokawa et al., 1997; Brierley et al., 2001; Mianzan et al., 2001). Physonect siphonophores use gas bubbles to maintain buoyancy (Mackie et al., 1987). These two groups may create specific challenges when mixed with, or if misinterpreted as mesopelagic fish in clean, high density layers. In this study the gas bearing siphonophores are at interest, because of their ability to produce backscattering which is very similar to backscattering from mesopelagic fish.

1.3.4.3 Siphonophores

In the early stages of mesopelagic research, the main consensus was that fishes with swimbladders were the main source of echoes in the deep scattering layers (Marshall, 1961). Several experiments with trawling of scattering layers, resulted in almost empty nets (Hershey et al., 1961; Boden et al., 1962). Observing these layers with submersibles uncovered that gas bearing siphonophores were locally abundant in some areas, and it was even suggested that these organisms were the major sound scatterer globally (Barham, 1963). It was also discovered that larger organisms usually were located at greater depths, and thus the siphonophores were distributed almost similarly to the resonance response of the gas inclusion. A siphonophore is long complex gelatinous organisms that comprise of a colony of individuals. Siphonophores are hatched from a single egg but grows up to become a colony. Siphonophores reproduce by producing gametes from the gonophores.

When fertilized the eggs are released into the water column and hatched into planula larvae. Then they become a siphonulae larvae, and it is at this stage the development of the pneumatophore begins. To maintain buoyancy the pneumatophore is filled up by gas (Mackie et al., 1987).

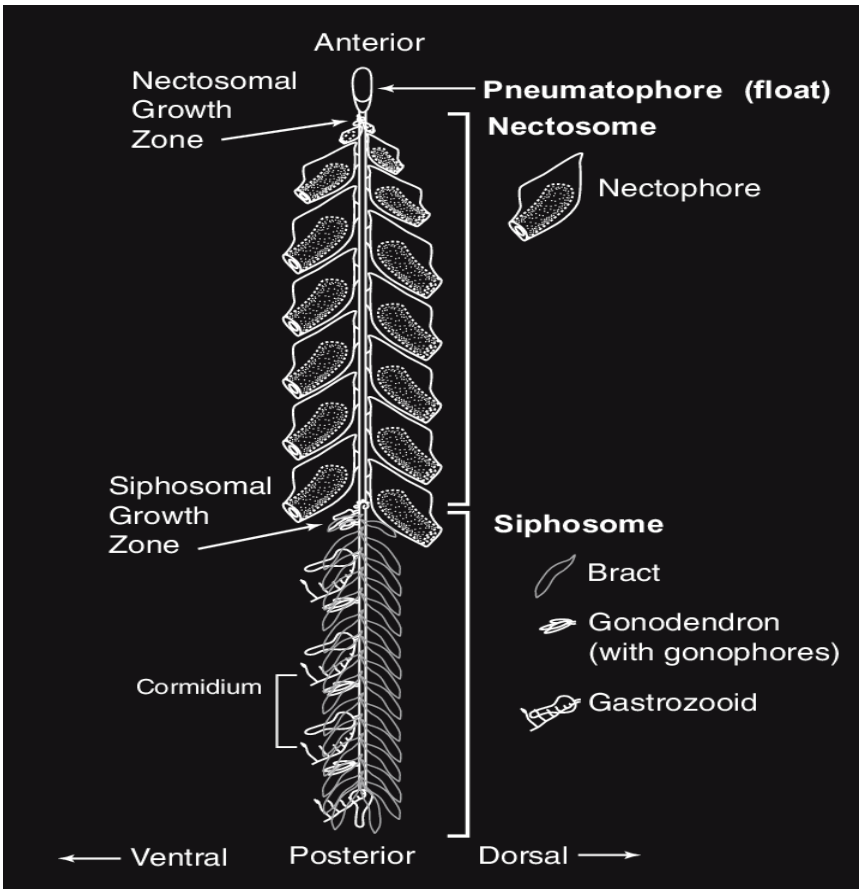

Figure 1.3.3. Schematic drawing describing the body plan of a physonect siphonophore. On the apex of the organism, the pneumatophore is located, which is used for maintaining buoyancy. Swimming bells (Nectopophores), which is used for propulsion, and a siphosome containing several zoids with different functions taken from (Dunn, 2005).

Siphonophores are organisms within the phyla Cnidaria and are widely spread across the oceans. They feed on plankton by staying motionless in the water column, catching zooplankton using their long tentacles (Mackie et al, 1987). Siphonophores are widely distributed both horizontal and vertical. The vertical distribution of siphonophores are dependent on several factors. Light has been bescribed by (Barham, 1963). Benfield et al., (2003), found that the siphonophores were able to adjust their vertical distribution dependent on temperature. The distribution of prey has been described as another factore (Pagès & Kurbjeweit, 1994). Oxygen may also play a part in their vertical distribution Robison et al.,1998). Siphonophores can have seasonal differences in their vertical distribution, just like the mesopelagic fish (Mackie, 1985; Silguero & Robison, 2000). Like

mesopelagic fish siphonophores undergo DVM (Pugh, 1984; Mackie, 1985; Mackie et al., 1987; Mills 1995; Youngbluth et al., 1996; Robison et al., 1998, Pugh, 1999). In some cases, the siphonophores can become very numerous, especially during mass blooms (Warren et al., 2001; Benfield et al., 2003; Knutsen et al., 2018).

1.3.4.5 Acoustic properties of siphonophores.

The gas inclusion in their pneumatophores are small, from which they produce the majority of the animal's echo. (Stanton et al., 1998) created a model for the acoustic scattering of siphonophores, where the acoustic properties of the siphonophores could be described as $L_{bs} = L_{bubble} + L_{tissue}$. He showed that these organisms can provide similar echoes as mesopelagic fishes and can be dominant in oceanic habitats. In the study of (Warren et al., 2001) siphonophores target strength were measured at levels between -59 dB to -70 dB. The pneumatophore is the important sound reflector, and recently several studies of the pneumatophores, response to sound have been conducted. In the paper by Knutsen et al., (2018), a theoretical scattering model were made to estimate the target strength of siphonophore pneumatophore at several diameters at different depths. The modelling exercise was made in order to understand the strong backscattering at 38 kHz in a specific bloom in a Norwegian fjord in 2015.

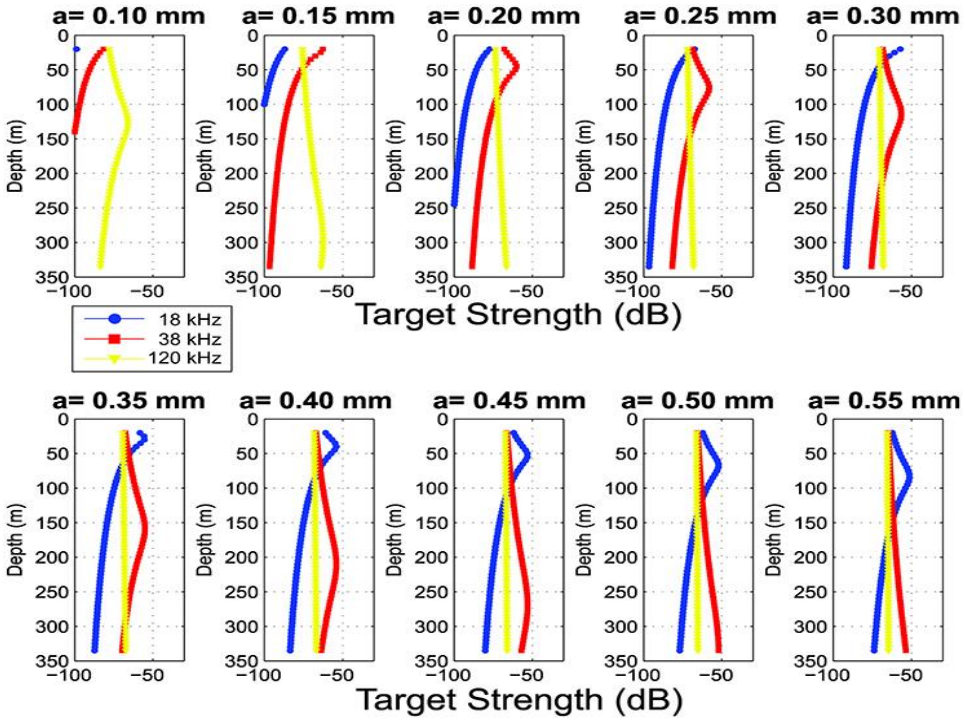

***Figure 1.3.4**. Different target strengths dependant on pneumatophore sizes and depth, taken from (Knutsen et al., 2018)*

In the study of (Knutsen et al., 2018) some measurements were made were the gas inclusion varied between 0.34 and 0.56 millimetres in spherical radius, but because these samples were over a year old, some deflation may have occurred. Like for mesopelagic fishes, the resonant frequency for siphonophores will be fairly low. With respect to biomass estimation of these animals, there may be other difficulties. These organisms will not be properly caught in trawls, as their tissue is damaged by the stress of capture, and many would pass straight through the meshes (Bigelow, 1913).

1.3.4.5 Role in the deep scattering layers.

Already in 1963, physonect siphonophores were suggested to play a major part in sound scattering layers. In a study done with a submersible, (Barham, 1963) discovered the species *Nanomia Bijuga* in the deep scattering layer, and a gas inclusion which resonates at 12 kHz were also described. The species were also observed as a fast swimmer, able to follow the layers migration properties. The individuals had the ability to regulate their gas inclusion due to the pressure changes. They can locally be the most abundant predator on zooplankton and they can be dominating in the mesopelagic layer. (Purcell, 1981; Robison et al., 1998; Gorsky et al., 2000; Hosia and Bamstedt, 2007). To form a deep scattering layer, the animals must be distributing in a certain density. McCartney, (1976) estimated that swimbladdered mesopelagic fish would at densities between 0.1 to 0.0001 fish/m^3 be able to form a layer to be clearly visible on an echo sounder. Siphonophores with the gas inclusion is also able to produce a layer in the lower end at that density scale. Siphonophores can aggregate in both thin and dense layers. Recordings of up to 50-100 siphonophores/m^3 have been observed by (Mills, 1995). Siphonophores can be locally very abundant. Knutsen et al., (2018), studied a local bloom of siphonophores and the density were measured to 20 siphonophores/m^3. This was in a fjord system in Kvænangen where the environmental factors were advantageous for the organisms to form a bloom.

1.3.4.6 Current standings

When estimating the global biomass, the assumption that all the bladdered scatterers be fish, could potentially lead to severe overestimation of biomass. Especially this is the case for some areas which can be dominated by strong scattering siphonophores. The lack of unbiased sampling gear

for this category of animals, makes the resulting sampling even more controversial. The knowledge of the gas inclusion and how it differs between species and individuals are yet not well studied. Estimating biomass with resonance and siphonophores in consideration have been done by Proud et al., (2018). In the model presented, the mesopelagic biomass could fluctuate between 1.8 to almost 16 gigatons. This model considers both the probability that the biomass is combined by siphonophores and fishes, and that there is different behaviour in the swim bladders. The author further suggests different methods to solve these problems by adding more frequencies to acoustic surveys, further studies of the species contributing to the DSL and finally obtaining more information on the acoustic properties of the siphonophores using modern profiling systems.

1.4 New acoustic methods

1.4.1 Multifrequency analysis

Multifrequency methods may be used to investigate and to separate target categories with different backscattering properties (Korneliussen & Ona, 2002). As mentioned earlier, different categories of organism's scatter sound differently, and these properties can be used to separate them.

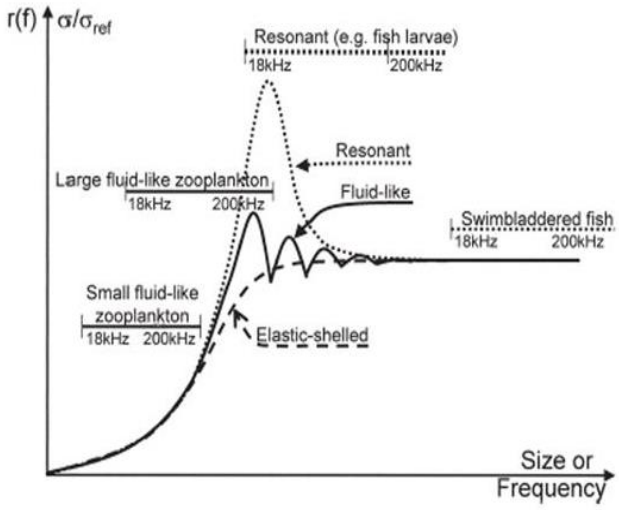

Figure 1.4.1. *How different target categories scatter sound. Figure taken from (Korneliussen & Ona, 2003)*

Swimbladdered fish are usually surveyed on low frequencies (18-38 kHz), while plankton are efficiently measured at high frequencies (120-333 kHz). Using several frequencies simultaneously, can be used as a tool to understand the composition of marine organisms in the water column (Horne, 2000; Ona & Korneliussen, 2000; Korneliussen et al., 2008). Mesopelagic layers often contain all the categories shown in figure 1.4.1, but the most common backscattering from pearlsides and lanternfish concentrations is higher backscatter at the lower frequencies, where the 18 kHz backscattering is found up along the resonance curve, and that the backscattering relative flat at frequencies above 38 kHz. This is consistent with bubble backscattering, where the bubble is of a size of 5-10 mm^3, rather than 1 mm^3.

1.4.2 Probing

When a pulse of high frequency is emitted, a lot of the sound energy is lost due to two factors, geometrical spreading, and absorption loss. The higher the frequency, the higher the absorption. Mesopelagic organisms live in usually deep waters, and they are weak scatterers. Low frequencies are most useful when measuring at great depths, but as mentioned, resonance can become a problem. Resonance is an unwanted effect on acoustic biomass estimation, since the backscattering at resonance is much higher than anticipated from a particular animal size. With traditional vessel acoustics, 18 and 38 kHz is usually applied, but there are for instance a difficulty studying target strength at depth due to the large pulse volume. The information about species composition is also limited at such depths since the separation of target or target categories are more difficult if they are mixed in the large pulse volumes. With 18 and 38 kHz, only the strongest targets is possible. These frequencies are not applicable for measuring zooplankton and other organisms without gas inclusions since their backscatter at these frequencies are weak.

By using a lowered transducer, organisms can be measured at different frequencies at close range, even at larger depths. When lowering the probe into the school, single targets can be studied, and target strength can be determined with better precision. The TS probe has the possibility of placing transducers either downwards or sideways, and a camera can be mounted. The camera system makes it possible to get insight of species composition in the layers. Lowering the probe into the layer or just above, gives a variety of possibilities. It measures mesopelagic fish at a short range, and it is possible to separate them as single targets. This gives an opportunity to measure target strength *in situ*, therefore also density estimation. With the probe either just above the layer with the transducer looking downwards, or in the middle of the layer with the transducer looking sideways are efficient ways to measure single targets with great resolution. Frequencies that are usually not applicable at those depths (120,200 and 333 kHz) can also be used. Then weaker targets can be separated and studied at these depths. These targets of interest may be an important food of both mesopelagic fish and siphonophores. The multifrequency information can also be used to roughly determine the species categories in the layer. Frequency response analysis is usually limited in vessel acoustics, as only upper water column can be reached. At greater depths only 18, 38 and 70 kHz are usable. With the help of the acoustic probe a normal frequency response analysis can be made at depths down to 1500 meters, which is the limitation of the transducer. With the help of frequency response, and a mounted camera, a more precise estimate of the species

composition can be made, as some of the categories can be well photographed with no avoidance. These are copepods, krill, jellyfish and similar organisms. (Ona and Pedersen, 2006).

1.5 Objectives

The objectives of this study are: (1) to compare the measurement of mesopelagic communities with both hull mounted transducer with TS-values gathered from literature, with measurements from the TS-probe with *in situ* target strength measurements. (2) To evaluate potential resonance in the swimbladders of mesopelagic fish if there are large differences in the density estimates (3) to evaluate potential presence of siphonophores in the scattering layers.

2 Material and methods

2.1 Survey description

Data was collected during the multipurpose Crisp survey, with the research vessel G.O Sars November 19th, 2017, to December 4th, 2017. The area where the probing samples were conducted is shown in (Fig. 2.1). The purpose of the survey was to test different acoustic equipment on several biological targets. Studies on herring, blue whiting and the deep scattering layers were conducted, only data on deep scattering layers were used in this study. Acoustic data was collected with hull mounted transducer, and an acoustic probe. The results from the two different observation platforms were compared. The investigations on mesopelagic fish conducted both in fjords in northern Norway, and in the Norwegian Sea at Vøringplatået.

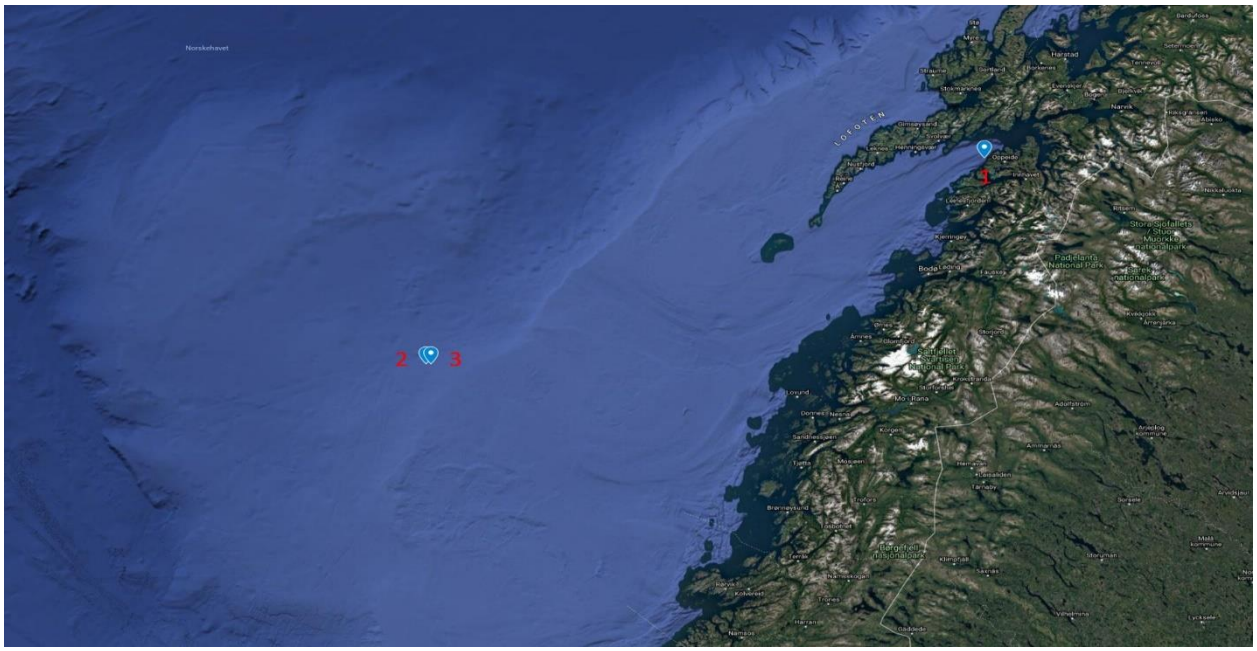

Figure 2.1. *Map of all three probing stations. One station in the inner parts of Vestfjorden November 25th (1) 2017 and two stations located at Vøringplatået November 29th (2) and 30th (3) 2017.*

2.2 Data collection

2.2.1 Ship data collection

The vessel data was collected with a Simrad EK80 split beam echo sounder, with 18, 38, 70,120,200 and 333 kHz transducers. Data was recorded continuously, and relevant data were chosen in the post processing program LSSS (Korneliussen et al., 2006). All frequencies were used in post processing except 333 kHz, due to limited reach. Since a comparison between vessel data and probing data were of interest, the acoustic data from both observation platforms were compared as close as possible with respect to time. The length of the transects interpreted was one nautical mile, and if possible, performed before and after probing. The aim was to investigate areas or volumes as similar as possible. Raw echo sounder data was saved in the EK80 software and transferred to LSSS to be further analysed. By using a package developed in LSSS, the data were down sampled to EK60 data before interpretation. The echo sounder system was calibrated before the survey, during optimal conditions with standard ICES methods (Ona, 1999; Demer et al., 2015).

Table 2.2. *Calibration data from hull mounted transducer*

	Simrad EK80, narrow-band mode					
Transducer type	ES18	ES38-7	ES70-7CD	ES120-7C	ES200-7C	ES333-7C
Transmission frequency [kHz]	18	38	70	120	200	333
Transmission power [W]	2000	2000	600	200	105	40
TS Transducer Gain [dB]	22.01	26.8	28.02	26.89	26.95	26.1
Equivalent beam angle [dB]	-17.0	-20.7	-20.7	-20.7	-20.7	-20.7
Sample interval, ms	0.0280	0.048	0.048	0.04	0.0032	0.024
Ramping slope, %						
Absorption coefficient [dB km^{-1}]	2.57	9.48	22.1	36.5	51.7	77.1
Half power beam widths (along/athwart ship) [deg]						
Transducer angle sensitivity (along ship and athwart ship)	15.5	18	23.0	23	23	23
Sound speed (measured) [m s^{-1}]	1472	1472	1472	1472	1472	1472

2.2.2 Choosing of area for post processing

For the scrutinizing of vessel data, a stretch of 1 nautical mile was chosen. Areas were chosen after where probing had occurred. If possible one area before and one after the probing were selected. If data were lacking, or had noise errors, areas further away were used. To be able to compare samples, it's important that the scattering layers don't deviate very much over the time of probing, typically 1 hour. Usually the NASC-values between successive distances of one nautical mile were similar. This is shown in (Fig.2.2.2), and (Fig 2.2.3) Where the autocorrelation was measured from both the shallow and deep scattering layers. The NASC-values were read from the echogram shown in (2.2.1.) and were the autocorrelation were calculated in MYSTAT. The autocorrelation was plotted in an ACF-plot were the correlation were plotted in the y-axis, and the spatial lag were plotted on the x-axis. The autocorrelation is increasing for each layer over time and justifies the usage of one nautical mile as a representative.

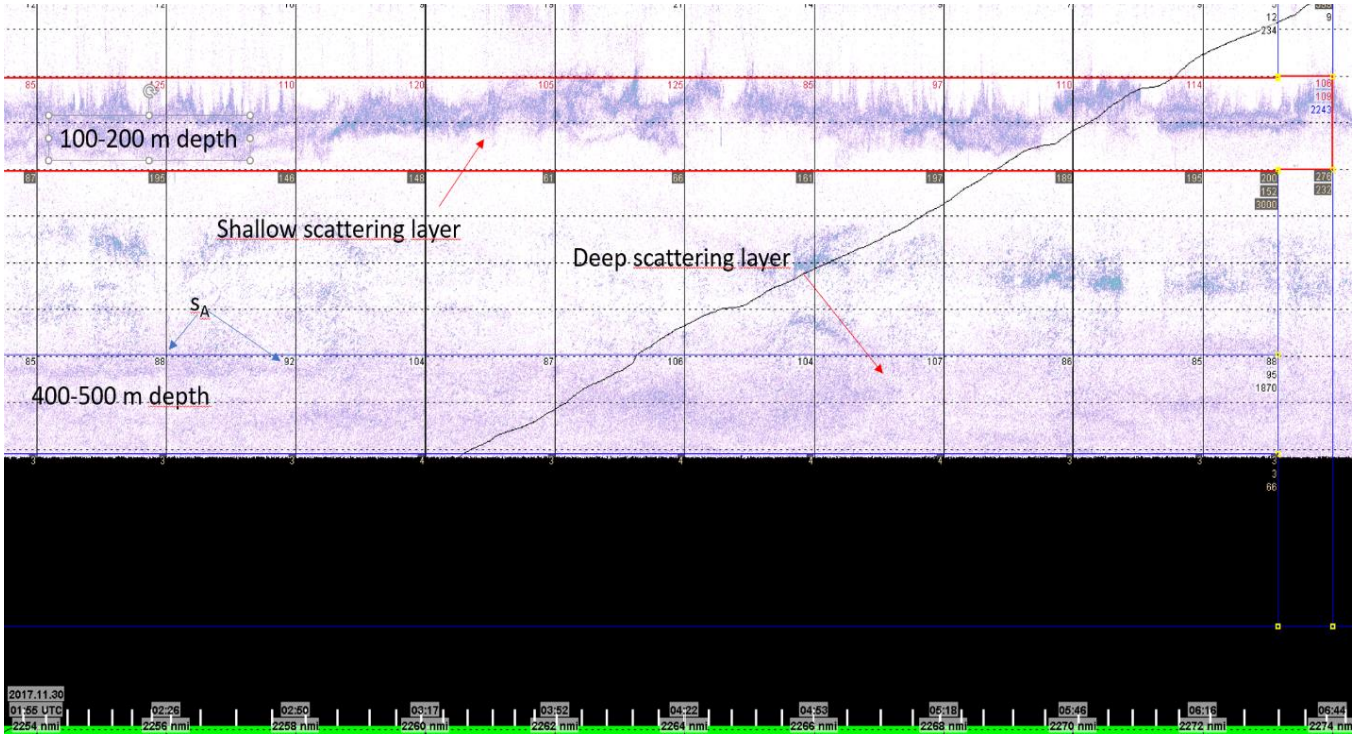

figure 2.2.1. *Echogram of 20 nautical miles. Measurement of autocorrelation were selected for this area. Mesopelagic layers usually have the same structure for a large geographical area. By measuring the NASC-values from LSSS and calculating autocorrelation, an argument for choosing only one nautical mile as a representative for the whole area is possible.*

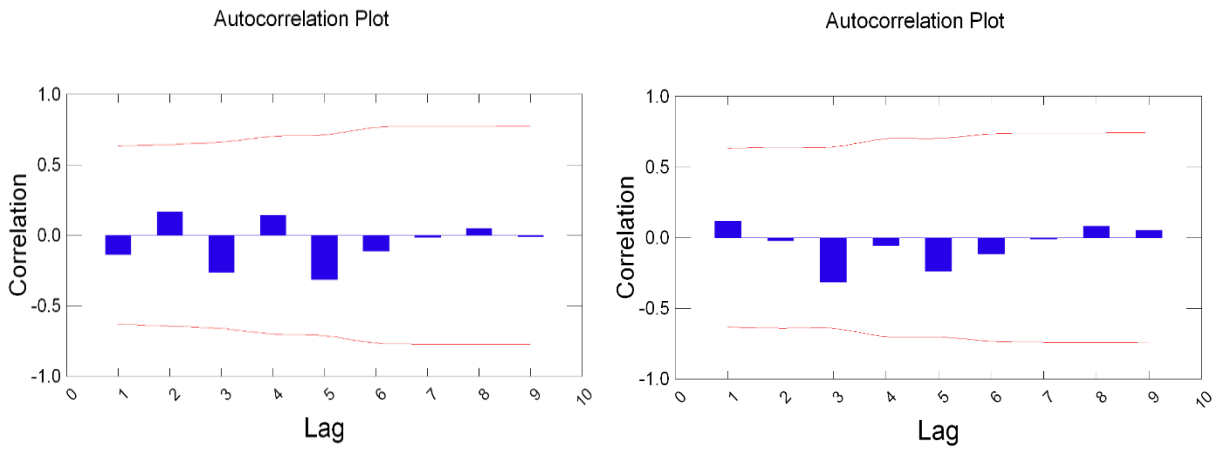

Figure 2.2.2. Autocorrelation plot for the shallow scattering layer (left) and the deep scattering layer (Right). Where NASC-values have been read from LSSS and plotted in MYSTAT. This plot shows the autocorrelation for the depth between 100-200 meters. This plot shows the autocorrelation for the depth between 400 and 500 meters.

Table 2.2.2. *Overview of areas chosen for post processing*

Date	Area	Time UTC	Log (Nmi)	Latitude	longitude
November 25th 2017	Vestfjorden	22:45-22:51	1625-1626	67.748	14.062
November 29th 2017	Vøringplatået	10:49-11:02 15:35-15:43	2212- 2213 2216-2217	66.613	6.59
November 30th 2017	Vøringplatået	00:07-00:19	2247-2248	66.68	6.604

2.2.2 Example of one station with vessel data

The area for the second probe station was in the Norwegian Sea, at Vøringplatået. This area will be described in detail to explain the methodology for this study. Scrutinizing, and echograms for each station are found in appendix I. Two areas were chosen for scrutinization. The areas chosen for scrutinization were one nautical mile passed between 10:49-11:02 UTC, and 15:35-15:43 UTC. Probing was conducted during dusk, which means a potential diel vertical migration took place during the sampling. A change occurred both at high and low frequencies, as shown in (Fig.2.2.5 and 2.2.6). Since there are suggestions that mesopelagic fish do not fast migrate horizontally (Gjøsaether, 1981), the total biomass may be similar before and after the vertical migration.

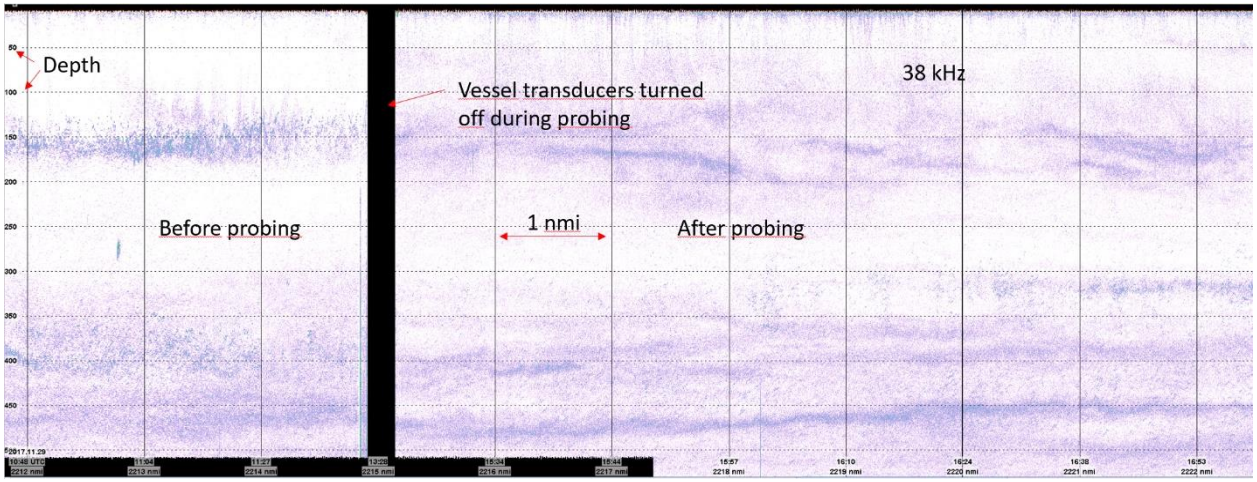

Figure 2.2.5. *Ten nautical miles of area where probing occurred, showing dial vertical migration at 38 kHz. The scattering layer at 150-200 meters are narrower before probing.*

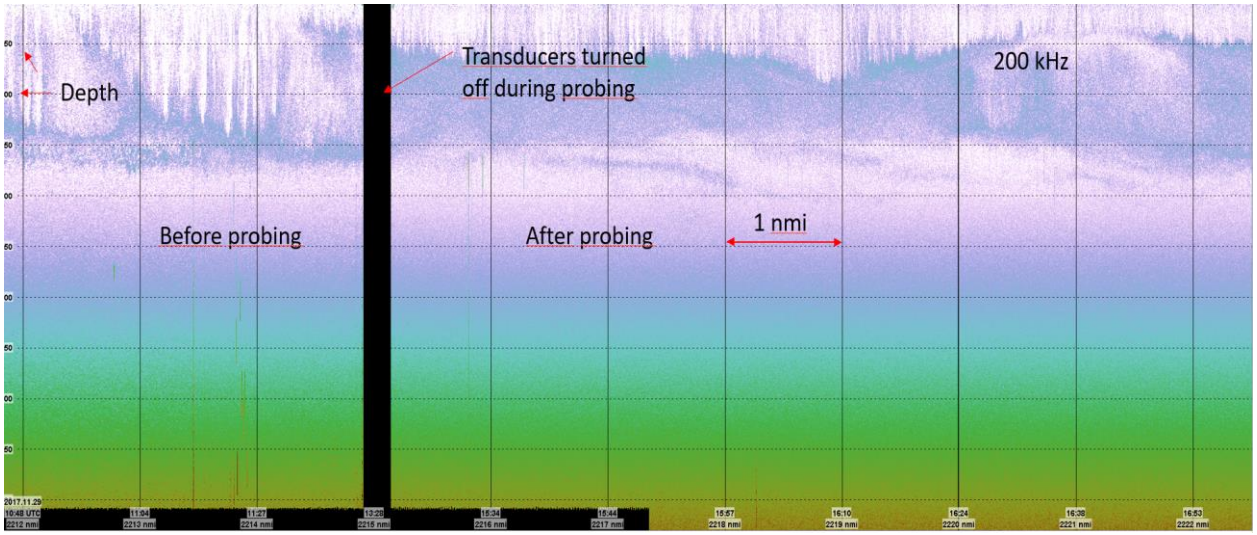

Figure 2.2.6. *Ten nautical miles of area where probing occurred, showing dial vertical migration at 200 kHz. The zooplankton layer appearing at 150 meters before probing, stretches from 50-150 meters after probing.*

In this area, there are both fish and zooplankton plankton evident, and there are two scattering layers(Fig.2.2.5). Zooplankton is especially visible on the 200 kHz echogram (Fig 2.2.6), but due to the range limitation, zooplankton may also be found deeper. However, under about 150 meter no strong scatterers are seen down to the maximum range of about 250 meters. Two areas were chosen for scrutinization, one area before probing from ship log 2212- 2213, and one after probing from ship log 2216-2217.

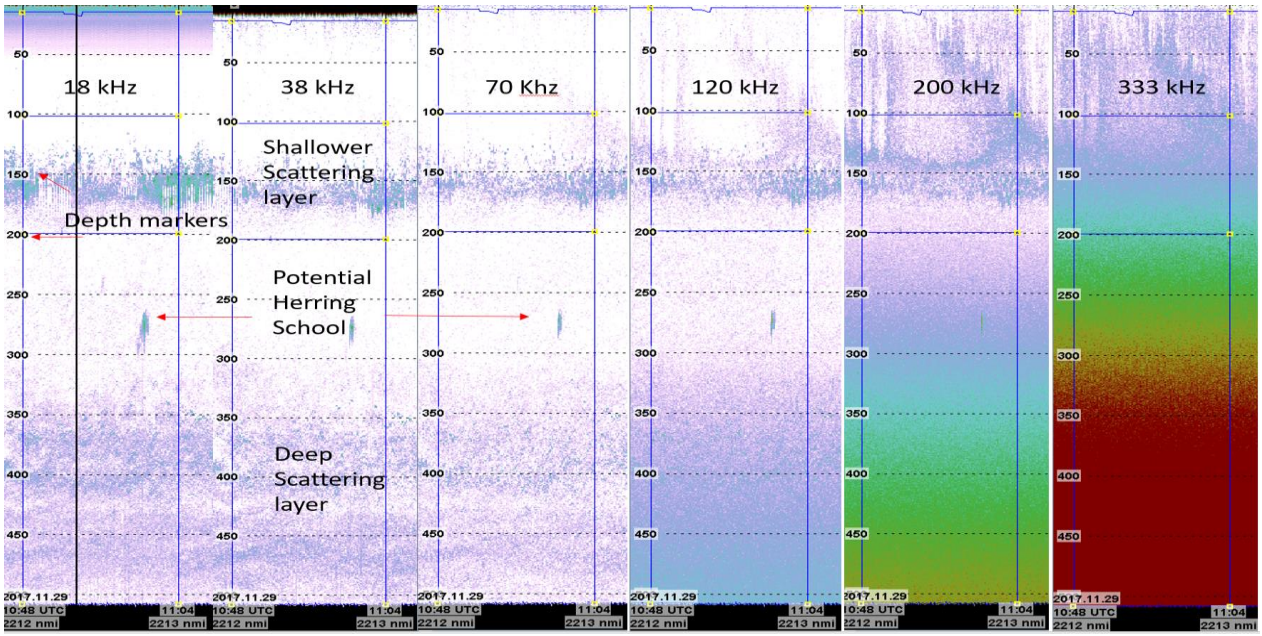

Figure 2.2.7. *Echogram from the nautical mile before probing, on 6 different frequencies. The small aggregation between 250 and 300 meters are possibly a herring school and were removed before scrutinizing. The depth is shown at the y axis of the echogram. At 18, 38 and 70 kHz there is two evident scattering layers, while the higher frequencies, 120, 200 and 333 kHz shows a dense zooplankton aggregation in the upper 150 meters.*

In this sample there are two distinct scattering layers. One relatively thin shallow layer, and one larger deep layer. In previous studies usually, pearlsides live in these shallower layers, and glacier lanternfish in the deeper layers (Giske et al. 1990). In this study both layers are scrutinized as mesopelagic fish. It appears that there is an increase in the density of the shallow layer just before the dial vertical migration starts, increasing the mean backscattering, especially evident at 18 kHz.

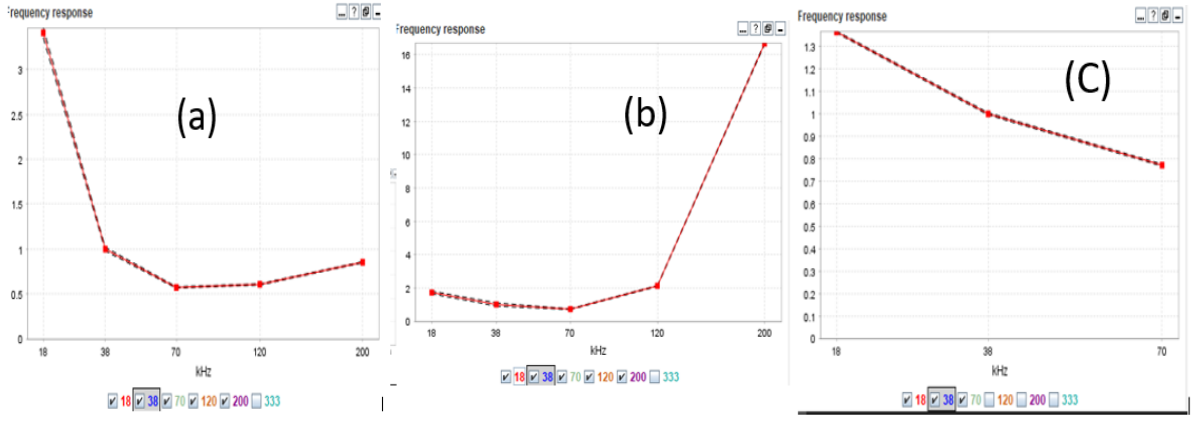

Figure 2.2.8. *The frequency response measured in the lower part of the upper layer, at approximately 130-190 m depth (a), and 80-140 m depth (b) and for the depth layer between 350-500 m (c). Notably only 18, 38 and 70 kHz are applicable due to range limitation in the deeper layer.*

Notable higher backscattering 18 and 200 kHz(Fig.2.2.8). Fish and other bladdered organisms usually have strong responses on low frequencies (Korneliussen & Ona, 2003). Mesopelagic fish like pearlsides and glacier lanternfish have strong backscattering on 18 and 38 kHz, (Scoulding et al., 2015). This could explain the frequency response seen for this layer. Copepods are targets which are expected to be in the Rayleigh scattering region, where their response will increase rapidly with high frequencies, (Simmonds & Maclennan, 2005).

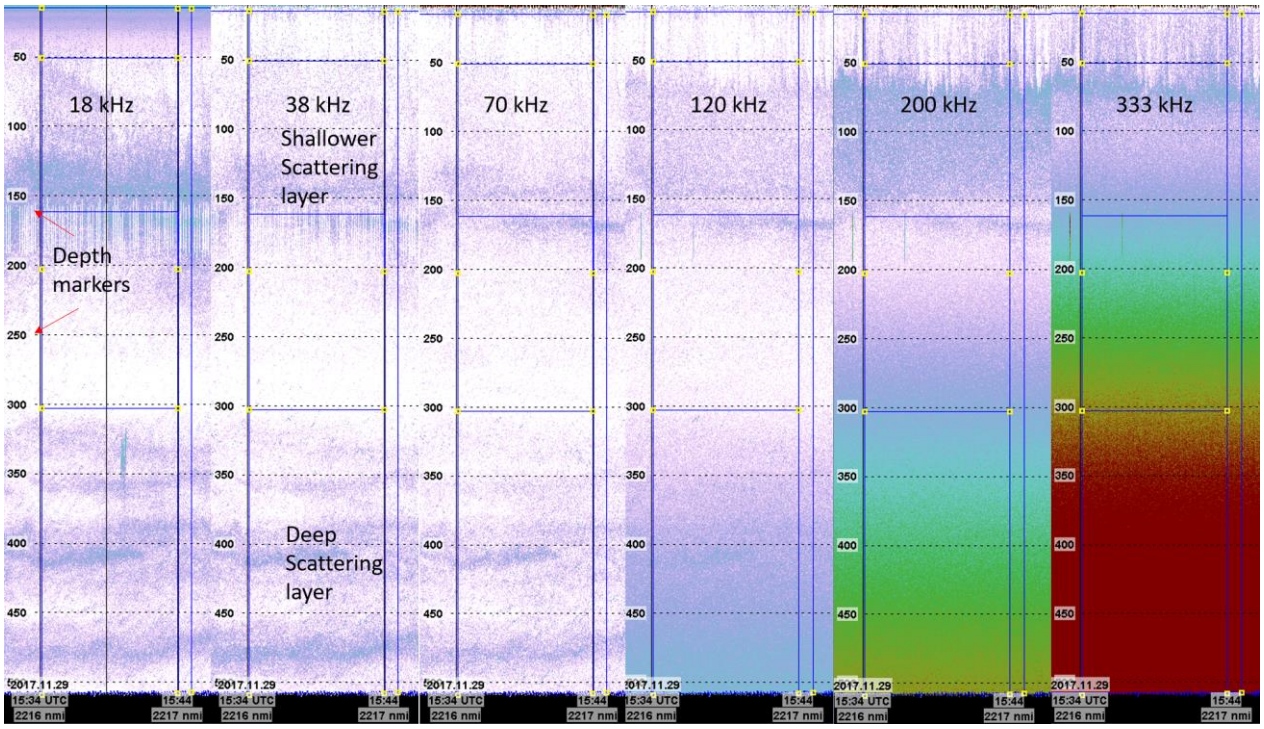

Figure 2.2.9. *Echogram from the nautical mile after probing, shown on 6 frewuencies.*

After probing the layer had diluted and it is more difficult to distinguish fish an zooplankton targets. There are still two scattering layers, but the the especially the shallow scattering layer are distributed over a larger depth, but appear less dense (Fig.2.2.9). Notably there is a dense distribution appearing above the shallow scattering layers, which is possibly copepods. Due to absorption, there is not possible to determine if plankton have migrated from depths. In this station both before and after probing, large fish seems to be absent, and the backscattering could be categorized in two categories, mesopelagic fish and zooplankton.

2.3 Probe data collection

For the acoustic sampling using a lowered platform, The TS-probe were used. This instrument was developed by IMR (Institute of Marine Research). The probe is put together of three different layers. An outer metal frame, a movable motorized transducer platform and a protected cylinder containing the computer and sensors (Fig.2.3.1). The cylinder contained 4 Simrad EK80 wideband transducers (echo sounders). The probing was performed from the hangar of the ship. The probe was connected to a winch with a crane when moved outwards and the probe lowered into the ocean. The probe was either lowered into the layer of interest, or a full profiling of the water column were done. Both echo integration data, and *in situ* target strength measurements could be made on the data collected on the probe. Due to the fibre-optic connection between the probe and the vessel, real time view echograms were possible together with other parameters like total depth and temperature (Fig.2.3.2). The transducers were either mounted horizontally or vertically as shown in figure 2.3.1. The stereo camera mounted on the probe were used on all station, and photos were taken opportunistically and if possible during the sampling. The goal was to inspect the species composition in the scattering layers. To get precise measurements, the probe transducers were calibrated after ICES- standards (Foote et al., 1987, Demer et al 2015). The probe has three extendable arms (Fig 2.3.1) where a calibration sphere is attached underneath. The sphere is then moved with the help of the nylon wires and the motorized transducer platform. Different spheres were used for the different frequencies. For the smallest spheres, an additional weight is added to make them stable in the water column.

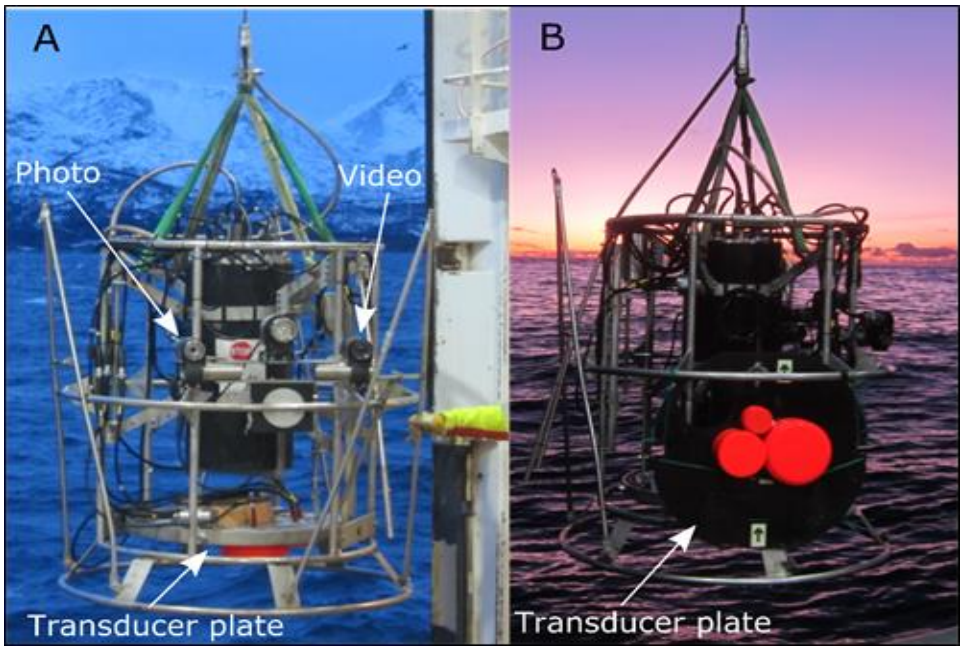

Figure 2.3.1. *Description of probe with transducers looking down (A), and transducers looking sideways(B). Photo: Rokas Kubilius*

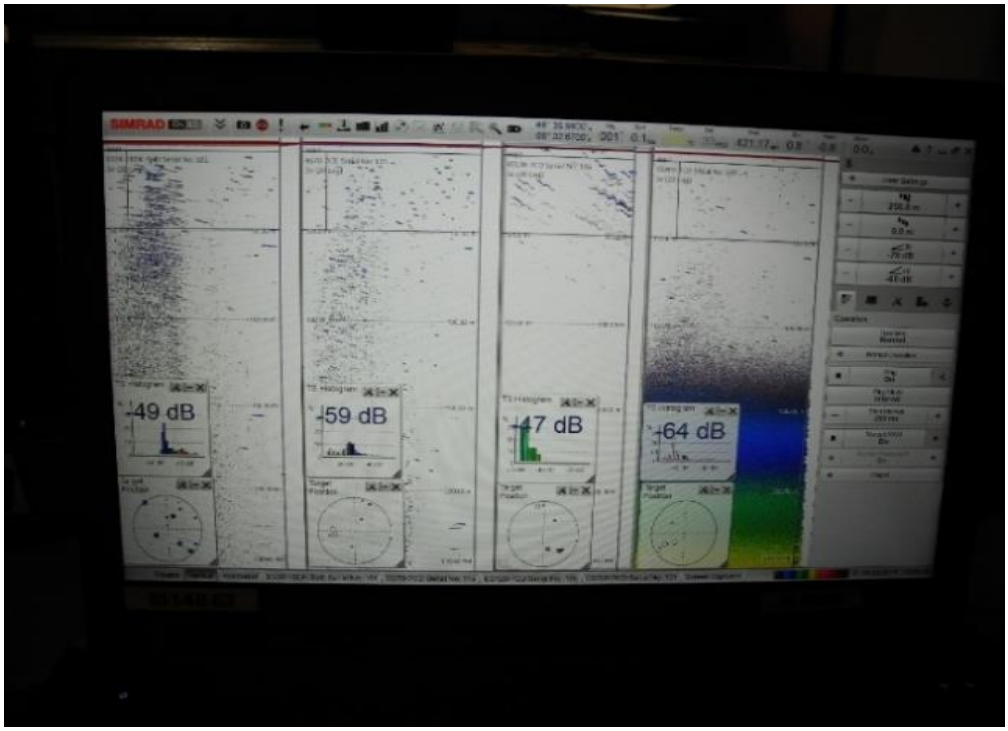

Figure *2.3.2. EK80 display during the probing. The screen is split into four sections. One representing each frequency.*

Table 2.3.1. *Calibration data for TS-probe*

Simrad ek80 **Narrowband mode**					
Transducer type	ES38D	ES38-18DK	ES70-7CD	ES120-7CD	ES200-7CD
Transmission frequency [kHz]	38	38	70	120	200
Transmission power [W]	400	100	500	400	150
TS Transducer Gain [dB]	25.27	19.17	26.98	27.1	26.66
Equivalent beam angle [dB]	-20.7	-12.5	-20.7	-20.7	-20.7
Sample interval, ms	0.04	0.048	0.048	0.04	0.032
Ramping slope, %	25.7	10.28	2.79	1.63	0.98
Absorption coefficient [dB km^{-1}]	9.36	9.36	21.87	36.10	51.14
Half power beam widths (along/athwart ship) [deg]	7.06/7.04	17.02/17.11	7.26/7.11	6.91/6.76	6.64/6.1
Transducer angle sensitivity (along ship and athwart ship)	23.0	10.0	23.0	23.0	23.0
Sound speed (measured) [m s^{-1}]	1479	1479	1479	1479	1479

***Table 2.3.2**. List of probing stations*

Location	Date	Time UTC	Method/ lowering speed ms^{-1}	Frequencies (kHz)	Depth sampled (m)
Vestfjorden	November 25th 2017	18:29	Investigation of the shallowest scattering layer	38,70,120, and 200 looking downwards	66-120
Vøringplatået	November 29th 2017	12:38-13:21	Deep profiling 0.5 ms^{-1}	38,70 and 200 pointing sideways, and 120 pointing downwards	10-550
Vøringplatået	November 30th 2017	11:11-12:47	Deep water profiling. 0.267 ms^{-1}	38, 70, and 200 pointing sideways 120 pointing downwards	10-761
Vøringplatået	November 30th 2017	12:47-14:17	Deep water profiling. Probe lowered with the speed of 0.274 ms^{-1}	38, 70, and 200 pointing sideways 120 pointing downwards	10-764
Vøringplatået	November 30th 2017	15:38-17:17	Deep water profiling. Probe lowered with the speed of 0.265 ms^{-1}	38, 70, and 200 pointing sideways 120 pointing downwards	10-757

Probing stations were chosen opportunistically, and when time was permitted during the survey. Three areas were investigated during this survey, and one example of one probing station is described in chapter 2.3.2

2.3.2 Example of one probing station

Location: Vøringplatået Time 12:38 UTC. The target strength probe was mounted with 38, 70, and 200 kHz looking sideways, and 120 looking downwards. The probe was lowered at a speed of 0, 5 ms^{-1} down to 550 meters, and up again. The echogram displayed in figure 2.3.5 is the echogram from one vertical profile. 38, 70 and 200 kHz were measuring horizontally, and the output in LSSS is a sideways echogram, where the depth markers represent the distance from the probe, rather than the depth. At 120 kHz the transducer was mounted vertically, and the depth markers would represent vertical distance away from the probe. Just as with the vessel data, the two scattering layers are present at especially 38 kHz (Fig. 2.3.5). Only the descent was chosen for post processing.

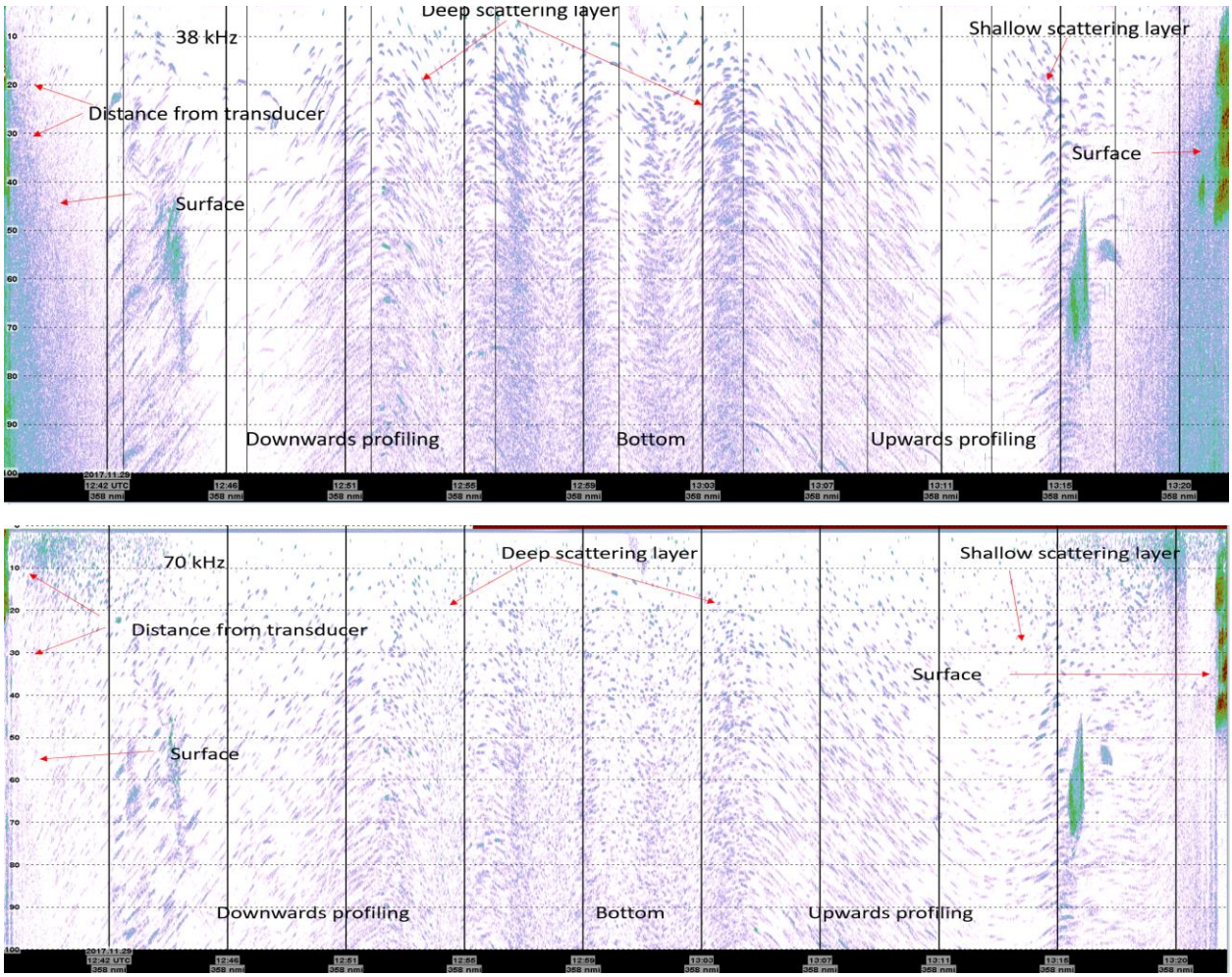

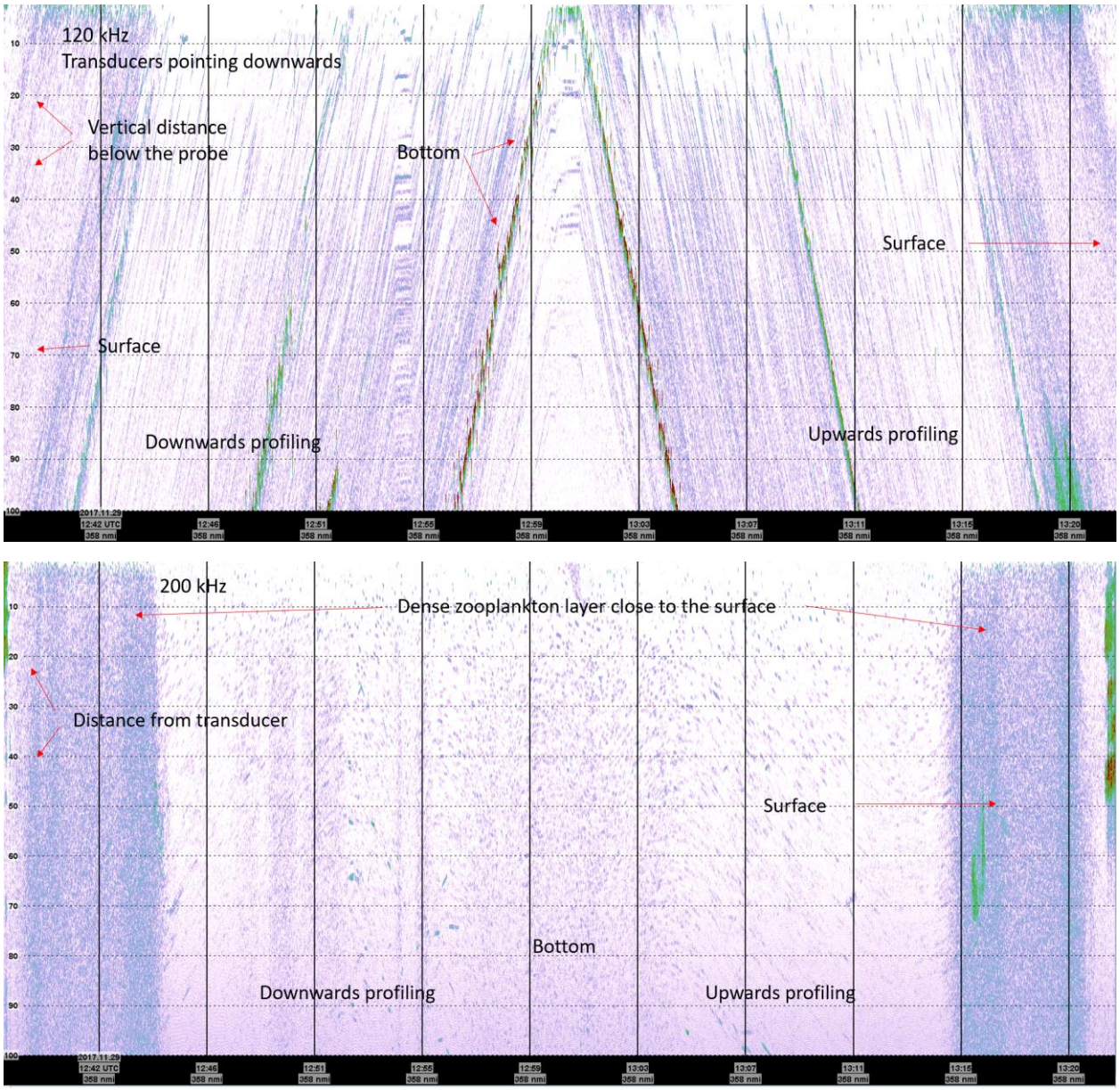

Figure 2.3.3 *overview of probing station 29th November 2017. Figure displays the frequencies, 38,70, 120 and 200 kHz. The echogram of 120 kHz is different due to the vertical mounting. The bottom is present at the middle of the echogram. Deep scattering layers are visible at the lower frequencies, while dense zooplankton aggregations are visible at 200 kHz. All echograms are showing a full profiling of the water column.*

2.4 Post processing

2.4.1 LSSS Scrutinising

LSSS a program developed by MAREC (www.marec.no), and initiated the IMR, is a program designed to handle and process large amounts of acoustic data. In this post processing program, there is possibilities to interpret the recordings from multiple echo sounders simultaneously. Echograms can be manipulated, and new depth layers can be created, were density of fish or other marine organisms can be measured. LSSS can both be used for large scale surveys used in fisheries management, and for smaller scientific investigations, like here. LSSS can handle echo sounder data from several frequencies simultaneously. This gives an opportunity for studying the frequency response of organisms, and to categorize target categories to species. The interpreted data can be converted to different file formats, and can be further used in models, input for setting of quota or scientific studies. (Korneliussen et al., 2006). In this study, LSSS is used for scrutinizing of both vessel and probe data. Abundance were estimated for allocating backscattering in NASC-unites (Maclennan et al., 2002). Acoustic classes were identified with the use of several frequencies and the relative frequency response (Korneliussen & Ona, 2002). *In situ* target strength measurements were extracted using LSSS's target strength filters further described in chapter 2.5.2.1. After the scrutinization, measured density was stored to database to selected regions, and extracted to excel from the listuser11-format for further analysis.

2.4.1.1 Scrutinization techniques

After opening LSSS the first step was to find areas usable for scrutinization. Since the vessel echo sounders were put into passive mode (off) during probing, the area or time just before probing were easily accessible. Mesopelagic layers usually have a high autocorrelation, and one nautical mile is usually representative for many successive miles (figure 2.2.1). If possible, areas without other schools of fish were chosen. Due to trawling and possible noise from other sonars and transducers, nautical miles without noise were selected. If this was not possible, noise was corrected by LSSS's noise removal tools. Most of the areas used, may be inhabited by plankton, mesopelagic organisms and in some of them, larger single targets from larger fish. Since there were no trawl catches, all mesopelagic observations were scrutinized as a mix of glacier lanternfish and pearlsides. These fishes are the two most common mesopelagic fishes in Norwegian waters, and even though they tend to separate (Giske et al., 1990) there is no biological sampling from the different areas to

determine that. There could also be a presence of smaller fish and larvae with similar acoustic properties. Sometimes larger fish mixed with the mesopelagic layers and had to be separated. Since mesopelagic fish and their food were the subjects of interest, all other targets were just scrutinized in such a way for separating them from the rest. A way to remove plankton echoes from fish echoes and separate small and large fish, is to threshold the mean volume backscattering strength. Several routines of thresholding were used to separate between targets. Thresholding is applied to separate between targets of different backscattering strengths. There is no described standardized way to use volume scattering strength to separate between targets, but usage of the ping plot in LSSS, gives insight on the trend of volume scattering. Strong targets like fish usually have a higher volume scattering strength than plankton and will stand out as clear peaks in the ping plot.

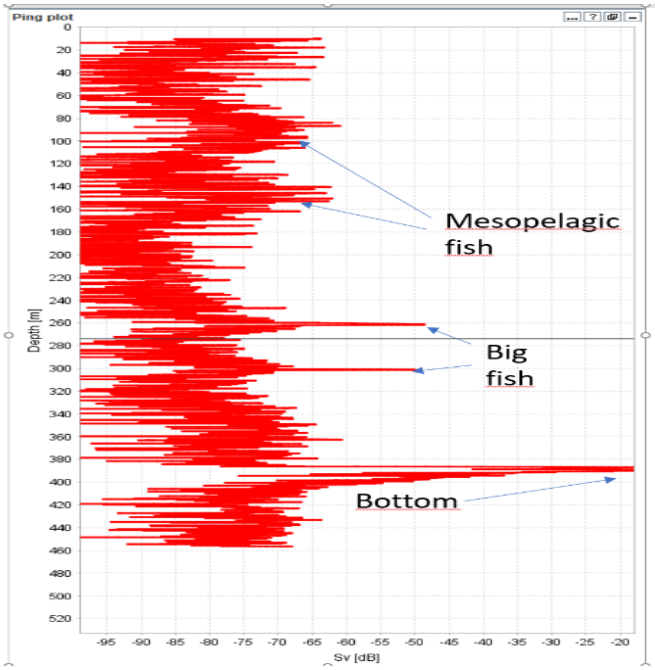

Figure 2.4.1. *Example of ping plot containing strong targets like large fish and the bottom. S_v-values are read in the x-axis, and thresholding are performed based on the observations. In this case the S_v of the large fish exceeds -55 dB*

By using lower and upper thresholding, weaker targets and stronger targets can be separated. Usually fishes have a volume scattering strength, (S_v), higher then –70 dB and can be separated from plankton this way. Plankton are weak scatterers and will have to distribute in dense layers if they should exceed S_v =-70 dB. If the sample includes large fish, or dense schools these can be seen in the ping plot as outliers. In order to do this, there must be a clear separation from the different targets. A good example is shown in figure 2.4.3, where there are presence of plankton,

smaller fish and larger fish targets. A problem arises when weak targets aggregate in a way that their volume scattering strength reaches the same level as the stronger targets. Then this procedure is more difficult. A way to check if the thresholding is working, is to compare the top and bottom threshold. The function can either remove the weak targets, or the stronger targets. If these two methods give a similar result, the thresholding method is working. The most common method in the different stations were thresholding in three different ways. Echoes from -70 to -82 dB were allocated plankton. If the remaining echoes belonged to small fish, the backscattering were allocated to mesopelagic fish if they were found at normal depths. Some of the samples which contained larger fish, the ping plot were frequently applied. Where large fish separates in such a manner as shown in figure 2.4.1, it is possible to threshold away all other targets, just with the remaining strong ones. When mesopelagic targets at 18 kHz were close to resonance frequency, there were difficulties separating them from the larger targets, which were present in the same layer. This were especially evident in some of the shallower scattering layers.

2.4.1.2 Categorization

In LSSS, different acoustic categories are used to describe targets. When the thresholding has separated different acoustic classes of organisms, they are divided into categories.

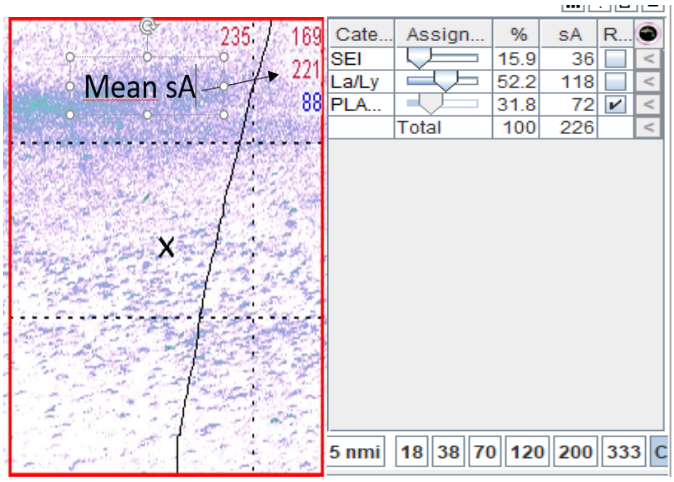

Figure 2.4.2. *Example of categorization. Acoustic classes are allocated three categories. By using the ping plot, large fish, mesopelagic fish and zooplankton are separated. In the categorization table, allocated backscattering together with the percentage of the total backscattering is shown.*

Here is an example of how different classes are categorized. By using the thresholding techniques described, three acoustic classes were made. The backscattering was given to mesopelagic fish, plankton and large fish, in this case saithe (Fig.2.4.2). When for instance the thresholding is -70dB, only NASC-values from this scattering strength or stronger are measured, and this number can be given to mesopelagic fish. Then lower the threshold back to -82 dB were the remaining value were given plankton. Due to noise from back radiation, upper 50 meters were not usable, when scrutinizing the 18 kHz data. The deep scattering layers were not reachable by 120 and 200 kHz. The same procedures were implemented on the probe data, but because of the high resolution, sometimes thresholding could be done visually. Since the volume sampled with the probe transducers, the smaller targets were resolved into single targets. Then the difference between fish and plankton were much more visible. The ping plot were used in the same way as with the vessel data, but there were also possibilities to study target strength of individual targets and compare them with literature target strength. In all samples NASC- values were allocated to plankton, mesopelagic fish or large fish. When scrutinizing zooplankton in the probe data, another approach had to be made. In the shallow parts of the profiling's, the density of zooplankton was of such a high magnitude, that it exceeded a volume scattering strength of -70 dB. In some of the samples it was possible to separate out some fish with a threshold of –60 dB. In the weaker layers, -70 dB were enough to separate the targets (Fig2.4.3). There is a possibility that fish echoes could be mixed in the measurement.

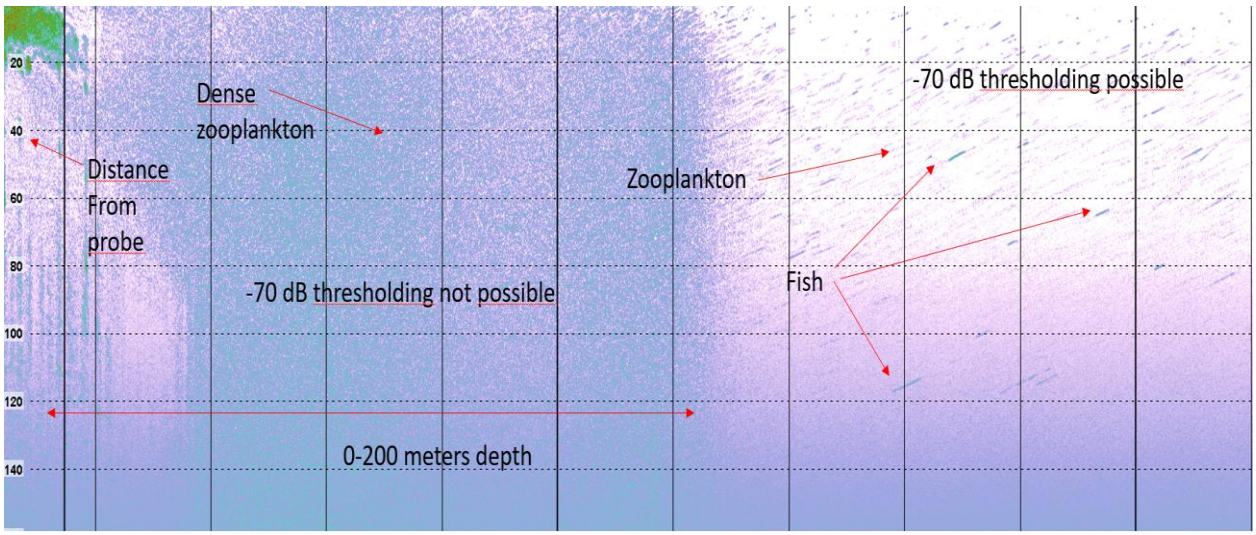

Figure 2.4.3. *Example taken from probing station 3, 30th November. There is a dense zooplankton layer in the upper water column. The volume scattering coefficient is stronger than –70 dB. This makes thresholding more difficult. Large fish may be separable from the layer, using –60 dB thresholding, but may include smaller fish in the plankton layer.*

2.4.2 Post processing of probe data

2.4.2.1 Data preparation for probing data

Probing data are read differently in to LSSS and must be prepared before depth profiles can be created. During probing, where the transducers were mounted vertically, but otherwise are read in the same way as vessel data. The depth axis is now, however range from the probe. When mounted sideways, the depth of the probe will now be along the distance, or ping axis, and the depth or pressure unites must be manually interpreted from the pressure sensor and the exact time. The goal was to measure the acoustic data with the same grid size as the vessel data, 10 meters. Since some of the probing data were read sideways, another approach was made. Together with the profiling, depth was measured with the probe pressure sensor, and giving exact depth for each second of descent and ascent. The average descent speed was computed by plotting depth vs time. At some stations this function was working well, and depth could be measured against time. In the station were one of the transducers were pointing downwards (120 kHz), the depth markers in LSSS gave usable information, together with the data from the depth sensor. With the sideways profiling, the depth markers in the echogram were used to measure the distance away from the probe. For the data on the 30th November, depth sensor data were lacking. As the transducer on 120 kHz were pointing downwards and, on this station, we were able to locate the bottom echo as a function of time (Fig.2.4.5). By studying the echogram from 120 kHz, there were also a possibility to check if the lowering speed were constant. By locating when the probe reached the bottom, and knowing the starting time of the descent, the average speed could be calculated. First the depth sampled is divided on the total seconds surveyed. With the lowering speed available the possibility to find the time the probe uses to profile 10 meters. Since the ping rate is readable directly in LSSS, and grid is established by how many pings have been transmitted for each 10 meters of descent. All calculations of grid sizes are found in Appendix III.

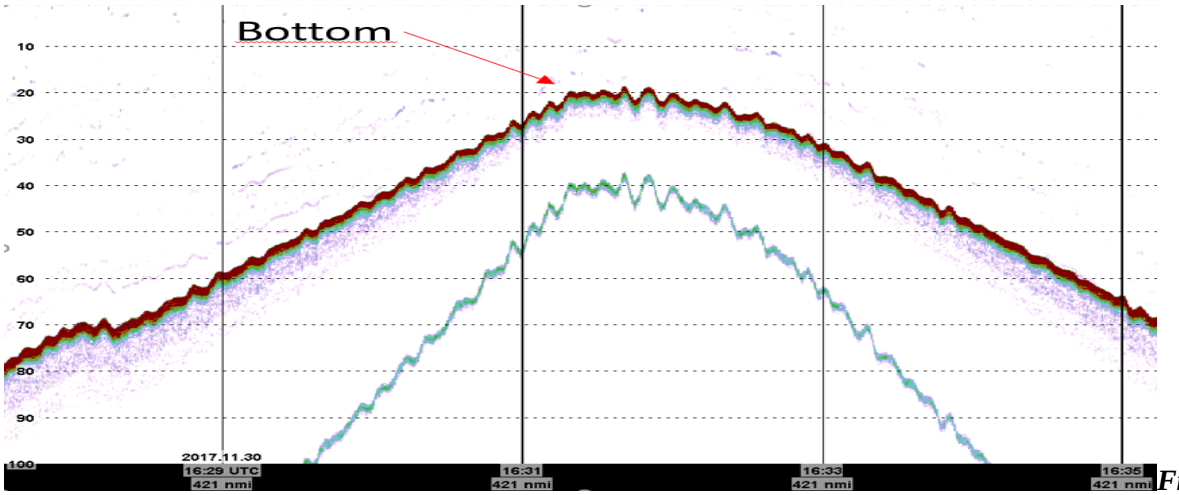

Figure 2.4.5. *Echogram from 120 kHz showing the appearance of the bottom echo during probing. This can give information about when descending ended, and the start of ascending*

Station number (date)	Time duration UTC	depth (m)	Lowering speed ms^{-1}	Grids size (Pings)
1 (November 25th)	18:31-18:40	90-160	NA	NA
2 (November 29th)	12:42-13:00	10-550	0.5	90
3 (November 30th) (1st profiling)	11:11-11:58	10-761	0.267	75
3 (2nd profiling)	12:47-13:32	10-761	0.274	73
3 (3rd profiling) Data were recorded during ascension	16:31-17:19	10-764	0.265	150

The probing data were scrutinized in the same manner as the ship data, but the approach was different. In the first station the probing data were only scrutinized from 80 to 170 meters down.

Since the density and measurements repeats itself in the range direction, scrutinizing took place 10 to 30 meters from to the probe. The ping plot were used in the same manner to separate targets as with the vessel data. While the vessel data usually had 10 measurements for each depth cells, the probing data had normally two, 10-20 m away from the probe, and 20-30 meters away from the probe. This ensures two objectives, high resolution, and at 20 meters away from the probe, avoidance from the probe itself have not been observed. This means that measurements further away from the probe, will just repeat the same measurement.

2.5 Conversion to density estimates

2.5.1 Ship data

The scrutinized data were then extracted using LSSS, ListUser11-format. These files were exported to Excel. The measurements are in this format split in different pelagic channels. These data then represent a depth layer of 10 meters where the NASC-values are averaged for approximately one and a half minute. Average Backscattering were calculated for each depth channel and plotted against depth in Excel for the whole volume sampled. A NASC-value is just a measurement value for the mean gathered acoustic energy for the volume, in order to obtain a more precise distribution on the depth distribution of mesopelagic fish, information on the reflection property of the mesopelagic fish was added

2.5.1.2 Biomass conversion for vessel data

Abundance and volume density were estimated both for ship and probe data. The formula for measuring area density is described in the introduction. For measuring density, a parameter for backscattering cross section is needed. Since there is no catch data from these areas, and there is up to date no 20 log l formula for pearlsides and glacier lanternfish, the target strength calculated in (Scoulding et al., 2015) were used. Assuming there were an even mix between pearlsides and glacier lanternfish, the TS for them were averaged. For copepods, the target strength for 3 mm copepod at 200 kHz from (Stanton et al., 2000) were used.

Table 2.6.1. *TS-values taken from (Scoulding et al., 2015) used to convert s_A values to biomass*

Frequency kHz	18	38	70	120
Target strength B Glaciale dB	-54.2	-62.1	-64.5	-65.6
Target strength M.Muelleri dB	-53.6	-60.8	-62	-62.9
Backscattering cross section B. Glaciale	$4.77*10^{-5}$	$7.74*10^{-6}$	$4.45*10^{-6}$	$3.46*10^{-6}$
Backscattering cross section M.Muelleri	$5.48*10^{-5}$	$1.04*10^{-5}$	$7.92*10^{-6}$	$6.44*10^{-6}$

Average backscattering cross section both species	$5.13*10^{-5}$	$9.10*10^{-6}$	$6.19*10^{-6}$	$4.95*10^{-6}$

Table 2.6.2 *TS-values for a 3 mm copepod taken from (Stanton et al., 2000)*

Frequency kHz	200
Target strength for copepods (dB)	-110
Backscattering cross section copepods	$1.25*10^{-10}$

Then the procedure described in section 1.1.3.3 were followed. The target strength was converted to the backscattering cross section, then averaged between the backscattering cross section of pearlside and glacier lantern fish,

$$\sigma_{bs} = 4\pi * 10^{\left(\frac{TS}{10}\right)} \qquad (17)$$

When the average backscattering cross section is known, area density (ρ_a) were calculated by using formula 14. In this study the volume density of animals were of interest, and the formula for density formula (15) were applied, to calculate individuals/m^3.

2.5.2 Probe data

After the preparation and scrutinization of the probing data, they were exported using ListUser11-format in the same way as the ship data. In the probing data, two measurements were averaged. This was chosen due to the high resolution of targets in the area 10-30 from the probe. The average of these measurements was made and plotted against depth cells of 10 meters in the same manner as the vessel data. In the probe investigations, also *in situ* target strength were continuously measured from the probe. For each station, the average target strength was measured in the layers in front of the probe. TS-measurements were conducted in all layers were mesopelagic fish were scrutinized. The target strength filters are more closely described in chapter 2.5.2.1. These values were extracted from LSSS by using the export function for TS-data and were exported to Excel for

averaging. Since TS is in a logarithmic unit, it was converted to linear mode before averaging (See formula 17). This formula was applied for all the measurements before averaging. Then the mean was converted back to decibel,

$$\mathrm{TS} = 10 * log_{10}(\frac{\sigma_{\mathrm{bs}}}{4\pi}) \qquad (21)$$

In the deep profiles, mean target strengths from 38 kHz to 70 kHz were calculated for each layer. Once whilst the probe was descending, and again while ascending. The 120 kHz system were mainly used as a bottom detector. In the sample at 25th November 2017, 38, 70 and 120 kHz systems were applied.

2.5.2.1 Single target detection filters (SED-filters).

Target strength measurements were collected with the TS-probe at different locations. To be recognized as a single target, some criteria must be met, in order to distinguish real targets from noise and multiple targets inside the pulse volume. First the minimum TS whereas targets are identified. If an echo is lower than a set target strength, the echo is not accepted. This value is usually used to exclude smaller organisms, but in this case the organisms in the mesopelagic community is usually weak targets, thus a fairly low threshold was applied. For the recognition of single targets, a specific length of the echo should be met. This upper limit is usually set from 1.8 times the pulse durations for covering large targets which tends to stretch the received echo. If the echo is much longer than the transmitted pulse, there is a probability that there are several targets accepted as one. To exclude such targets, if an echo exceeds a reference value it is not accepted. When a single target is detected, the position of the targets is measured by the phase angle in the split beam system. The phase angles may be stable throughout the pulse for a clean, single target. If there are two or several targets at the exact same distance, but in different parts of the in the beam, the phase angles will vary. A stable phase angle is needed in this filter. Targets are usually located randomly across the acoustic beam, and targets are weaker thus further from the acoustic axis. This is accounted for by the split echo sounder, but the maximum gain compensation is set

for the valid part of the beam, where the calibration is valid. Targets too close to each other are also rejected. In all target strength extractions these filters were applied:

Table 2.6.2. *Filters for target strength measurements*

Min TS (dB)	-70 dB
Pulse length determination level (dB)	6
Min echo length	0.8 (Relative to pulse duration)
Max echo length	1.8 (Relative to pulse duration)
Max gain compensation	6 dB
Do phase deviation check	yes
Max phase deviation	8 (Phase steps)

2.5.2.2 Biomass conversion for probing data

The direct target strength was applied. The in-situ target strength measurements are used directly in the estimation. The target strength is converted to backscattering cross section (σ_{bs}). The depth cells created in the probing data were 10 meters. In the biomass conversion the backscattering cross section from the target strength measurements were used, but the formulas for calculating density were the same as the vessel data. In the profiles were sideways transducers were applied, both NASC and TS had to be measured sideways.

2.6 Analysis of stereo camera photos

The camera mounted on the probe were used together with the profiles. By using the exact time photos are taken, depth could be measured. Photos of interest were further analysed. Siphonophores were keyed to the closest family with the help of Dr Aino Hosia from University of Bergen (UiB). Observations of siphonophores were plotted against depth. Photos were also used to give insight of the planktonic community in the different layers. Mesopelagic fish and other photos of interest were also noted

3 Results

Echograms from the vessel data were converted to density estimates by using the literature values for TS and σ_{bs}. The output from each station were a vertical profile where the mean density was measured for each depth cell of 10 meters. This gives an insight of where the majority of the scatterers is in the sampled volume. At the vessel stations, vertical measurements were repeated several times for one nautical mile. The standard deviation was calculated from the mean and plotted as error bars in the vertical profile. Most of the volumes investigated had two distinct layers. One thinner layer often located in the upper 200 meters, and one deeper layer which usually were located between 400 and 600 meters depth with the exception to the station in Vestfjorden, where the bottom depth were less than 400 meters. A typical example of the distribution of scatterers in the samples at Vøringplatået is shown in (Fig.3.1). Both layers backscattering properties were weak, with echoes from small fishes. Usually the biomass was very low in the volume between the two layers, shown both in the echogram and vertical profile. The distribution is typical as described in (Giske et al., 1990), where both pearlsides and glacier lanternfish are present, and the pearlsides usually distributes in the upper layer, glacier lanternfish are found below 250 meters.

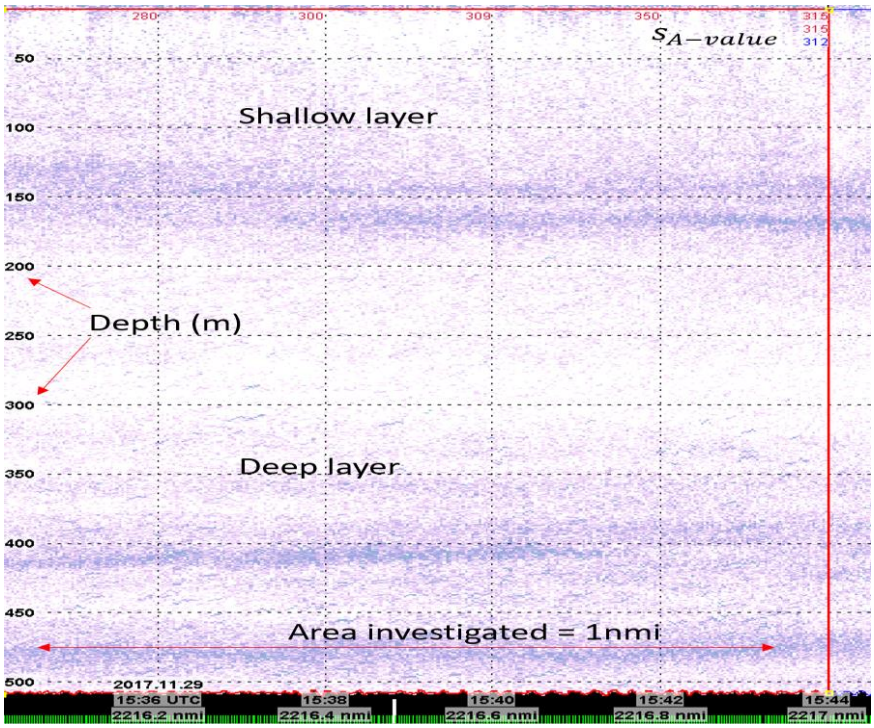

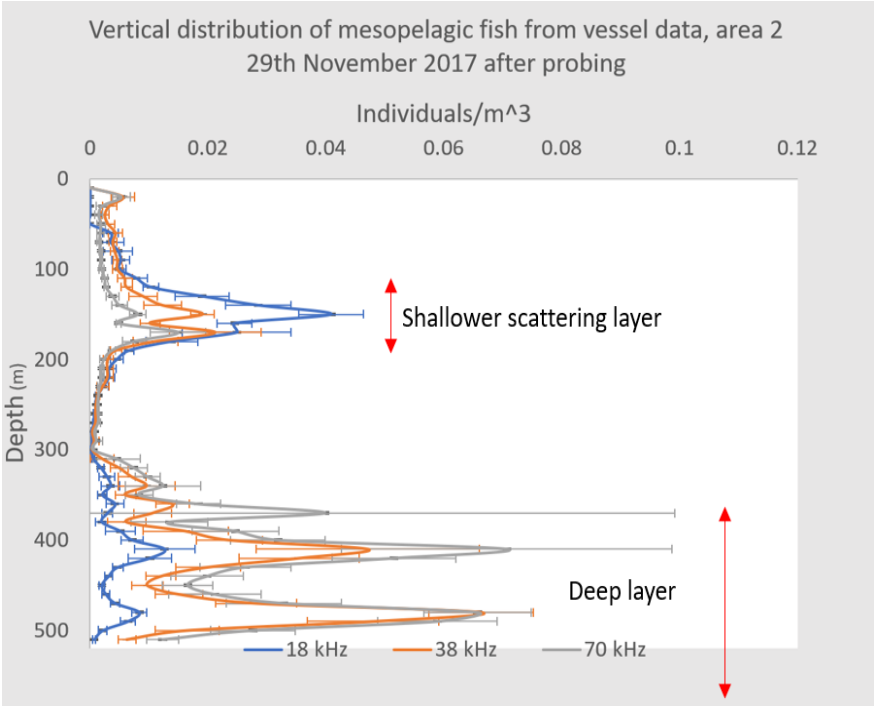

Figure 3.1. *Echogram, and corresponding depth profile from the same area. Both echogram and graph show two layers where the majority of the scatterers distribute. One layer stretching from 100-200 meters depth, and one from 350-500 meters. The biomass in the deep scattering layers have three peaks in biomass, while the shallow scattering layer only have one.*

The density was measured by using a reference value, which were averaged in (Scoulding et al.,2015). The measurements from that study were performed in another location, and possibly at a different depth. The precision of the abundance estimates depends on the accuracy of the reference value. In all the probing samples, TS and σ_{bs} were collected simultaneously, with the backscattering from the different layers.

3.1 *In situ* target strength measurements

The results of the target strength measurements showed differences from literature values used in the vessel data (Table 3.1). At 38 kHz the target strength had a range between -55 to -59.7. At 70 kHz the mean TS were weaker, but less variable than 38 kHz. In (Scoulding et al.,2015), the mean TS for 70 kHz were between -62 to -64.5 for the two species of mesopelagic fish, while in these measurements, the mean TS varied between -59 to -63 dB. The TS measured in the station 1, were the all the transducers were mounted vertically, the TS for 120 kHz were more than 3 dB higher

for pearlsides and close to 6 dB higher than glacier lanternfish. All the measurements display a higher measured TS than the value taken from literature. Notably the literature values were measured dorsally and, and these measurements were for the most part done ventrally. The measurements done in Vestfjorden with all transducers mounted vertically, the measured target strengths close to -59 dB at all frequencies (Fig 3.1.1). At probe station 3, November 30th, 2017, all measurements at 38 kHz were normally distributed with a mean TS close to -55 dB (Fig.3.1.3). These measurements are more than 6 dB higher than the literature value used for measuring mesopelagic fish. These measurements were used directly together with the backscattering values for each station. In the parentheses, the number of measurements for each station are mentioned. The mean target strengths represent the mean of these values converted to linear form, before converted back to its logarithmic units. TS was always applied together with the same samples backscattering. Not all my TS measurements can be compared with the literature value, since the measurements are done in lateral form.

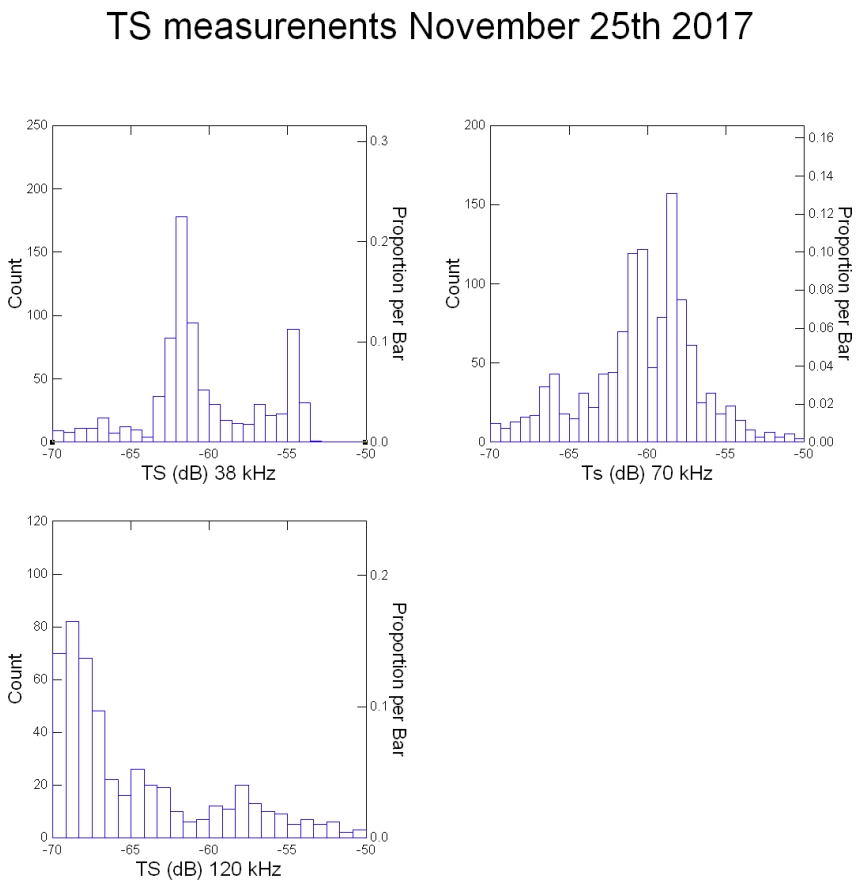

Figure 3.1.1. *Target strength distributions from the probing station, November 25th, 2017. TS in dB are plotted at the x-axis, the number of measurements at the left y-axis, and the proportion each measurement contributes to the whole sample at the right y-axis.*

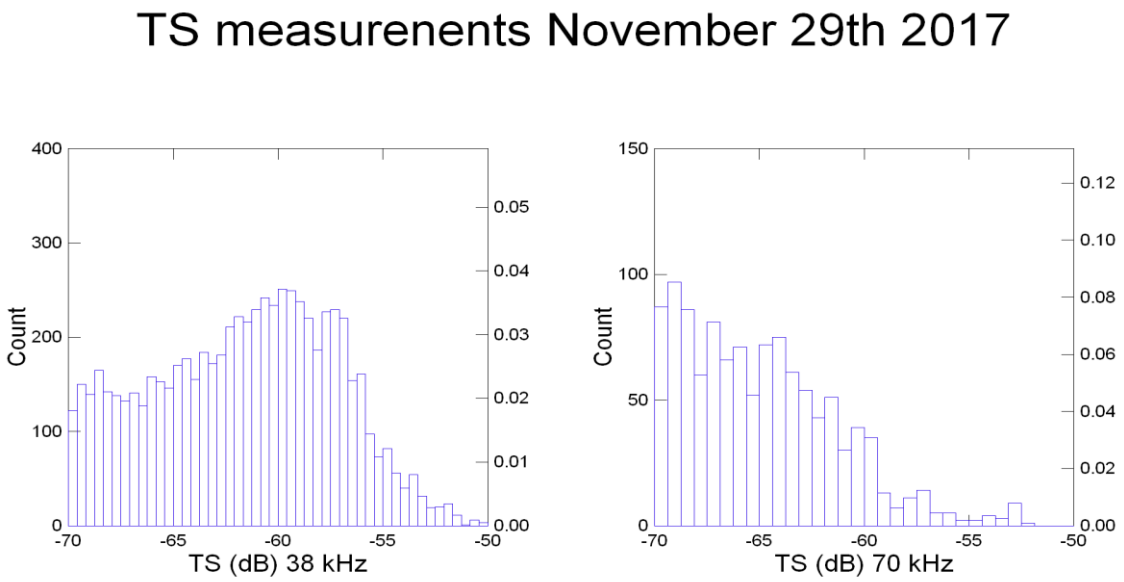

Figure 3.1.2. *Target strength distributions from the probing station, November 29th, 2017. TS in dB are plotted at the x-axis, the number of measurements at the left y-axis, and the proportion each measurement contributes to the whole sample at the right y-axis*

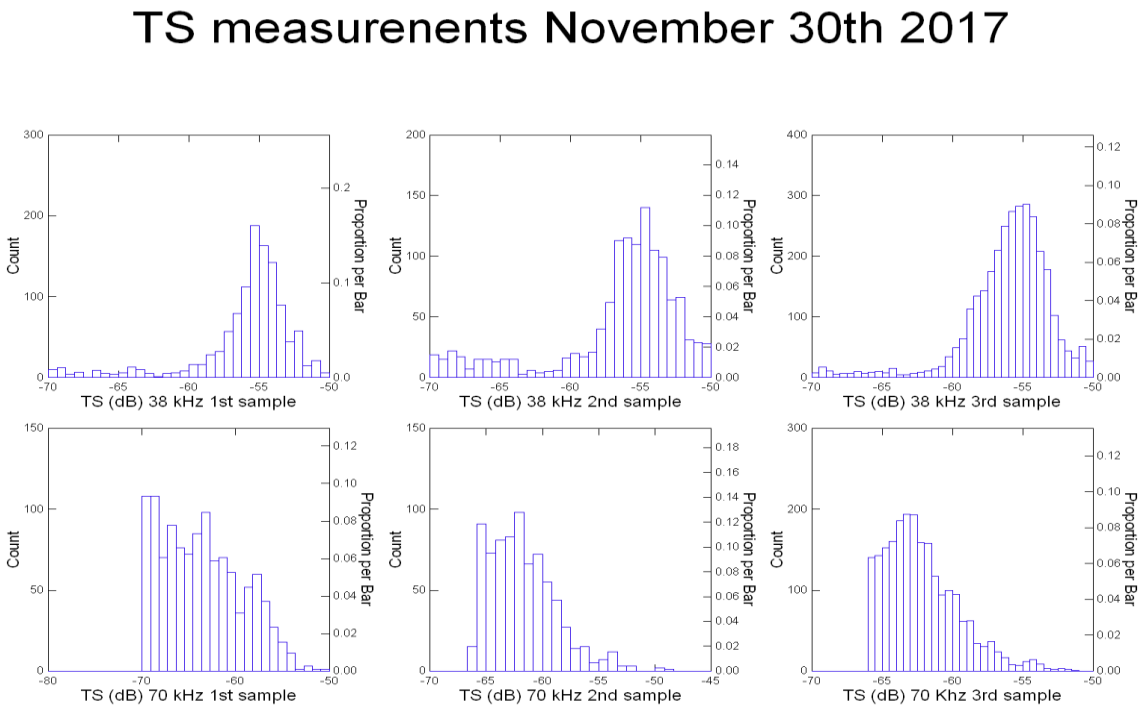

Figure 3.1.3. *Target strength distributions from the probing station, November 30th ,2017. TS in dB are plotted at the x-axis, the number of measurements at the left y-axis, and the proportion each measurement contributes to the whole sample at the right y-axis*

Table 3.1. Target strength distribution for each area. N= number of measurements for each sample. Samples was either measured with dorsal or ventral looking transducers.

Date	**Time UTC**	**Dorsal/ ventral**	**Longitude (deg)**	**Latitude (deg)**	**Day night**	**TS 38 kHz dB (n)**	**TS 70 kHz dB (n)**	**TS 120 kHz dB (n)**
November 25th, 2017	18:31-18:38	Dorsal	15.2705	68.114	Night	-58.9 (791)	-59.0 (1204)	-61.2 (496)
November 29th, 2017	12:40-13:02	Ventral	6.625	66.612	Dusk	-59.7 (4129)	-63.0 (1135)	NA
November 30th, 2017 1	11:17-11:56	Ventral	6.544	66.616	Day	-54.9 (1170)	-61.4 (1150)	NA
November 30th, 2017 2	12:56-13:27	Ventral	6.544	66.616	Dusk	-55 (1300)	-62.9(931)	NA
November 30th, 2017 3	16:39-17:16	Ventral	6.544	66.616	Night	-55.2 (3176)	-62.4 (3095)	NA

3.2 Density estimates of mesopelagic fish, vessel vs probe data

Estimates of ρ_v fish were plotted against depth. The depth was plotted on the y axis, and the density of fish per cubic metre were plotted on the x-axis. Error bars were made for the vessel data where the estimate was an average of several repeated recordings. Vessel data, and probing data were compared using a Wilcoxon signed rank test. The rank test is a non-parametric test, which determines if the population mean rank differ. In this case, density estimates from the vessel data were ranked with the probing data. Measurements from the same depth were used in the rank test. Usually the vessel data measurements were limited down to 500-600 meters due to the way data were stored in EK80. Data were compared only to this depth, but by studying the probing stations. Even though the probing data had a longer range of measurements, by studying results there are no evidence for any major scattering layer below 500 m (Fig. 3.2.3-3.2.9.) Data for all frequencies measured were compared in MYSTAT. When performing the rank test, the critical value was selected as 0.05, and these hypothesises were made:

H_0= there are no difference between the probing data and the vessel data.

H_A= there is a difference between the probing data and the vessel data.

All results from the rank tests are found in Appendix II. In these plots, all the backscattering was allocated to mesopelagic fish, and the presence of siphonophores and other scatterers which have the similar echo as mesopelagic fish were not accounted for. These targets are difficult to separate from mesopelagic fishes, as they exhibit the same backscattering pattern in the frequency domain and in amplitude.

3.2.1 November 25th, 2017

The measurements show on the vessel data a relatively similar distribution of mesopelagic fish on 38, 70 and 120 kHz (Fig. 3.2.1). The peak in biomass were all located at 150 m depth. The lowest peak was measured at 18 kHz, with a density estimate of 0.06 fish/m^3, while the highest estimate was twice as high at 120 kHz, with 0.12 fish/m^3. 38 and 70 kHz measured similarly with a peak of 0.1 fish/m^3 fish. A possible reason for the high estimate at 120 kHz, could be the inclusion of zooplankton with a volume scattering strength than –70 dB. The biomass is present from 50 to 150 meters, but the density decreases rapidly below 150 meters.

The measurements on the probing data show that the biomass measured are smaller than in the vessel data, and with $p<0.05$ there is a significant difference between the data at 38 kHz (Table 3.2). At the vessel data, and this is scrutinized as mesopelagic fish, while in the probing data, the thresholding process becomes easier. In the vessel data, the density is as 0.1 fish/m^3, while in the probing data the highest values are 0.05 fish/m^3. In the probing data, 38 and 120 kHz measures similarly, but it appears to be a higher biomass measured at 70 kHz both in the same layer as the other two frequencies, but there is also a layer with 0.04 fish/m^3 at 100 meters depth(Fig 3.2.2.).

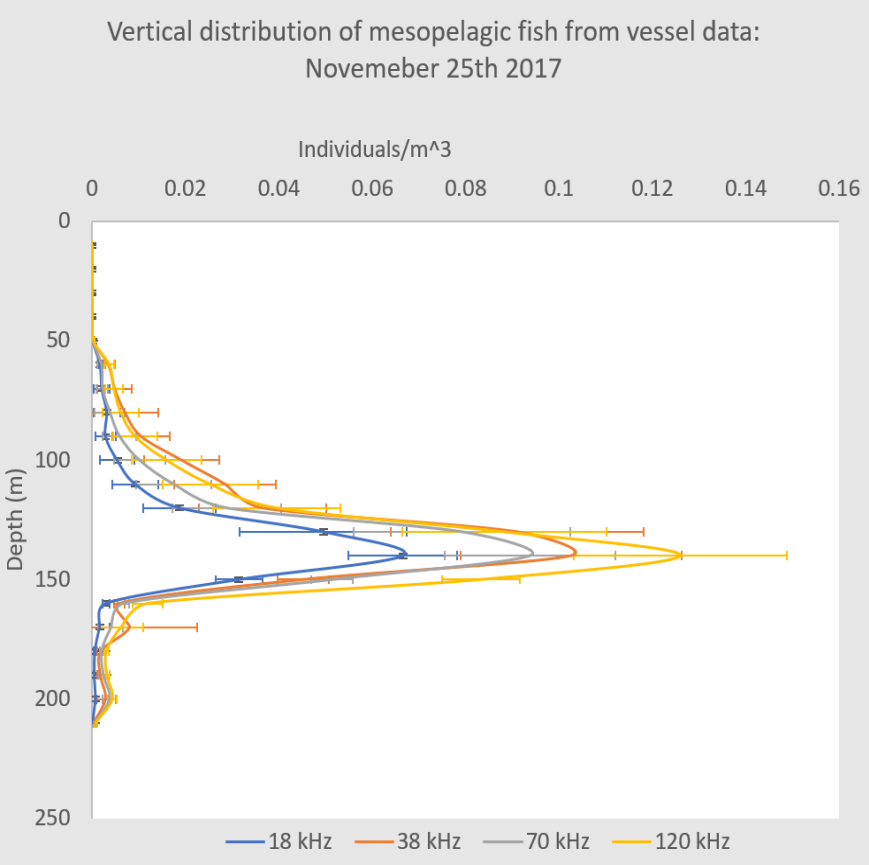

Figure 3.2.1. *Density distribution of mesopelagic fish measured at 4 frequencies. The error bars represent the standard deviation for each 10-meter depth channel. The depth profiles distribute in a similar fashion, with some differences in biomass estimates.*

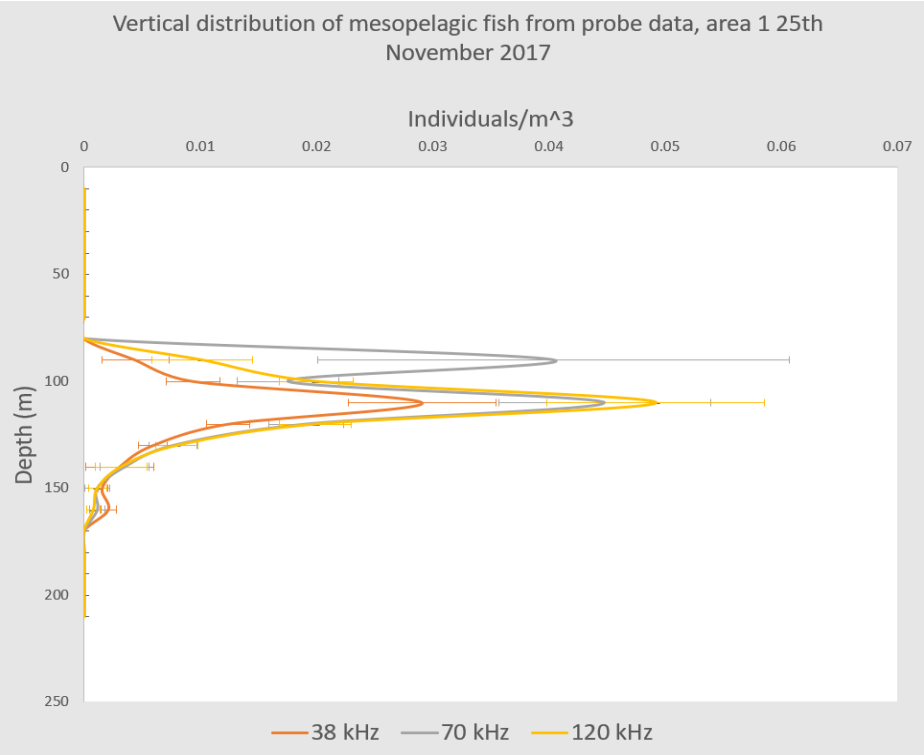

Figure 3.2.2. *Vertical distribution of mesopelagic fish shown on three frequencies. All the transducers were mounted vertically in this investigation. The volume sampled at this probing station were between 90-160 meters.*

Table 3.2. *Wilcoxon rank test for samples at November 25th.*

Frequency	P-value	Accept/reject 0 hypothesis
38 kHz	0.017	reject
70 kHz	0.327	accept
120 kHz	0.161	accept

3.2.2 29th November 2017

The density measured in the vessel data, show a denser shallow layer in the station before probing. This layer was present between 100-200 meters depth. (Fig3.2.3). This may be happening because the station was during dusk, and the dial vertical migration were starting. The measurements before probing, showed densities of 0.15 fish/m^3 at 38 and 70 kHz with error bars suggesting some outliers in the measurements. The deep scattering layer has a density of 0.05 fish/m^3. Notably the biomass is estimated to be very low compared to 38 and 70 kHz (Fig. 3.2.3).

In the second sample from the vessel data, after probing, the density of the upper layer had diluted, but targets seem to be more evenly distributed in more depth cells. The density is smaller in the shallow scattering layer with the highest value between 0.02-0.05 fish/m^3at 18, 38 and 70 kHz. It appears that there is a higher biomass at 18 kHz after probing. There is a smaller layer between the two scattering layers in the probing data, this possibly fish displaying several migratory behaviours, since the probing were done during dusk (Fig.3.2.4).

At the probing station, biomass was measured in all parts of the water column. With $p<0.05$ in both stations at 38 kHz there is a significant difference between the vessel and probe data (Table. 3.3). In the shallow scattering layer, the density is measured to 0.06 fish/m^3 at 70 kHz and 0.02 fish/m^3 at 38 kHz. In the DSL there are two peaks at 70 kHz at 350 and close to 500 meters at 70 kHz with densities from 0.04 to 0.05 fish/m^3. At 38 kHz there are one peak above 500 meters at 0.04 fish/m^3. While there are more distinct layers in the vessel data, the biomass appears to be more dispersed in to several layers both at 38 and 70 kHz (Fig 3.2.4). The probing was performed during dusk and vertical migration might influence the results.

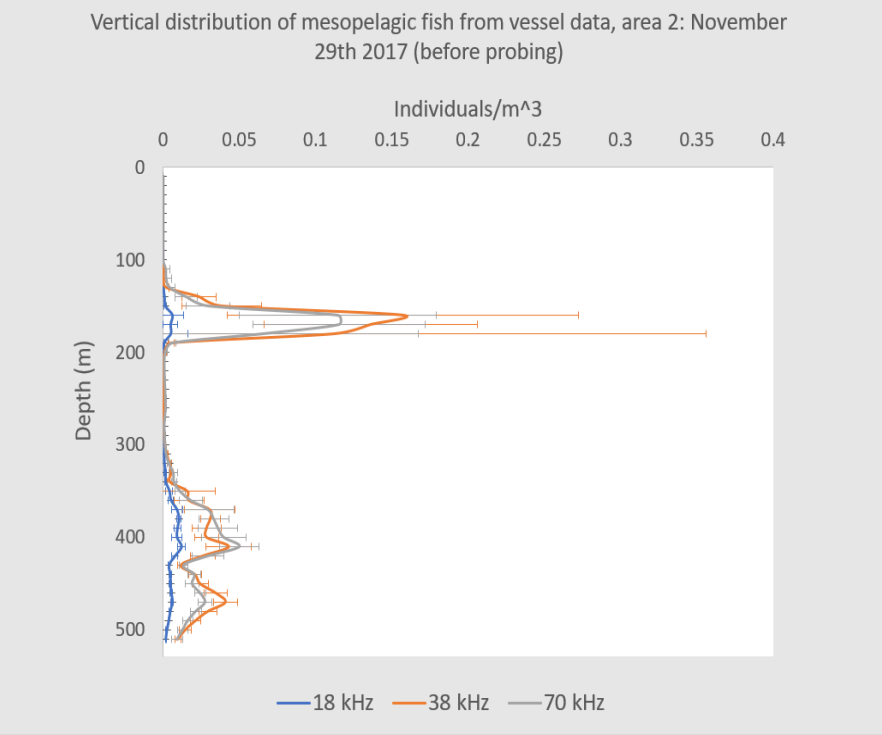

Figure 3.2.3*. Vertical distribution of mesopelagic fish down to 500 meters on three frequencies. Notably there is a denser layer in the upper 200 meters.*

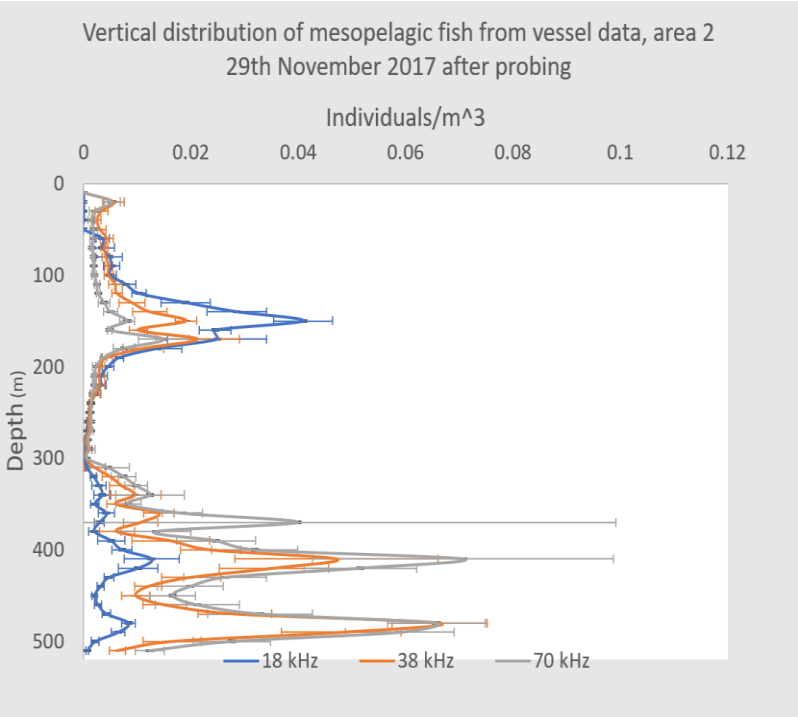

Figure 3.2.4. *Vertical distribution of mesopelagic fish on the vessel station after probing. The shallow scattering layer has diluted as described in (Fig. 2.2.5.) in material and methods.*

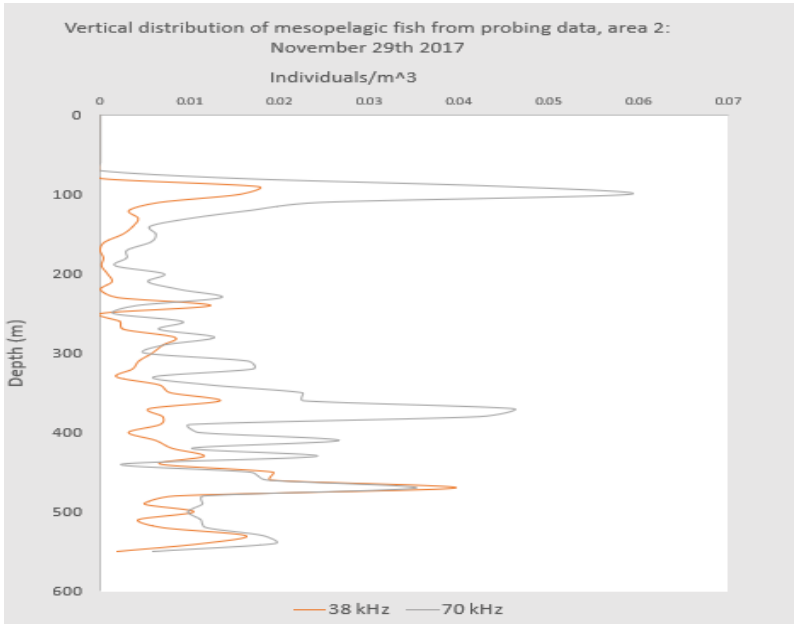

Figure 3.2.5. *Vertical distribution of mesopelagic fish measured with TS-probe profiled from 10-550 meters depth. Transducers with frequencies 38 and 70 kHz were mounted horizontally, and fish were measured from 10-30 meters away from the probe.*

Table 3.3. *Wilcoxon signed rank test results*

Before/after probing	Frequency	P-value	Accept/reject h_0
Before	38	0.007	Reject
Before	70	0.4.91	Accept
after	38	0.001	Reject
after	70	0.881	Accept

3.2.3 30th November 2017

The vessel sample were done during night, and there are two clear layers. One shallow scattering layer with densities up to 0.08 fish/m^3, measured at 38 and 70 kHz between 100 and 200 meters, and one layer with the density of 0.02 fish/m^3 between 300 and 500 meters, and some smaller aggregations close to the surface (Fig. 3.2.6). The measurements at 38 and 70 kHz are almost similarly distributed, while the measurements at 18 kHz becomes less dense with depth.

In the first probe sample, the density is similar in the deep scattering layer at 38 and 70 kHz with densities up to 0.02 fish/m^3, but the shallow scattering layer are several times stronger on 70 kHz than 38 kHz with 0.025 fish/m^3 to 0.005 fish/m^3 (Fig 3.2.7). This profiling was done during sunlight and could explain the low biomass in the shallow scattering layer, due to the main biomass might be distributed at greater depths.

The second profiling was done during dusk, and the biomass does not form as distinct layers as with the first profiling. The biomass seems to be more dispersed in all the parts of the water column, from 600 meters and up to 100 meters. Biomass estimates peaks with fish densities of 0.035 fish/m^3 at 70 kHz at 500 meters depth and, a notable difference between frequencies at the shallow scattering layer measuring 0.02 fish/m^3 at 70 kHz, and 0.005 fish/m^3 at 38 kHz (Fig 3.2.8).

The third profiling were conducted during night, and it is evident that a migration maybe has taken place. There are stronger measurements at both 38 and 70 kHz in the upper 200 meters, while the biomass in the DSL are lower than in the previous profiles. Especially at 70 kHz there are several layers both close to the surface and down to 200 meters with densities of 0.06 fish/m^3(Fig. 3.2.9). The results of the Wilcoxon rank test suggest with a $p<0.05$ in all samples at 38 kHz that there is a difference between the vessel data and the probe data. At 70 kHz, $p<0.05$ for the first two stations

while p>0.05 at the last station (Table 3.4). In all three probing stations there is a layer of biomass in the upper 200 meters at 70 kHz, while only present at 38 kHz in the third profiling.

3.4.1 vessel data

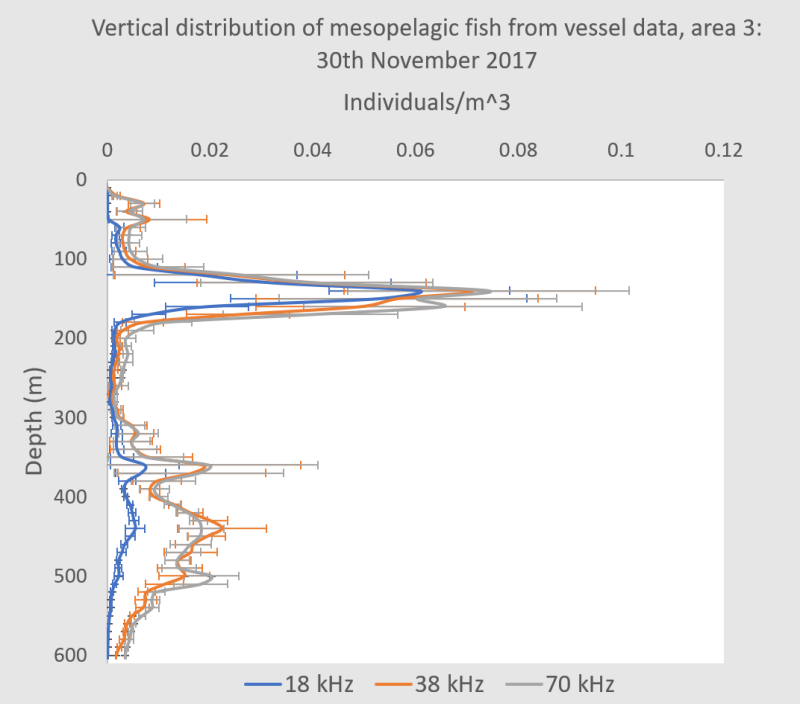

Figure 3.2.6. *Density of mesopelagic fish on three frequencies from vessel data 30th November 2017. As in the vessel data from 29th October, the layer with the highest density measured were the shallow scattering layer.*

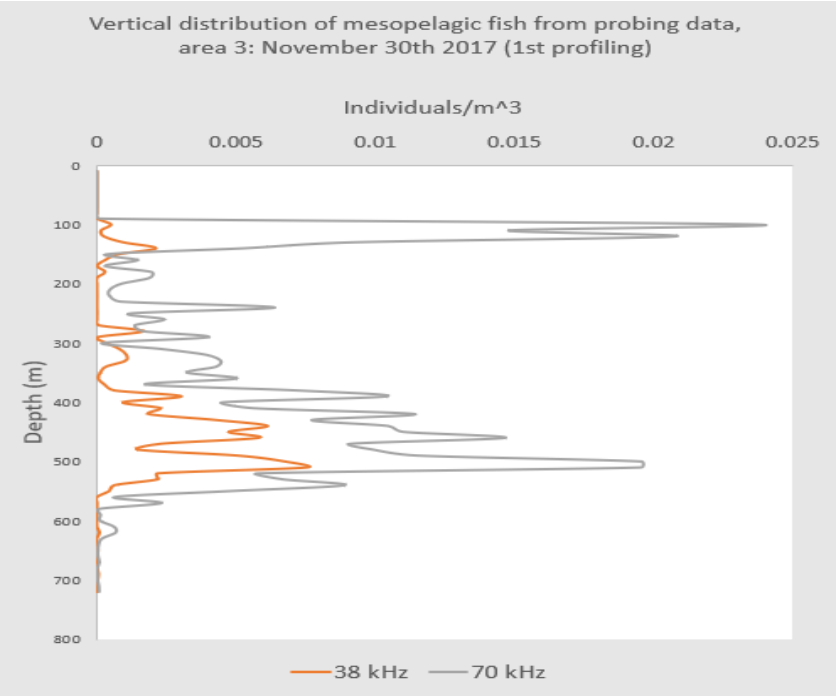

Figure 3.2.7. *Vertical distribution of mesopelagic from probing data, with frequencies 38 and 70 kHz mounted horizontally, during the first profiling. Data was collected during sunlight from 10-761 meters depth.*

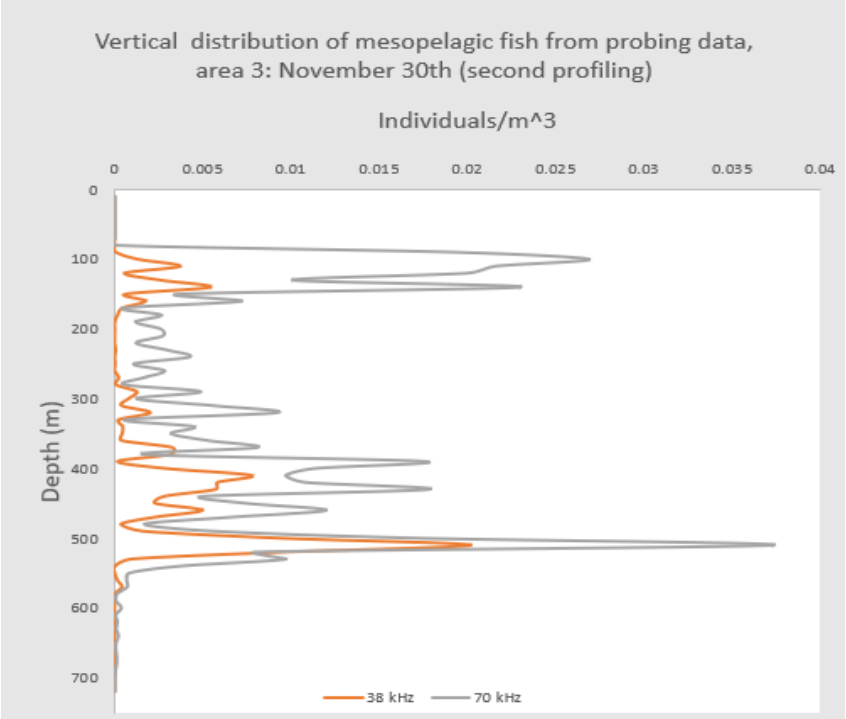

Figure 3.2.8. *Vertical distribution of mesopelagic fish from probing data, second sample, during dusk from 10-761 meters*

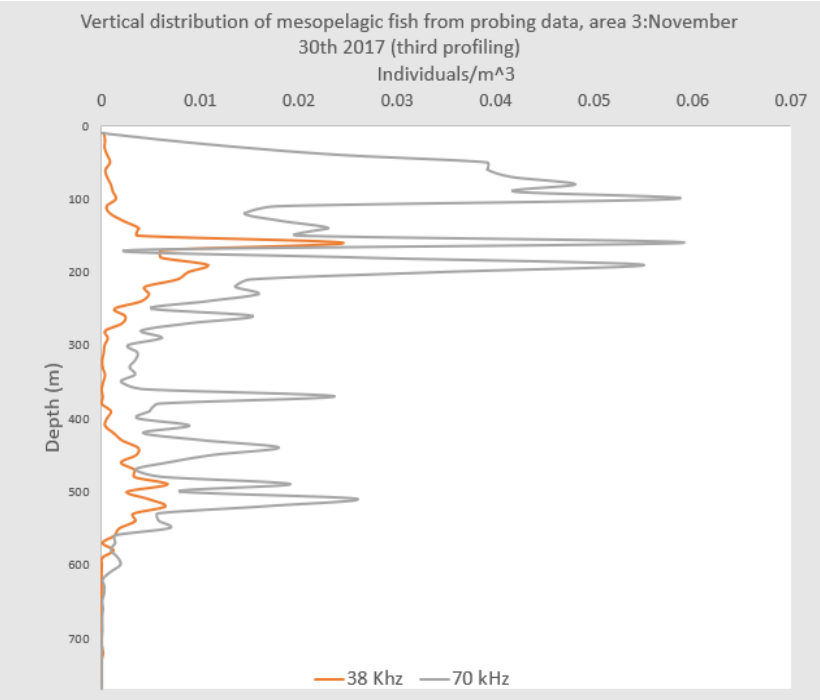

Figure 3.2.9. *Vertical distribution of mesopelagic fish from probing data, 3rd sample, at night from 10-764 meters. Notably fish were measured during the ascent of the probe at this sample.*

Table 3.4. Results of Wilcoxon signed rank test.

n Profiling	Frequency	P-value	Accept/reject h_0
1st profiling	38	>0.0001	reject
1st profiling	70	>0.0001	reject
2nd profiling	38	>0.0001	reject
2nd profiling	70	>0.0001	reject
3rd profiling	38	>0.0001	reject
3rd profiling	70	0.457	accept

At all stations the density of mesopelagic fish is fairly low, with even low densities in the scattering layers.

3.3 Photo observations

By using the stereo camera mounted on the probe opportunistically, some interesting observations were made. The aim was to take pictures of mesopelagic fish, and siphonophores at depth for comparing with echograms. The total number of photographs taken were 1654. Clear photographs of mesopelagic fish occurred only twice (Fig. 3.3.1), while several classes of zooplankton appeared. Glacier Lanternfish have been described as able to avoid an acoustic probe up to 7 m (Ona et al., 2018 in prep.), which can explain why only two clear pictures of mesopelagic fish were taken. Another problem with the stereo camera photos, were the lack of clear photos, many photos only showed reflections of some organisms, not in focus, and there is a possibility that some of these objects were mesopelagic fish. As shown in (Fig. 3.3.1) glacier lanternfish captured by the camera, reflects the strong flashes from the camera.

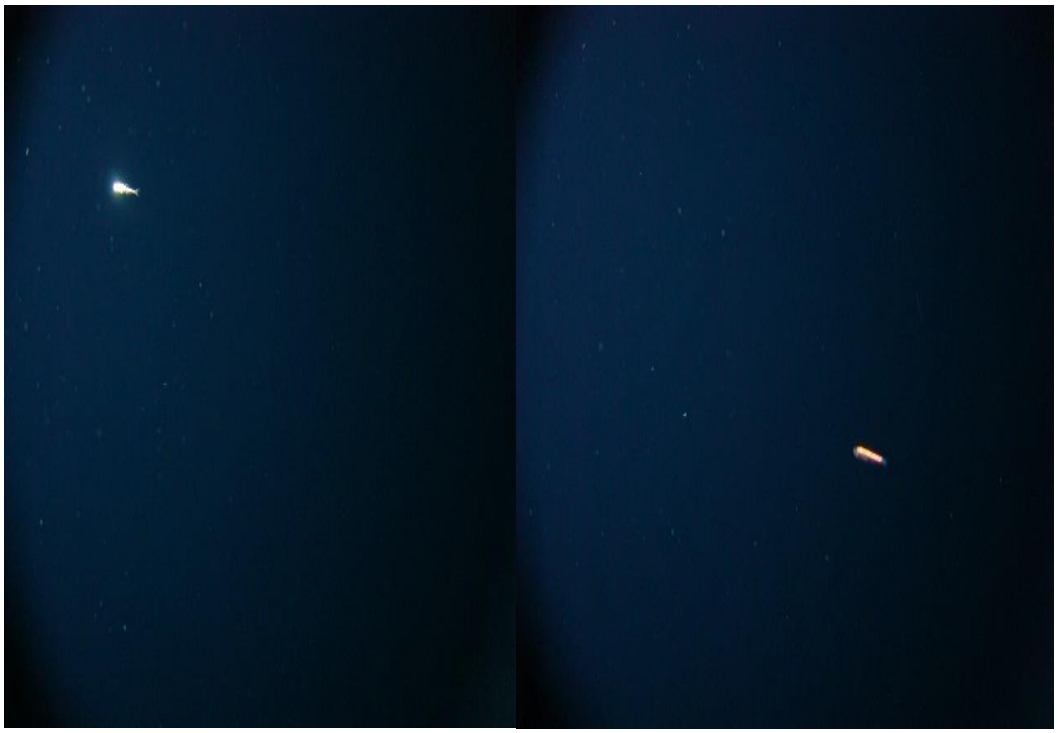

Figure 3.3.1. *Photo observations of a two glacier lanternfish taken in the middle of the DSL, at approximately 450 meters. The fishes show a strong reflection with a gold-like colour.*

Siphonophores were present at all sites in the photo sampling, and by using the time the photos were taken, observations could be plotted against depth. Due to the unclarity of the photos, all siphonophore observations were keyed to the family *Nanomia*. Siphonophores were present in both scattering layers, but also close to the surface, above the DSL and close to the

bottom below 700 meters. In the photo detections, they do not appear to distribute in one specific layer (Fig.3.3.2). Notably the 25th November the probe was only lowered down to 120 meters, and kept at that depth, and that could partly explain why there were only observations at that depth. Due to the unclear photos, pneumatophore size was not possible to measure. There were no indications of any dense layers of siphonophores as described in (Knutsen et al., 2018). Siphonophores present at all sampling sites at all depths, so this may suggest that they contribute to the backscatter measured in this study.

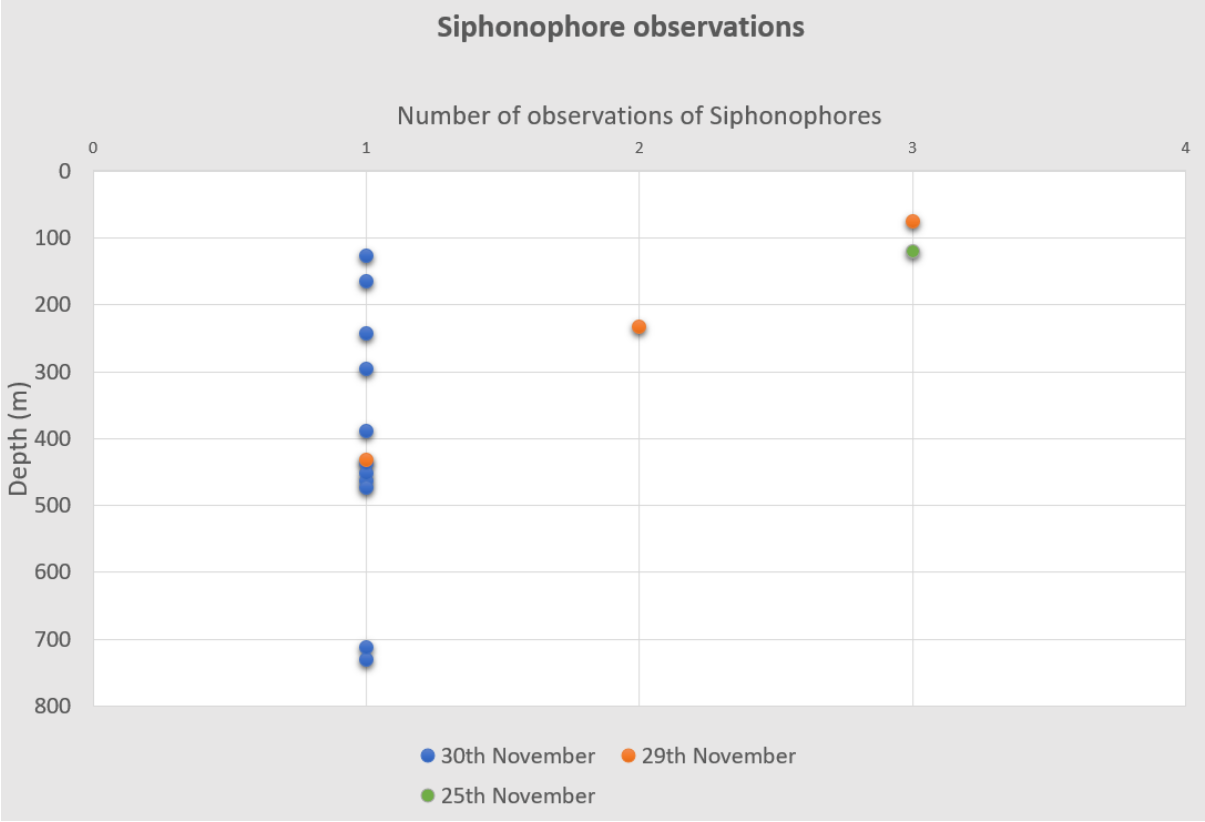

Figure 3.3.2. Number of siphonophore observations compared with depth. At November 29th and 30th observations were *made during the full profiling, while at November 25th the probe was lowered into the SSL. Siphonophores were observed from the surface down to 750 meters and were present throughout the water column.*

3.4 Peculiar observations at 70 kHz

At all probing stations, the biomass estimated were higher at 70 kHz. In the echograms there are targets on 70 kHz which are not visible on 38 kHz. These are single targets, with the same appearance of those in the deep scattering layers. Acoustic data were scrutinized in the same manner at both frequencies, but the density distributions were different (Fig.3.2.2, 3.2.5, 3.2.7, 3.28, and 3.29). Especially in the upper 200 meters these targets seemed to aggregate. This phenomenon is present at both site 2 and 3. By measuring the target strength of these organisms, it distributes around –60 dB, which excludes the possibility for it being a krill or other zooplankton without a gas inclusion (Fig.3.4.1). In almost all depth channels in the vertical profiles, biomass estimates were higher at 70 kHz. In all probe profiles targets are resolved as single targets, and the possibility that aggregations of weak targets having a higher S_v than –70 dB is low. Notably in all three profiles in station 3, there are biomass registrations between the two described scattering layers at 70 kHz while there is nearly none at 38 kHz.

Below is an example from probing station 2, 29th November 2017, where there is a low distribution of targets at 38 kHz and a high density at 70 kHz between 0-200 meters depth (Fig.3.4.1). The targets are appearing very close to the probe, with no sign of avoidance. By using the stereo camera, physonect siphonophores were appearing at the same depths (Fig 3.4.2).

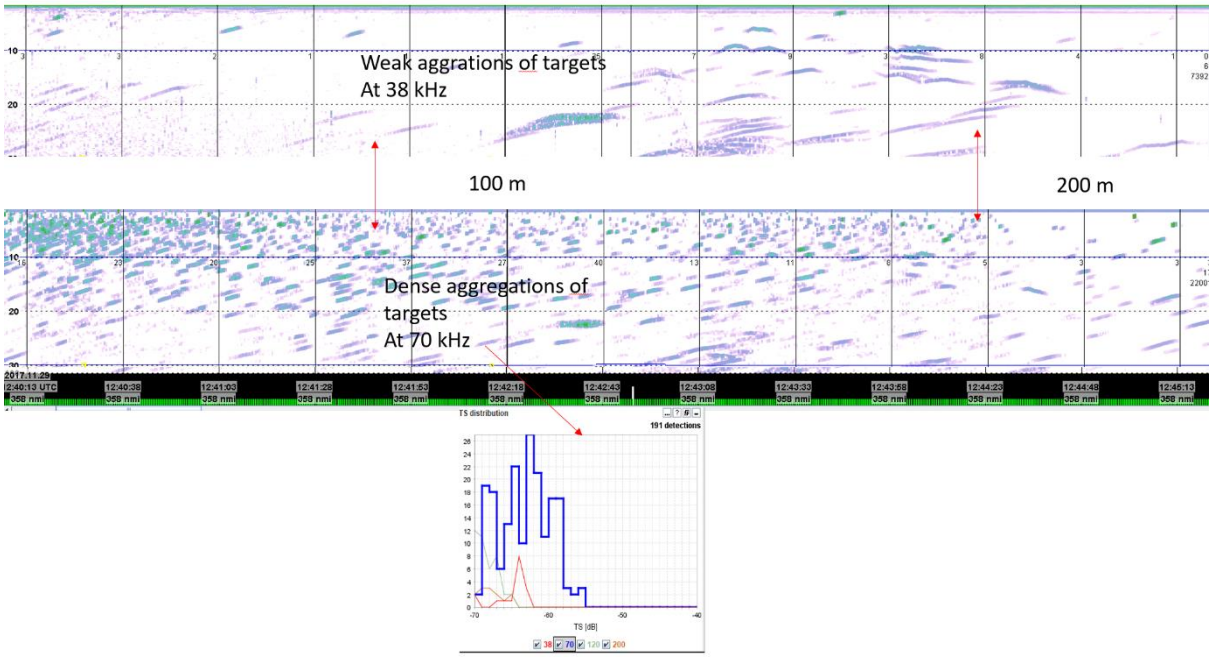

Figure 3.4.1. *Two echograms showing the same part of a depth profiling. The echogram at 38 kHz, displays few targets, while the echogram at 70 kHz shows several strong targets. The target strength distribution in this sample shows that there are stronger targets in this aggregation. These targets aggregate densely, also close to the TS-probe and seem to be non-avoiding*

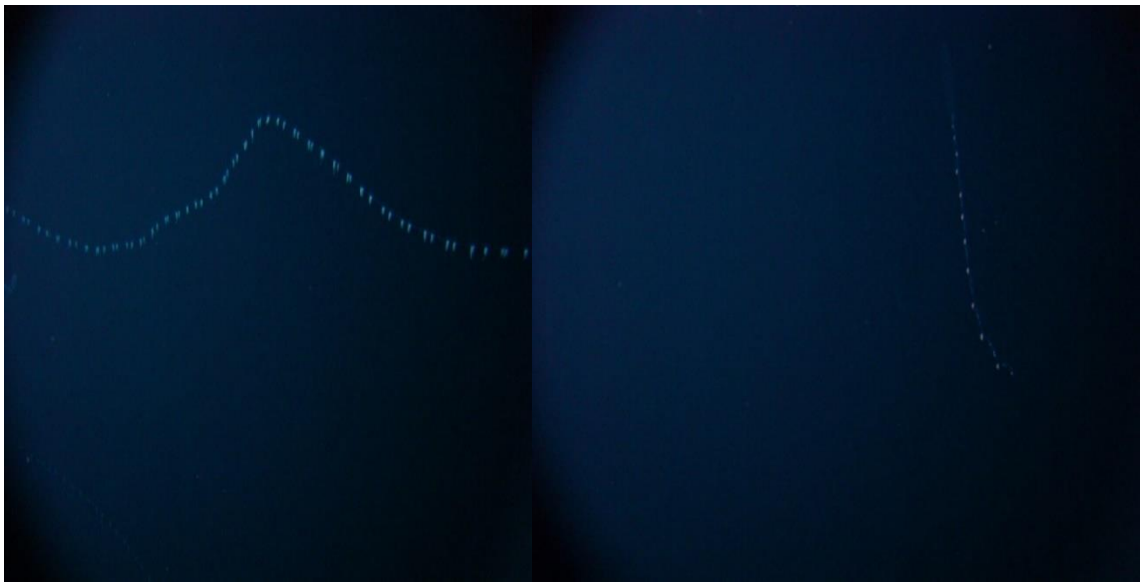

Figure 3.4.2. *Photographs taken by the stereo camera at 75 meters depth, showing three physonect siphonophores*.

This phenomenon was also observed in Vestfjorden (Ona et al., 2018 in prep.). By investigating a layer on three different frequencies, multiple strong targets, not present at 38 kHz, appeared on 70 and 120 kHz, which led to a backscatter several times higher(Fig.3.4.2). By the first look from the vessel data, this appeared to be a classic shallow layer inhabited by pearlsides (Giske et al., 1990). By drawing a school box around these targets, the average TS were extracted. In this case targets were found with TS about -60 dB at the three frequencies. In this case the scattering properties of these organisms suggest that they could be a different target than pearlside. When investigating this layer, two images of physonect siphonophores were captured (Fig. 3.4.3).

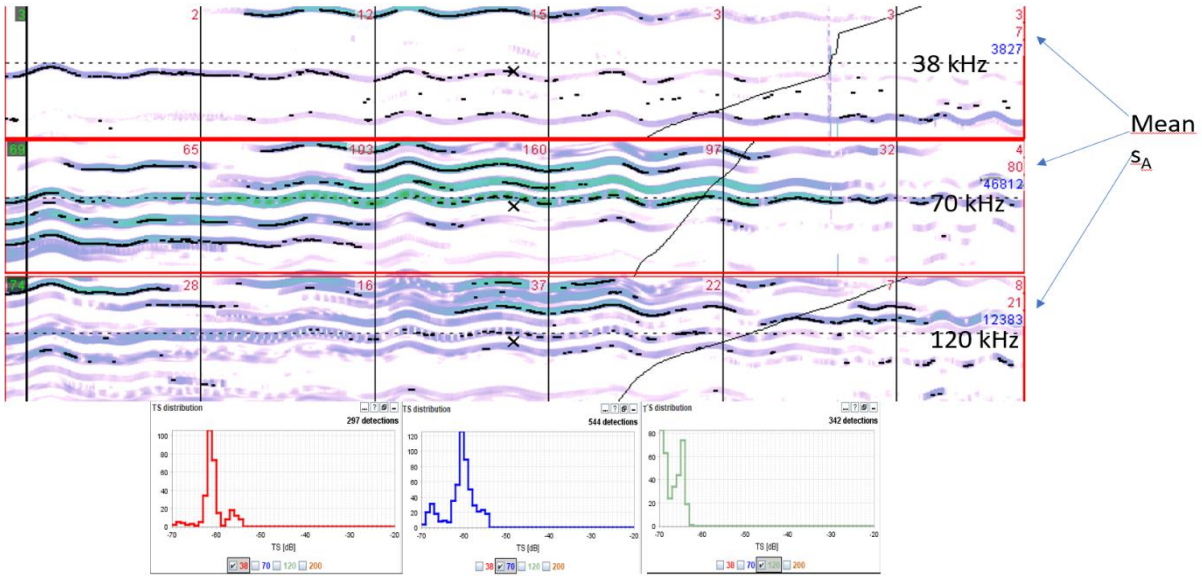

Figure 3.4.3. *Echograms from a selected area from the first probing station. These three selected echograms show the same area, but the detection of targets is different. Notably there are more strong targets at 70 kHz, the backscattering is more than 10 times higher at 70 kHz than 38. Notably the TS-distributions are close to –60 dB at all measurements. These measurements were done at approximately 100 meters depth, and siphonophores were photographed at 119 meters.*

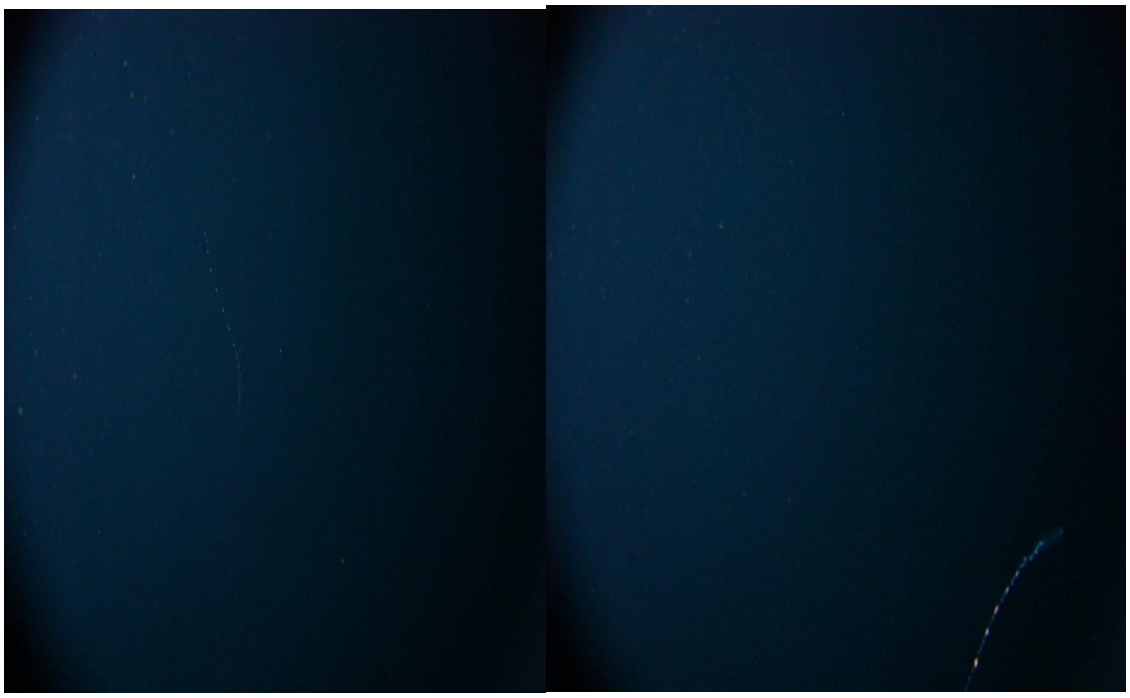

Figure 3.4.4. *Observations of two physonect siphonophores, family Nanomia at 120 meters depth.*

An echogram from 38 and 70 kHz showing the same samples (Fig 3.4.5-3.4.6), shed some light upon the observations at 70 kHz. In the 38 kHz echogram there are a clear separation between the shallow scattering layer at the deep scattering layer. In the area between 200-300 meters depth there are almost no targets,

while at 70 kHz there are several strong targets present. At 70 kHz other smaller targets appeared which could possibly be krill or other larger zooplankton, but since almost all the targets in this range from the probe could be resolved as single targets, the thresholding procedure made separation possibly. The target strength of the stronger targets is between -60 and -70 dB and are higher than the measured TS for the northern krill (Calise & Knutsen, 2011), which were present in all photo samples.

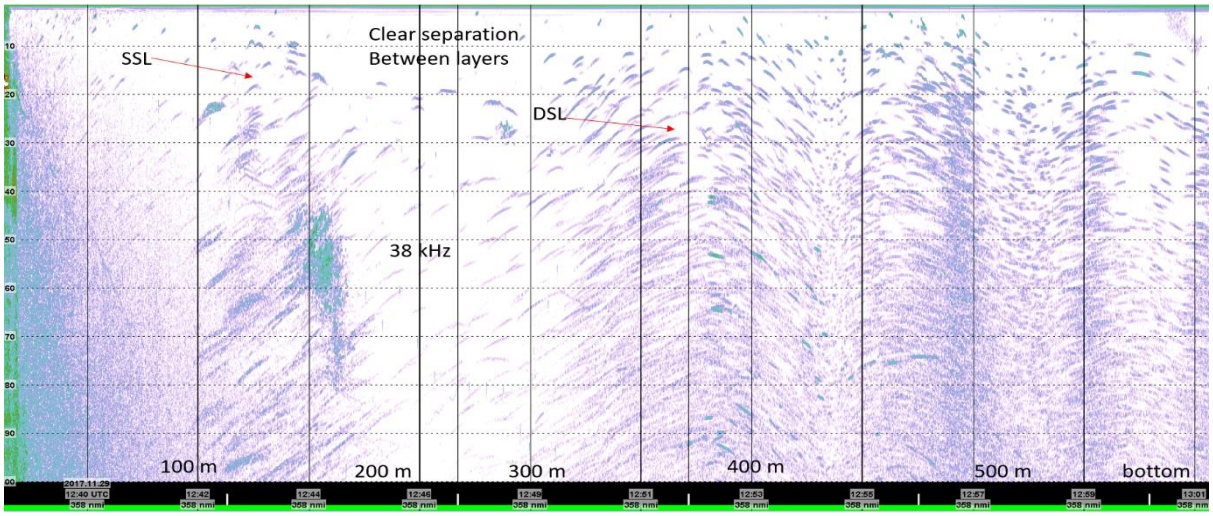

Figure 3.4.5. *Selected echogram from the probing station November 29th, 2017. The echogram shows a clear separation between the shallow and the deep scattering layer, with a few targets between 200-300 meters.*

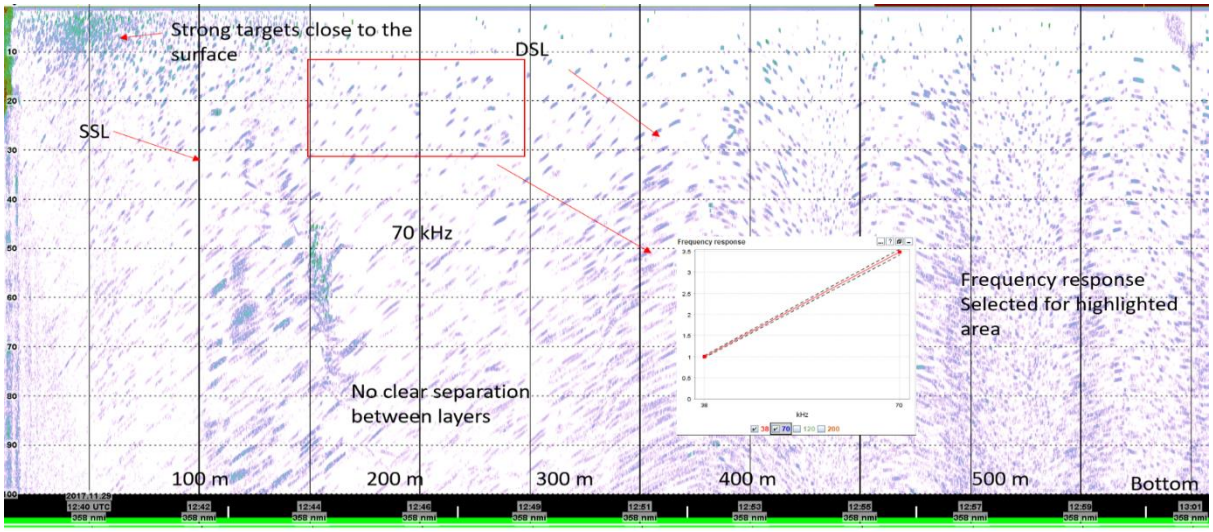

Figure 3.4.6*. Echogram of the same area with 70 kHz. In this sample there are several targets in the intermediate area between 200 and 300 meters, and the frequency response for this selected area shows that backscattering is 3.5 stronger than 38 kHz*

In all these measurements, all backscattering with a S_V higher than -70 dB, were allocated mesopelagic fish. If these targets present at -70 dB are not mesopelagic fish, there would be a positive bias.

3.5 Zooplankton distribution

In all three samples, small zooplankton are distributed in the upper 200 meters of the water column. The identification of zooplankton is made on the basis of the frequency response which could resemble "small fluid like zooplankton" (Fig 1.4.1.). Large zooplankton like krill will have a higher backscattering at the higher frequencies, and less at 38 kHz while smaller zooplankton like copepods will have an exponential increasing backscattering with frequency (Stanton et al., 1996). The highest registrations of zooplankton are from the probing data. This is due to the different thresholding in the upper layer. At the 1st site, the density is at 6000 zooplankton/m^3 at 150 meters depth, while the probing data suggest a density of 4000 zooplankton/m^3 at 100 meters (Fig 3.5.1). At the second site the vessel registrations are weaker than the probe registrations, but this is due to the different approaches of scrutinizing (Fig 3.5.2). As mentioned in the method chapter, the zooplankton layer was so dense at station 2 and 3, that the -70dB threshold were not working. While the density differs between peaks at 4000-9000 zooplankton/m^3, the major difference between the probing data and the vessel data is the possibility to measure at greater depths. At this station there are some weaker registrations with densities at approximately 500 zooplankton/m^3. At the third sites there were strong densities up to 14000 zooplankton/ m^3. There is one notable difference, with a dense layer of plankton at 500 meters depth with densities up to 6000 zooplankton/m^3 (Fig.3.5.3).

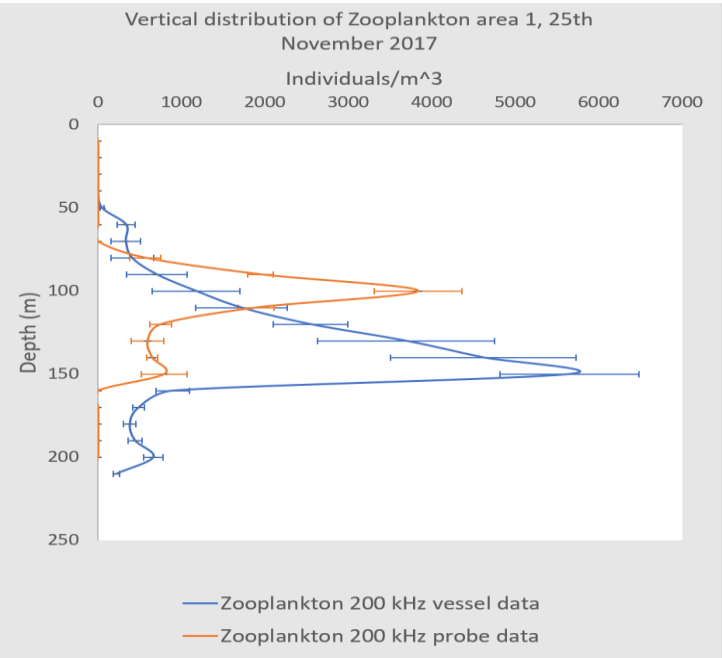

Figure 3.5.1. *Vertical distribution of zooplankton in area 1, November 25th, 2017. Volume sampled with vessel data from 50-210 meters, and between 80-160 meters sampled with the TS-probe.*

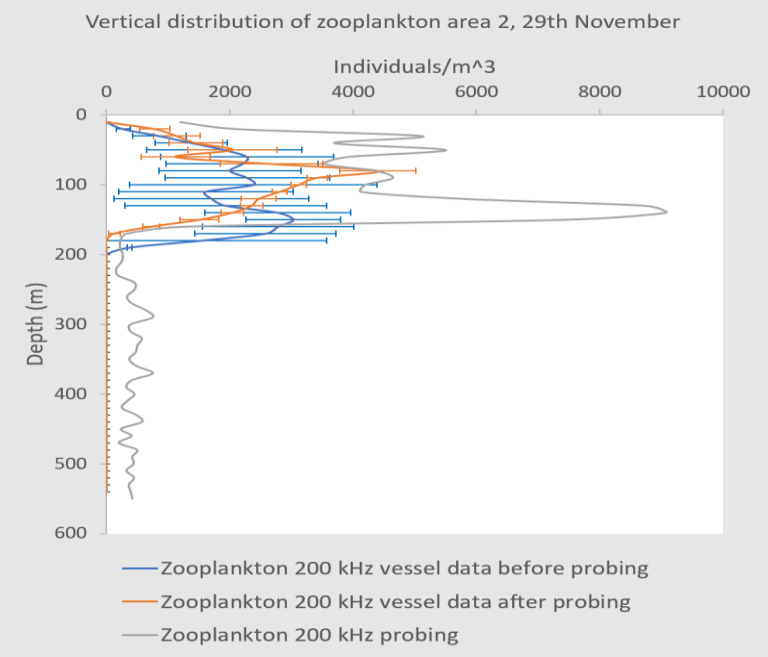

Figure 3.5.2 *Vertical distribution of zooplankton from November 29th, 2017. The upper 200 meters were sampled with the hull mounted transducers, and the entire water column sampled with the TS-probe.*

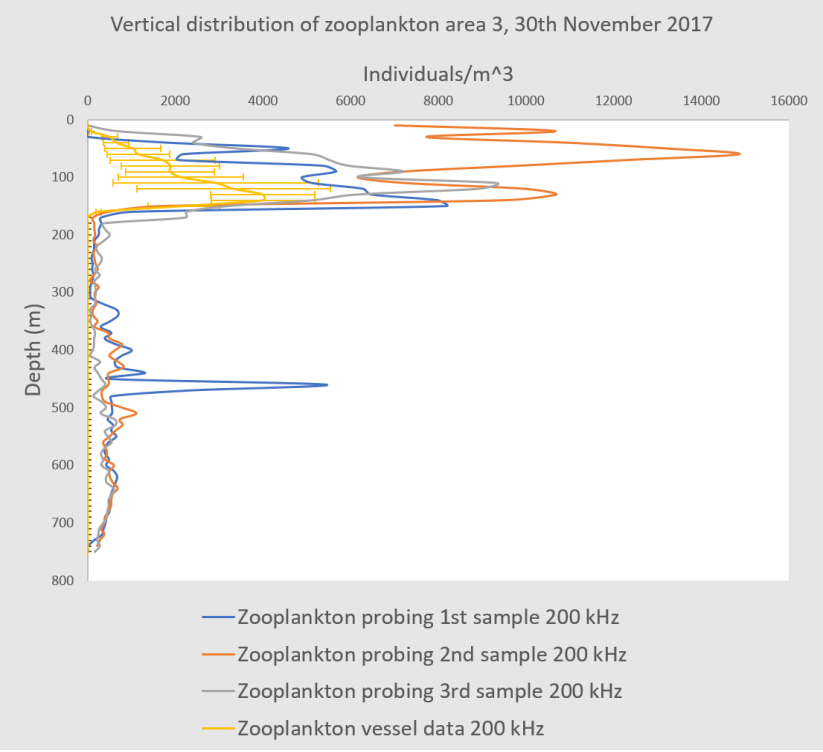

Figure 3.5.3. *Vertical distribution of zooplankton from November 30th, 2017. Showing vessel data and all three profiles conducted. The upper 200 meters were investigated with the hull mounted transducers, and the entire water column down to 760 meters were sampled with the TS-probe.*

While the stereo camera was mainly used to identify mesopelagic fish and siphonophores, the macro function could be used to identify the species in the zooplankton aggregations. Whilst turned off during most of the samples, zooplankton like copepods could not come into focus. But when turned on more species of zooplankton could be identified. The figure below (Fig.3.5.4) shows a peculiar observation during the third probing station. In the two first areas, zooplankton tended to distribute in the upper 200 meters in the water column, but there were also some weaker layers present at depth. The macro function from the stereo camera were used to identify the targets at this depth (Fig 3.5.5).

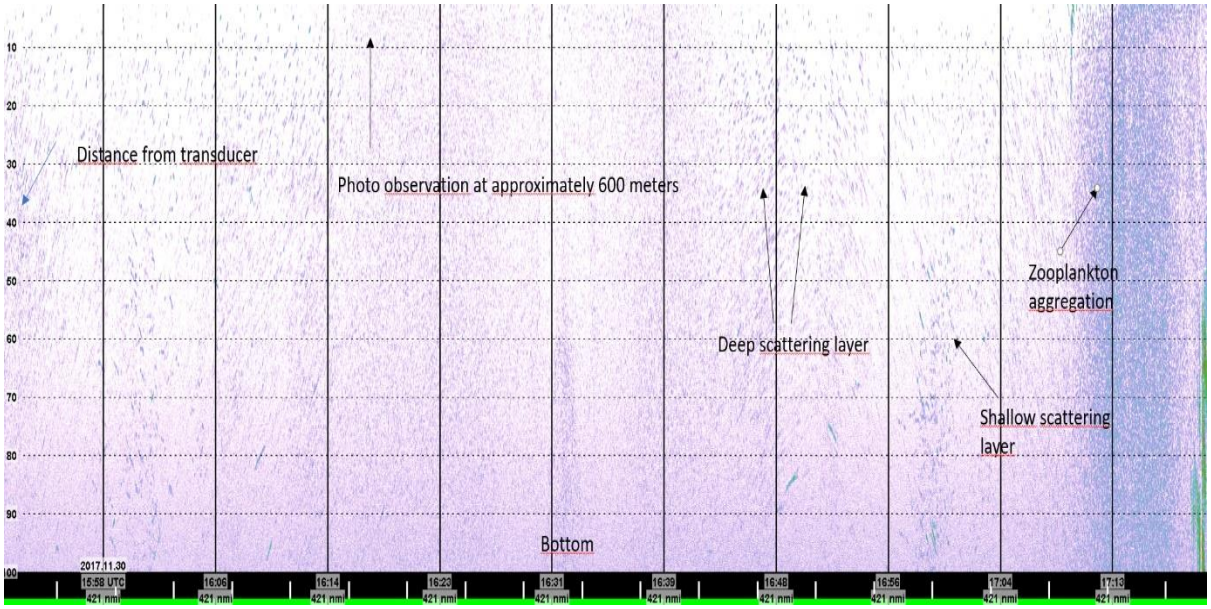

Figure 3.5.4. *Echogram showing the third descent of the probe in area 3, 30th November 2017 at 200 kHz. In an area below the DSL a weak aggregation of targets appear, which could potentially be copepods. Closer to the surface there are a denser zooplankton aggregation, which appeared in all echograms.*

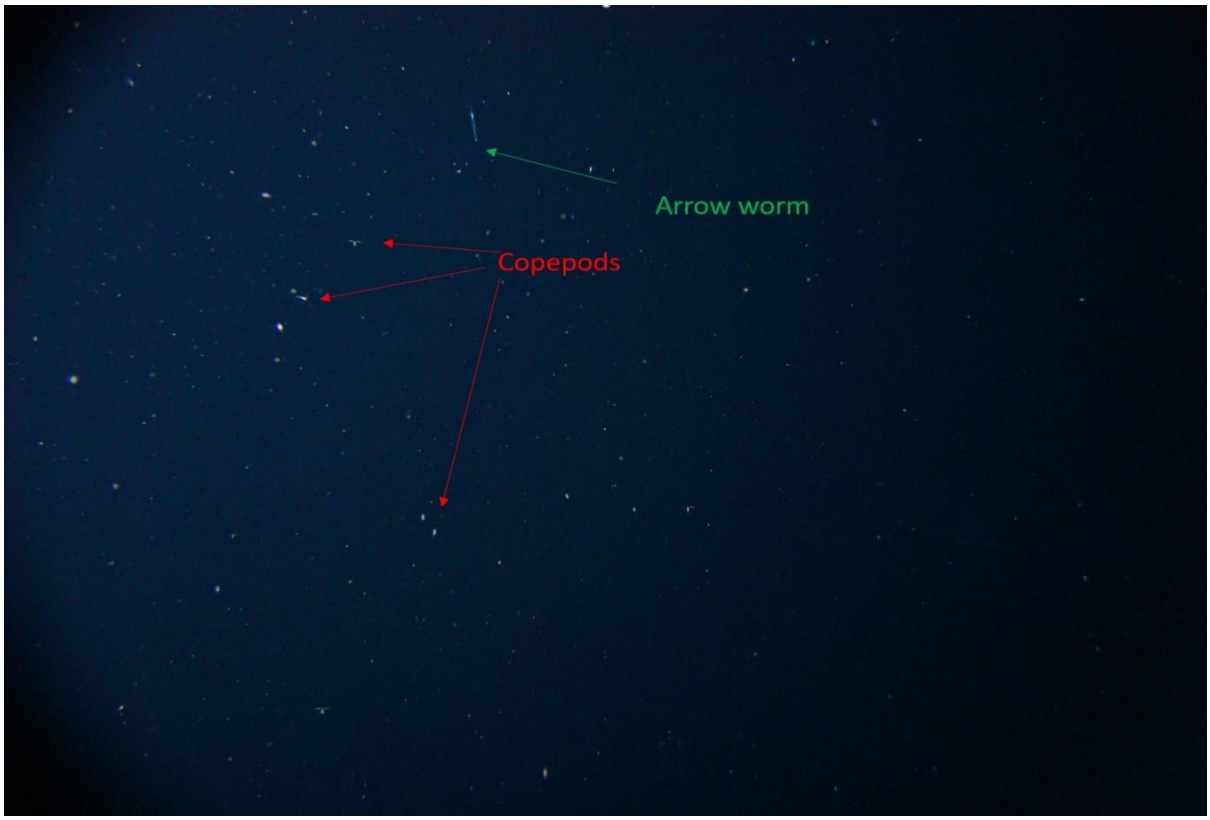

Figure 3.5.5*. Photo showing both an arrow worm, and an aggregation of copepods at the approximate area which were marked in the echogram in figure 3.5.4.*

In the photo samples, copepods, arrow worms, krill and other species of zooplankton were discovered. The stereo cameras macro function was useful to identify zooplankton at depth and help the scrutinizing of the acoustic data. With knowledge of the scattering properties of zooplankton, it can be used to roughly estimate the distribution of different groups of animals in plankton layers. As an important food of both mesopelagic fish and siphonophores, the discovery of aggregations in deep layers may help describe the behaviour seen in by both groups. While most zooplankton still were in shallow waters, it may indicate that some copepods have started their overwintering process below 500 meters depth, which is described by (Hirche, 1996).

4 Discussion

4.1 Sources of error

4.1.1 Separating species or species categories

In all the samples, backscattering with the volume scattering strength >-70 dB at the appropriate depth were given to mesopelagic fish. According to experienced interpreters this volume backscattering strength is often used to discriminate between weaker scatterers like zooplankton and fish. Mesopelagic layers are however known to be inhabited by multiple species (Tont, 1976). The largest potential error source in this study is the presence of other species. This may be fish with similar acoustic properties to glacier lanternfish and pearlsides, gas bearing zooplankton and aggregations of weaker targets which is not separable from fish targets and possibly noise. One of the weak points in my thesis is the lack of appropriate trawl samples, as only large meshed trawls were used during the survey. There are no trawl samples in this study to give an insight to the species composition in the different layers, and all scrutinizing are done with the assumption that glacier lanternfish and pearlsides are abundant fishes in mesopelagic layers in these waters (Gjøsaether, 1981; Mazhirina, 1988). If other species are scrutinized as mesopelagic fish, the biomass estimates would be even lower. Presence of larger fish in the TS measurements from the probe could theoretically be a large source of error in the mean TS estimates. Not many large fish in a sample is needed to skew the average TS. In this study, the camera was not mounted in the same direction as the transducers. This excludes the possibility to compare photos, and echoes with knowing the species studied. Anyhow, the sampling volume of the camera is very limited compared to the acoustic sampling volume, and some important groups also tend to avoid the probe so much that they often are out of reach of the camera, estimated to be 5 to 7 meters in clear water (Ona et al., 2018 in prep).

4.1.2 Avoidance

There is a clear evidence that mesopelagic fishes avoid the TS-probe. In (Ona et al., 2018 in prep.) avoidance from lantern fish were measured to 7 meters away from the probe. Outside this range, the density remained constant to 100 m range. This were accounted for by starting the measurement 10 meters away from the probe. It appears that especially the first 10 meters the density of fish was lower. It is a bit difficult to interpret this from the echogram directly, because the effective

beam with is also smaller at short distance (Fig. 4.1). If there is a sharp decrease in both NASC-values and area density, towards the transducer, then avoidance occur. Avoidance from camera lowered systems have previously been described by (Koslow et al., 1995).

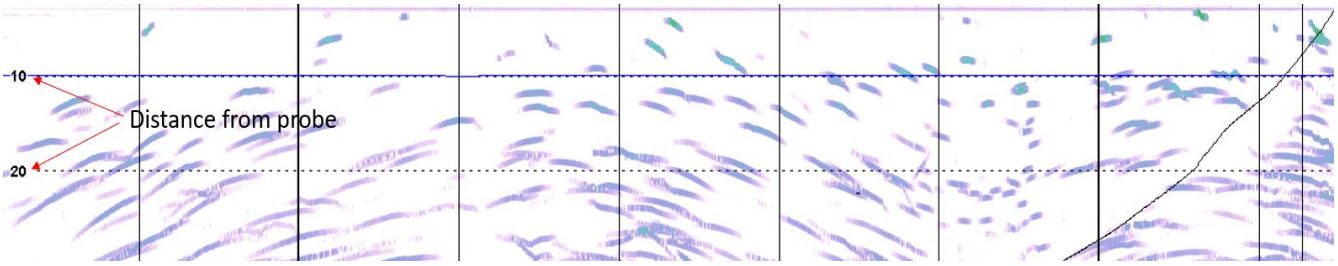

Figure 4.1. *Echogram showing deep scattering layer, with several single targets.*

Due to this effect, there have been difficulties obtaining good photos of mesopelagic fish, with a few exceptions. This may be explained by looking at the echograms. The probe uses flashes, when photos are taken, and the mesopelagic fish are known to be light sensitive (Staby & Aksnes, 2011). When the transducers are mounted horizontally, the avoidance problem is reduced (Ona et al., 2018). Even though siphonophores, dominate the picture identifications, there are probably much more pearlsides and glacier lanternfish relatively but outside the reach of the cameras used. Plankton targets at registered well at 200 kHz do not avoid the TS-probe in the same way. With the low densities measured from both vessel data and probe data, also the probability of having a mesopelagic fish in range of the camera becomes small. The camera may not work properly as ground truthing of deep scattering layers, but as a good tool together with echograms. Other camera systems which is decoupled from the ship movement may work better than from a lowered probe. It is possible the pressure wave and pumping movement from the vessel heave, transferred to the descending device which is sensed by the fish (Ona et al., 2018 in prep). More promising results have been obtained with bottom mounted cameras and freely dropped camera systems on for example the very sensitive Orange Roughy (*Hoplostethus Atlanticus*), (Driscoll et al., 2012).

4.1.3 Survey design

The acoustic sampling from the vessel and the probe were not conducted at the exact same time, this means that it may not measure the exact same biomass and vertical distribution. As measured in the material and methods, mesopelagic layers have a high autocorrelation (Fig 2.2.2), but there are possibilities that some event might have changed the density of the fish. Even though the

autocorrelation plots shown suggests that the areas are very similar, changes in vertical may happen within one hour. Another source of error is the lowering speed of the probe. Even though the average lowering speed were calculated, and vertical grids were computed, there is a reasonable possibility for estimating the wrong depth. In this survey, an exact depth is not of the highest importance, due to the objective of finding the general densities in scattering layers. If a depth cell deviates with two meters, the main outcome of this study would not change.

4.1.4 scrutinization errors

When performing the post processing of the acoustic data, there are several sources of error. There is a possibility of misinterpretation of the targets due to lack of experience by the operator. Acoustic targets may be identified by using a trawl sample, but due to gear selectivity error sources will also appear here without knowledge of the catchability of the species of interest (Fernö and Olsen, 1994; Kloser et al., 2009; Kaartvedt et al., 2012). Trawl samples are not the ideal method for measuring siphonophores (Bigelow,1913). When performing the amplitude thresholding the principle are to remove weak aggregations of plankton from a mixture with stronger targets, like swimbladdered fish. When concentrations of weak targets increase, so does their volume scattering strength, and they become increasingly difficult to separate from other targets. In the probing station at 30th November, there are two separate aggregations of zooplankton (Fig.2.4.3). One which is possible to separate from fish targets, and one with a volume scattering strength which is impossible to separate. A bias would be given to either fish or zooplankton depending on the thresholding applied. In the probe stations some of the registrations on 70 kHz, can possibly be fish but are scrutinized as plankton. If the glacier lanternfish do possess an inflated swimbladder, their echo may become more similar to large zooplankton, and may lead to a negative bias. Several species common in Norwegian waters like *Myctophum Punctatum* and *Notoscopolus Kroeyr*i are described in (Bardarson, 2013) as bladderless mesopelagic fishes with target strength between –70 to -90 dB. Bladderless lanternfish could also fall under this category and would maybe be removed with bottom thresholding from the acoustic data. Generally, these error sources are reduced with the usage of the TS-probe, but due to time limitation and lack of knowledge of other species such an analysis could not take place in this material. The probe data generally shows that there are a mix of both fish and several other acoustic classes, like fluid like targets and small zooplankton. This

is generally supported by the photos taken (Fig. 3.4.2, 3.4.4 an3.5.5), especially for non-avoiding groups.

4.2 Discussion of the results

4.2.1 Differences measured using the two observation platforms

The major discovery in this study, is the very thin density of mesopelagic fish in scattering layers in the Norwegian Sea, and Vestfjorden. Even the densest measurement only measures approximately 0.15 fish/m^3 (Fig 3.2.3). The mesopelagic fishes studied in this survey are small fishes, with average weights close to one gram. This mean there would only be 0.1g/m^3 with fish at the densest areas, which is very low compared to other areas with a high abundance of mesopelagic fish, like the Oman gulf (Gjøsæter & Kawaguchi, 1980). Herring and some other pelagic fishes much larger in size than a mesopelagic fish can sometimes be found in densities of 22 fish/m^3 (Misund & Aglen, 1993). There is in all samples at 38 kHz significant difference between ship data and probe data (Table. 3.2-3.4). The result indicates that the target strength values used in the vessel data gives the wrong biomass estimates. The mean TS-values measured with 38 kHz from the probe, varied with 6 dB (Table 3.1). Since this is in the logarithmic domain, this means that the backscattering cross section, measured November 30th were over 2 times higher than November 29th. When measuring backscattering, a knowledge of correct backscattering cross section is needed. In this case, there may be a positive bias, because the literature TS-values are lower than those measured *in situ*. There are also two stations where the measurements at 70 kHz are different than the other frequencies (Table 3.4). In many cases are the biomass estimates 2-4 times higher on the vessel data than the probing data. This may indicate a stronger response in swimbladders at 38 kHz, but usually if the swimbladders were resonating, the difference in results should be even higher. This result may have several reasons. As described by (Neighbors and Nafpakitus, 1982), the swimbladders of myctophids may become filled by lipids, or become inflated (Marshall, 1960; Butler & Pearcy, 1972; Neighbors & Nafpakitus, 1982; Yasuma et al., 2003; Yasuma et al., 2010). This could change the resonance frequencies of pearlsides. It is possible that the swimbladders change volume at great depths (Hershey et al., 1961; Godø et al.,2009). In these samples, the deep scattering layers are located from 400-600 meters, and it is possible that swimbladder sizes changes with depths together with the resonance frequency. In the vessel data the backscattering were stronger at 18 kHz in the shallower depths, but relatively similar to 38 kHz at depth. In the TS-measurements done by (Scoulding et al., 2015) the TS for pearlsides and

lanternfish and lanternfish were respectively, -60.8 dB and -62.1 dB which were averaged to -61.1 dB. In this study, *in situ* target strength measurements differed between -59.7 dB to -54.9 dB. This could explain the skewed biomass estimates from the vessel data, and the importance of measuring target strength *in situ* at several locations. Due to the resolution, and thus the simpler thresholding process together with the *in-situ* target strength measurements, the results obtained by the probe are definitely more precise. Target strength measurements of these groups are more or less impossible from the vessel. Especially at 38 kHz the biomass estimates are significantly smaller at all stations. With a more correct reference TS-value the vessel data may also be more precise. These results are presented without the inclusion of several other species. In these stations, all echoes thresholded up to S_v>-70dB, were allocated mesopelagic fish, while the stereo camera photos indicate that physonect siphonophores are present in the samples. Siphonophores are difficult to sample due to its fragility, (Hosia & Båmstedt, 2007) and is often shredded in trawls.

4.2.2 Unknown targets strong at 70 kHz

The more numerous observations at 70 kHz, may suggest that there are organisms near the resonance frequencies at the probing samples. There was a higher density of mesopelagic targets at 70 kHz than 38 kHz. The targets which appears on the higher frequencies, could be mesopelagic fish with inflated or partly lipid-filled swimbladders. Problems related to resonance frequencies of swimbladders at frequencies higher than 38 kHz have been described (Kloser et al., 2002; Godø et al., 2009). In some studies, myctophids have shown to have a non-linear relationship when it comes to size and swim bladder size. In some individuals the gas in the bladders are lost or filled with lipids (Marshall, 1960; Butler & Pearcy, 1972; Neighbors & Nafpakitus, 1982; Yasuma et al., 2003; Yasuma et al., 2010; Bardarson, 2013). It is also possible that small bladders containing gas can be resonant at such high frequencies as 70 kHz, and if there are a population of juvenile fish with such small bladders or adult myctophids with reduced bladders, this observation is likely. To be able to be near the resonance frequency at 70 kHz, the gas bubble must be very small. Another explanation could be that juvenile stages of mesopelagic fishes could contain such a small bladder. In (Folkvord et al., 2016) juvenile pearlsides with mean lengths at 10-12 mm was found to distribute in the upper 75 meters of the water column. In many studies they have been found in shallower layers than the adult pearlsides. (Kaartvedt et al., 1988; Giske et al.,1990; Baliño & Aksnes, 1993; Rasmussen & Giske, 1994; Bjelland, 1995; Goodson et al., 1995; Bagøien et al., 2001, Staby et al, 2011). This

could correspond with the observations done close to the surface at both profiling stations. This could lead to a negative bias, if these fishes do not appear at 38 kHz. In (Davison et al., 2015), a reduced TS with as much as 30 dB were possible if the gas in the swimbladder were lost. This must be from the resonance top of the bladder to only flesh, as the usual relationship between a fish with a swimbladder and one without is about 10 dB at same size (Foote, 1980). There is a possibility that mesopelagic fish have been scrutinized as zooplankton, if they are weaker targets. This could lead to an underestimation.

An alternative hypothesis is that the strong backscatter at 70 kHz may come from small, near resonant gas bubbles in gas bearing siphonophores. In previous studies siphonophores were measured to be resonant at low frequencies (Barham, 1963; Warren et al., 2001), with measured TS at 24 kHz of -64.5 dB. Pneumatophore sizes has been described in different sizes, with lengths between 0.15 mm (Lavery et al., 2007), to 3.27 mm (Barham, 1963), but there may be a possibility that for some siphonophores, the pneumatophore is of such a small size that they can be near resonance at higher frequencies. During this study, the department of natural history were visited, and some photos of pneumatophores were obtained.

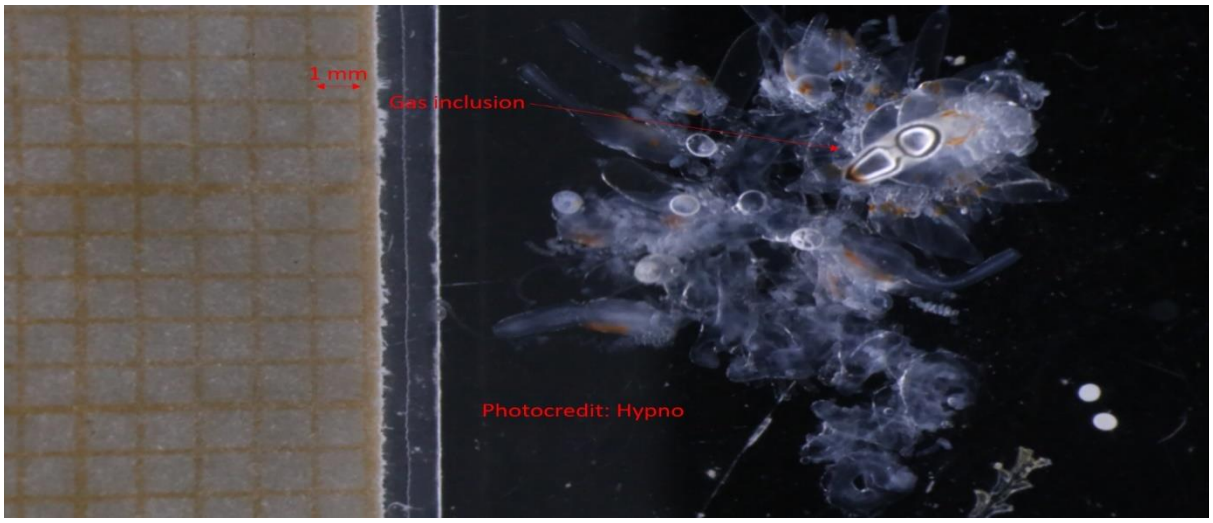

Figure 4.2.1. *Photograph of a Nanomia Cara, which are the most abundant siphonophore in upper waters in the North Atlantic ((Williams & Conway, 1981; Mackie et al., 1987; Hosia et al., 2007). In this photo the pneumatophore is shown together with a millimetre paper. The pneumatophore is closer to the camera, than the paper and will possibly make the pneumatophore appear larger than it potentially is, the diameter seems smaller than one millimetre.*

Even though this siphonophore is not in its natural habitat, the pneumatophore diameter is less than 1mm. Physonect siphonophores do undergo earlier life stages where the pneumatophore also is

present. One of them is the siphonulae-stage (Mackie et al., 1987). In the study (Benfield et al., 2003) the siphonulae stage were studied on *Nanomia Bijuga* in the Gulf of Maine. A model was made for several pneumatophore sizes, where a pneumatophore size close to 0.2 mm in diameter which could be close to resonance frequency at both 70 and 120 kHz. Siphonulae stages for *Nanomia Cara* has been observed as numerous in the winter months in Norwegian fjords (Hosia & Båmstedt, 2007). If this pneumatophore size is present in the siphonophores identified in these samples, a possible explanation could be this. If the some of the gas bearing siphonophores should be near resonance at 70 kHz they could possibly be separable from some mesopelagic fishes.

4.2.3 Image identification

With the camera observations, there are evidence of physonect siphonophores in the deep scattering layers, and all observations are found in appendix IV. The ratio between mesopelagic fish and siphonophores in these layers are not known, and more studies should be performed. There are several topics regarding siphonophores, which may be of interest in the study of their role in the deep scattering layers. If the siphonophore echoes are similar to mesopelagic fish echoes, the backscattered values in this survey would be positively biased towards mesopelagic fish. If these siphonophores are resonant at 70 kHz, there may be a possibility to distinguish between them acoustically. It is also possible that mesopelagic fish and siphonophores distributes differently due to different behaviours.

4.2.4 Migrating behaviour of the scattering layers

This study was conducted during the winter in northern Norway, and the day length was short. This would possibly influence how the mesopelagic fish behaved in this study. Even though there were suggestions in the acoustic data, that there were some dial vertical migrations. Both pearlsides and glacier lanternfish stay at depths during the winter period (Dypvik et al., 2012; Staby et al, 2011), but it is also suggested that lantern fish migrate, in correspondence to copepods. In this study, the majority of copepods were present in the shallower layers (Fig3.5.1-3.5.3), even though they were also present below 500 meters (Fig3.5.4 and 3.5.5). If the density of zooplankton were sufficient for the population of lanternfish, a feeding approach on overwintering copepods would be possibly a safer approach than migrating. Pearlsides have been observed overwintering at depth, and this approach would reduce the risk of predation, together with feeding on the migrating zooplankton

observed with the stereo camera (Giske et al., 1990; Bagøien et al., 2001). Juvenile pearlsides are suggested to perform DVM in the winter months due to for the purpose and advantages of maturing early (Staby et al., 2011). There are also suggestions that some lanternfish do not migrate at all (Kaartvedt et al., 1988; Baliño & Aksnes, 1993; Kaartvedt et al., 2009; Dypvik et al., 2012). At the 3rd station, the biomass in the DSL decreased between dusk and night and could suggest that some animals may have migrated (Fig.3.2.7-3.2.9). But there were no suggestions that most of the biomass migrated, with the presence of a deep scattering layer during night (Fig 4.2.2). At station 2 November 29th it appeared that the shallow layer became more diluted during night-time. The DSL appeared to be relatively similar between day and night. With the observation of dense copepod aggregations in the upper 200 meters and some weaker at depth (Fig3.5.4-3.5.5), both migrating and non-migrating strategies could be possible.

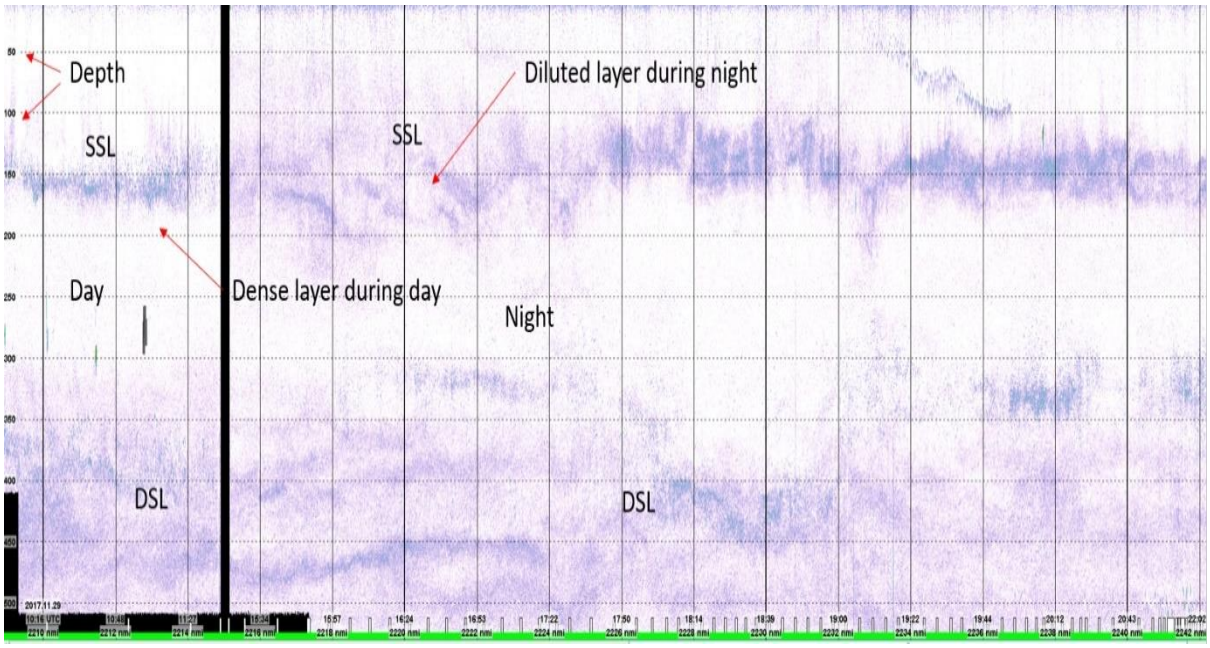

Figure 4.2.2. *Echogram showing dial vertical migration in the shallow scattering layer at November 29th, 2017. Notably the deep scattering layer appears similar both at day and night.*

4.3 Future studies

4.3.1 Acoustic studies

In (Proud et al., 2018) a model was made which predicted a biomass of mesopelagic fish in the world oceans to be between 1.8 to 15.9 Gigatons with a median of 3.8 Gigatons. This is up to date possibly one of the most accurate biomass estimations, due to its inclusion of resonance, loss of swimbladder, and its inclusion of physonect siphonophores. But the distance between both quartiles in this study are very large and could by further investigations become more accurate. When performing surveys, measuring mesopelagic fish abundance, usually a reference target strength has been used. In future studies, the TS-probe or a similar instrument could be used to measure the density directly. *In situ* target strength measurements, or full profiles could be done in the same design as for example trawl stations. By using the correct TS, the relationship between observed backscattering and the target volume density would be more correct. This would give a more precise biomass estimate, especially is also the dangerous siphonophore category could be identified and isolated.

The results presented here, may shine light on the importance on using several frequencies on surveys. If resonance on 38 kHz is found in several of the world oceans, there may be severe positive biases in previous biomass estimations (Davison et al.,2015). In this investigation no large deviation was found between the density estimates. In future studies, there should be a focus on further investigations of swimbladders of several mesopelagic fishes. One interesting aspect is if it follows a linear relationship or not, but it can also be of importance finding out what percentage of the population which involve individuals with inflated or lipid filled swimbladders. In the study by (Bardarson, 2013) a percentage of 71 percent of the glacier lanternfish had air in the swimbladder. With a broader knowledge of this ratio, this could be used in the biomass estimation, by separating gas a non-gas filled individuals as two acoustic categories and add them together in the post processing. It could be interesting to investigate the ecological interactions in these scattering layers. Mesopelagic fish and siphonophores both are planktivours (Gjøsaether, 1981;Gjösæter, 1973;Kinzer, 1977; Kawaguchi & Mauchline, 1982; Roe & Badcock, 1984; Dypvik et al., 2012; Robison et al., 1998; Gorsky et al., 2000; Hosia and Bamstedt, 2007), but they could possibly have completely different predators, which may lead to a different vertical distribution. Potential presence of their predators may also be used as an index to determine if they are present in this area

or not. The jellyfish *Periphylla Periphylla* have been suggested as a potential predator on siphonophores (Hosia & Båmstedt, 2007).

4.3.2 Wideband

Using multifrequency acoustics to investigate mesopelagic fishes have been proven difficult. At 18 and 38 kHz there are problems with possible resonance, regressing swimbladders, depth, and ontogenetic factors. But if there are resonance problems also at 70 kHz, a new approach may be needed. This need to be investigated further to find the optimal frequencies for measuring mesopelagic fish. To obtain more information about individual targets, a pulse with a wider spectrum can be used. A wideband sonar is an instrument with larger bandwidth than regular sonars and echo sounders (Simmonds and Copland, 1996). An important feature of wideband sonars is the received spectrum of echoes. This can be used to further determine acoustic differences between species. This method is extending the frequency response method, but on a smaller scale. Where the multifrequency response operates between 18 kHz and 333 kHz, a wideband spectrum can stretch between be more or less continuous from 30-400 kHz, divided into 5 or 6 bands. If there are resonance problems both at 38 and 70 kHz, other frequencies should be selected outside the resonance top of the organism. When operating a wideband echo sounder, spectrum analysis could be performed. This is the same principle as with multifrequency analysis, but there is much higher coverage along the frequency axis. In this case spectral analysis of single targets of both mesopelagic fish and siphonophores could be made, increasing the probability of individual separation. In order to achieve this, the targets must be measured at short range by a probe or a lowered device.

4.3.3 Further studies on acoustic properties of mesopelagic fish and siphonophores

Knowledge about target strength-length relationship is important in the acoustic surveying method. If myctophids have a negative linear relationship as suggested by (Scoulding et al., 2015), the strongest acoustic returns will come from juveniles. Usually young fish larvae are not the target group for commercial fishers. So, there is a possibility that the fish of interest give away the weakest reverberation. In (Davison et al., 2015), the difference between fish with gas filled swimbladders, and inflated or lipid filled have been described, can vary as much as 30 dB. This problem should

be met by further studies of swimbladders of several species of mesopelagic fish. Some species might be more visible on higher frequencies, but these frequencies are not applicable, since there is a strict range limitation for high frequencies applied.

To be a potential important ecological species, there are not too many investigations done on siphonophores. There should be more research on camera techniques, which may give reasonable estimates of both mesopelagic fish and siphonophores. A possibility is increasing the range of the camera. Ways to perform camera sampling, without scaring the fish should be further investigated, but some solutions have been found (Driscoll et al.,2012). To understand the acoustic properties of different types of siphonophores, pneumatophore sizes must be mapped for several species if possible, just like with commercial fish species. More studies should also be made with a submersible echo sounder, combined with a camera mounted in the same direction as the transducer where several targets are studied, possibly with wideband acoustics. This has been done with some success by (Kloser et al.,2016). If there is a possibility for calculating target strength for siphonophores, with images of the same animal present in the echogram, more precise knowledge of their acoustic properties could be made. To be able to make more realistic estimates on mesopelagic fish globally, the ratio between fish and siphonophores should be investigated for each site measured.

4.3.4 Mesopelagic fish as a potential fishery and resource.

If there should be a global fishery on mesopelagic fish, some criteria have to be met. Knowledge about true density is important. Development of proper sampling systems for mesopelagic fish and mesopelagic communities should be developed. In these samples from the Norwegian Sea and fjords, the volume density is not very high. Modern fisheries trawling usually use technologies that assumes that the fish density is high, or that they may be herded by large meshed towards an opening or a cod end. The behaviour of one fish is also often depending on the behaviour of the neighbouring fish in this process. Also, the fish must have some swimming capacity in order to not be overridden by the trawl panels during herding (Tuvia & Dickinson, 1969; Wardle, 1984; Wardle, 1986). If the mesopelagic fish have are found at low densities like this study suggests, the fish must act independently with respect to the neighbouring fish. Different catching strategies than those of schooling fish must therefore be developed. If there should become a future fishery, better

knowledge on the layer properties would also be needed. If a fishery is targeting clean layers pearlsides, which would be beneficial, methods for acoustic identification of such layers should be possible, both for efficient harvest, but also for reducing the risk of bycatch. It is also important to know the ecological roles of mesopelagic fishes before the serious harvesting starts, because knowledge of how fishing pressure might afflict populations, together with their abilities to bring carbon to the deep (St John et al., 2016) is still rather unclear.

5 Concluding remarks

The measured biomass of mesopelagic fish in the Norwegian Sea, and the fjord chosen are low compared to some of the densities observed in tropical seas (Gjøsæter & Kawaguchi, 1980; Gjøsæter, 1984). The objectives of this study were to compare results from the two different observation platforms. There is a difference between the vessel data and the probe data, especially at 38 kHz, but the difference is not large enough to suggest a possible resonance in the scattering layers. The measured TS is usually higher than the literature value, which leads to the overestimation from the vessel data, but the vessel data itself seems relatively reliable. Another objective was to assess if physonect siphonophores were present in the scattering layers. In this study siphonophores were found at all stations, in several parts of the water column, and it may suggest that they play a part in the backscattering from these layers.

There are several challenges when it comes to measuring mesopelagic fish precisely, and several potentially large bias sources in both trawling (Koslow et al., 1997; Kloser et al., 2009; Pakhomov & Yamamura 2010; Kaartvedt et al., 2012; Iriogoien et al., 2014), and acoustic surveys (Kloser et al., 2002; Godø et al., 2009; Davison et al., 2015; Scoulding et al., 2015; Proud et al., 2018). Lowered, short range acoustics, like from a probe may give more precise density estimates and also valuable TS-relationships in deep water (Johnson et al., 1956; Kloser et al., 2016). There are several difficulties of standardizing the target strength due to uncertainties with respect to swimbladder strategy (Butler & Pearcy., 1972; Neighbours & Nafpaktitis, 1982; Bardarson, 2013; Scoulding et al., 2015, and more investigations here on the most important groups may improve our understanding of the backscattering. Furthermore, knowledge is needed on competing scatterers in the mesopelagic layers is needed for more precise abundance estimates, and the understudied siphonophores such a target (Barham, 1963; Mackie et al.,1987; Warren et al., 2001; Benfield et al.,2003; Hosia & Båmstedt, 2007; Kloser et al.,2016; Proud et al.,2018; Knutsen et al.,2018). Overall more profound and dedicated research is asked for before selected species of this ecosystem is harvested in a sustainable manner.

6 References

Alverson, F.G., 1961. Daylight surface occurence of myctophid fishes off the coast of Central America Pacific Science, 15; 483

Andreeva, I., 1964. Scattering of sound by air bladders of fish in deep sound scattering layers. Soviet Physics Acoustics, 10, 17–20.

Bagøien, E., Kaartvedt, S., Aksnes, D.L., and Eiane, K., 2001 Vertical distribution and mortality of overwintering Calanus. Limnology and Oceanography 46, 1494-1510

Baliño, B.M. and Aksnes, D.L., 1993. Winter distribution and migration of the sound scattering layers, zooplankton and micronekton in Masfjorden, western Norway. Marine Ecology Progress Series 102, 35-50

Banon, R., Arronte, J. C., Rodriguez-Cabello, C., Pineiro, C. G., Punzon, A., & Serrano, A., 2016. Commented checklist of marine fishes from the Galicia Bank seamount (NW Spain). Zootaxa, 4067(3), 293-333.

Bardarson, B., 2013. Modelled Target Strengths of Three Lanternfish (Family: Myctophidae) in the North East Atlantic Based on Swimbladder and Body Morphology. University of St Andrews, Scotland, 97 pp.

Barham, E., 1963. Siphonophores and the Deep Scattering Layer. Science, 140(3568), 826-828.

Benfield, M. C., Lavery, A. C., Wiebe, P. H., Greene, C. H., Stanton, T. K., & Copley, N.J., 2003. Distributions of physonect siphonulae in the Gulf of Maine and their potential as important sources of acoustic scattering. Canadian Journal of Fisheries and Aquatic Sciences, 60(7), 759-772.

Bjelland, O. (1995). Life history tactics of two fjordic populations of Maurolicus muelleri. Cand. scient (Doctoral dissertation, thesis, University of Bergen).

Bigelow, H. B. (1913). Medusae and Siphonophorae collected by the US Fisheries steamer" Albatross" in the northwestern Pacific, 1906 (Vol. 44). US Government Printing Office.

Boden B. P., 1962. Plankton and sonic scattering. Rapp.P.-v., R~un. Conseil Permanent International pour l'Exploration de la Mer 153, 171-177.

Brierley, A. S., Axelsen, B. E., Buecher, E., Sparks, C., Boyer, H., and Gibbons, M. J., 2001. Acoustic observations of jellyfish in the Namibian Benguela. Marine Ecology Progress Series, 210, 55–66.

Brooks, A. L., 1977. A study of the swimbladders of selected mesopelagic fish species, in Oceanic Sound Scattering Predictions, edited by W. L. Anderson and B. J. Zahuranec (Plenum, New York), pp.

Butler, J. L., and Pearcy, W. G., 1972. "Swimbladder morphology and specific gravity of myctophids off Oregon," Journal of the Fisheries Research Board of Canada. 29(8), 1145–1150

Christensen, V., Walters, C. J., Ahrens, R., Alder, J., Buszowski, J., Christensen, L. B., ... & Kaschner, K., 2009. Database-driven models of the world's Large Marine Ecosystems. Ecological Modelling, 220(17), 1984-1996.

Clay, C.S. and Heist, B.G., 1984 Acoustic scattering by fish: acoustic models and a twoparameterfit. The journal of the Acoustical Society of America 75, 1077–83

Clay, C.S., 1992. Composite ray-mode approximations for backscattered sound from gas- filled cylinders and swimbladders. The Journal of the Acoustical Society of America, 92, 2173–80.

Clay, C.S. and Horne, J.K., 1994 Acoustic models of fish: the Atlantic cod (Gadus morhua) The Journal of the Acoustical Society of America, 96, 1661–8.

Davison, P. C., Koslow, J. A., & Kloser, R. J., 2015. Acoustic biomass estimation of mesopelagic fish: backscattering from individuals, populations, and communities. ICES Journal of Marine Science, 72(5), 1413-1424.

Demer, D. A., Berger, L., Bernasconi, M., Bethke, E., Boswell, K., Chu, D., Domokos, R., et al., 2015. Calibration of acoustic instruments. ICES Cooperative Research Report No. 326: 133.

Dragesund, O. and Olsen, S., 1965. On the possibility of estimating year-class strength by measuring echo-abundance of 0-group fish. Fiskeri Direktorates Skrifter Serie Havundersøkelser.13,47–75.

Dunn, C. W. (2005). Complex colony-level organization of the deep-sea siphonophore Bargmannia elongata (Cnidaria, Hydrozoa) is directionally asymmetric and arises by the subdivision of pro-buds. Developmental dynamics: an official publication of the American Association of Anatomists, 234(4), 835-845.

Duvall, G., & Christensen., 1946. Stratification of Sound Scatterers in the Ocean. The Journal of the Acoustical Society of America, 18(1), 254.

Dypvik, E., Røstad, A., & Kaartvedt, S., 2012. Seasonal variations in vertical migration of glacier lanternfish, Benthosema glaciale. Marine Biology, 159(8), 1673-1683.

Folkvord, A., Gundersen, G., Albretsen, J., Asplin, L., Kaartvedt, S., & Giske, J., 2016. Impact of hatch date on early life growth and survival of Mueller's pearlside (Maurolicus muelleri) larvae and life-history consequences. Canadian Journal of Fisheries and Aquatic Sciences, 73(2), 13.

Foote, K. G., 1979. On representations of length dependence of acoustic target strengths of fish. Journal of the Fisheries. Research Board of Canada, 36: 1490–1496.

Foote, K. G., 1980. Averaging of fish target strength functions. The Journal of the Acoustical Society of America, 67(2), 504-515.

Foote, K.G., 1985. Rather-high-frequency sound scattering by swimbladdered fish. The Journal of the Acoustical Society of America. 68, 688–700.

Foote, K.G. and Ona, E., 1985 Swimbladder cross sections and acoustic target strengths of 13 pollack and 2 saithe. Fiskeridirektoratets Skrifter Serie. Havundersøkelser 18, 1–57.

Foote, K. G., 1987. Fish target strengths for use in echo integrator surveys. The Journal of the Acoustical Society of America, 82(3), 981-987.

Foote, K. G., & Knudsen, H. P., 1994. Physical measurement with modern echo integrators. Journal of the Acoustical Society of Japan (E), 15(6), 393-395.

Giske, J., Aksnes, D., Balino, B., Kaartvedt, S., Lie, U., Nordeide, J., . . . Aadnesen, A., 1990. Vertical distribution and trophic interactions of zooplankton and fish in Masfjorden, Norway. Sarsia, 75(1), 65-81.

Gjøsæter, J., 1973. Food of the myctophid fish, Benthosema glaciale (Reinhardt), from western Norway. Sarsia, 52, 53–58

Gjøsæter, J., 1981a. Growth, production and reproduction of the myctophid fish, Benthosema glaciale, from westernNorway and adjacent seas. Fiskeridirektoratets SkrifterSerier Havundersøkelser, 17, 79-108

Gjøsæter, J., 1981b. Life history and ecology of Maurolicus muelleri (Gonostomatidae) in the Norwegain waters. Fiskeridirektoratets Skrifter, Serie Havundersøkelser 17,109-131

Gjøsæter, J. (1984). Mesopelagic fish, a large potential resource in the Arabian Sea. Deep Sea Research Part A. Oceanographic Research Papers, 31(6-8), 1019-1035.

Gjøsæter, J., and Kawaguchi, K., 1980. A review of the world resources of mesopelagic fish, Food And Agriculture Organization Of The United Nations. 151 pp.

Gjøsæter, H., Wiebe, P., Knutsen, T., & Ingvaldsen, R., 2017. Evidence of Diel Vertical Migration of Mesopelagic Sound-Scattering Organisms in the Arctic. Frontiers in Marine Science, 4

Godø, O. R., Patel, R. & Pedersen, G., 2009. Diel migration and swimbladder resonance of small fish: some implications for analyses of multifrequency echo data. Ices Journal of Marine Science, 66, 1143–1148

Goodson, M.S., Giske, J., and Rosland, R., 1995 Growth and ovarian development of Maurolicus muelleri during spring. Marine Biology,124,185-195

Gorsky, G., Flood, P. R., Youngbluth, M. et al., 2000. Zooplankton distribution in four Western Norwegian fjords. Estuarine Coastal and Shelf Science, 50, 129–135.

Hirche, H, and Niehoff, N., 1996. Reproduction of the Arctic Copepod Calanus Hyperboreus in the Greenland Sea-field and Laboratory Observations."Polar Biology 16.3, 209-19. Web.

Horne, J. K., 2000. Acoustic approaches to remote species identification: a review. Fisheries Oceanography, 9, 356–371.

Hosia, A., & Båmstedt, U., 2008. Seasonal abundance and vertical distribution of siphonophores in western Norwegian fjords. Journal of Plankton Research, 30(8), 951-962.

Fernö, A., & Olsen, S., 1994. Marine fish behaviour in capture and abundance estimation. Oxford: Fishing News Books.

Furusawa, M., 1988. Prolate spheroidal models for predicting general trends of fish target strength. The Journal of the Acoustical society of Japan (E) 9, 13–24.

Hershey, Backus, & Hellwig., 1961. Sound-scattering spectra of deep scattering layers in the western North Atlantic Ocean. Deep Sea Research (1953), 8(3-4), 196,IN3,201-200,IN4,210.

Irigoien X, T. A. Klevjer, A. Røstad, U. Martinez, G. Boyra, J. L. Acuña, . . . S. Kaartvedt., 2014. Large mesopelagic fishes biomass and trophic efficiency in the open ocean. Nature Communications, 5, 3271.

Jech, J.M., Schael, D.M. and Clay, C.S., 1995. Application of three sound scattering models to threadfin shad (Dorosoma petenense). The Journal of the Acoustical Society of America, 98, 2262–9.

Jennings, S., Kaiser, M., & Reynolds., J. 2001. Marine fisheries ecology. Oxford: Blackwell Science.

Johnson, H. R., Backus, R. H., Hersey, J. B., and Owen, D. M., 1956. Suspended echo-sounder and camera studies of midwater sound scatterers. Deep Sea Research (1953), 3, 266-272.

Kaartvedt, S., 1988. Significance of Vertical Migrations for Advection and Retention of Fjord-living Crustaceans, 114.

Kaartvedt, S., Knutsen, T., and Holst, J. C. 1998. Schooling of the vertically migrating mesopelagic fish Maurolicus muelleri in light summer nights. Marine Ecology Progress Series, 170, 287–290

Kaartvedt S., Røstad A., Klevjer TA., Staby A., 2009 Use of bottom-mounted echo sounders in exploring behavior of mesopelagic fishes. Marine Ecology Progress Series, 395, 109–118

Kaartvedt, S., Staby, A. & Aksnes, D. L., 2012. Efficient trawl avoidance by mesopelagic fishes causes large underestimation of their biomass. Marine Ecology Progress Series, 456, 1–6.

Kawaguchi, K., & Mauchline, J., 1982. Biology of myctophid fishes (family Myctophidae) in the Rockall Trough, northeastern Atlantic Ocean. Biological Oceanography, 1(4), 337-373.

Kinzer, J., 1977. Observations on feeding habits of the mesopelagic fish Benthosema glaciale (Myctophidae) off North West Africa. In: Andersen, N. R., Zahuranec, B. J. (eds.) Oceanic sound scattering prediction. Plenum Press, New York, pp. 381–392

Kleckner, R. C., and Gibbs, R. H., 1972. Swimbladder structure of Mediterranean midwater fishes and a method of comparing swimbladder data with acoustic profiles, Mediterranean Biological Studies, Final Report, Vol. I, pp. 230–281.

Kloser, R. J., Ryan, T., Sakov, P., Williams, A., and Koslow, J. A., 2002. Species identification in deep water using multiple acoustic frequencies. Canadian Journal of Fisheries and Aquatic Sciences, 59, 1065–1077.

Kloser, R. J., Ryan, T. E., Young, J. W. & Lewis, M. E., 2009. Acoustic observations of micronekton fish on the scale of an ocean basin: potential and challenges. Ices Journal of Marine Science, 66, 998–1006

Kloser, R., Ryan, T., Keith, G., & Gershwin, L., 2016. Deep-scattering layer, gas-bladder density, and size estimates using a two-frequency acoustic and optical probe. ICES Journal of Marine Science, 73(8), 2037-2048.

Knutsen, T., Hosia, A., Falkenhaug, T., Skern-Mauritzen, R., Wiebe, P.4., Larsen, B.R., . . . Berg E., 2018. Coincident Mass Occurrence of Gelatinous Zooplankton in Northern Norway. Frontiers in Marine Science, 5(MAY), .

Korneliussen, Rolf J., and Egil Ona., 2002. An Operational System for Processing and Visualizing Multi-frequency Acoustic Data. 59.2 (2002), 293-313. Web.

Korneliussen, R. J., Ona, E., Eliassen, I., Heggelund, Y., Patel,R., Godø, O.R., Giertsen, C., Patel, D., Nornes, E., Bekkvik,T., Knudsen, H. P., Lien, G., 2006The Large Scale Survey System - LSSS. Proceedings of the 29th Scandinavian Symposium on PhysicalAcoustics, Ustaoset 29 January – 1 February 2006.

Korneliussen, R. J., Diner, N., Ona, E., Berger, L., and Fernandes, P. G., 2008. Proposals for the collection of multifrequency acoustic data. ICES Journal of Marine Science, 65: 982–994

Korneliussen, R.J. and Ona, E., 2003. Synthetic echograms generated from the relative frequency response. ICES Journal of Marine Science 60, 636–40.

Koslow, J. A., Kloser, R., & Stanley, C. A., 1995. Avoidance of a camera system by a deepwater fish, the orange roughy (Hoplostethus atlanticus). Deep Sea Research Part I: Oceanographic Research Papers, 42(2), 233-244.

Koslow, J. A., Kloser, R. J. & Williams, A., 1997. Pelagic biomass and community structure over the mid-continental slope off southeastern Australia based upon acoustic and midwater trawl sampling. Marine Ecology Progress Series, 146, 21–35

Lam, V. & Pauly, D., 2005. Mapping the global biomass of mesopelagic fishes. Sea Around Us Project Newsletter, 30, 4

Lavery, A., Wiebe, P., Stanton, T., Lawson, G., Benfield, M., & Copley, N., 2007. Determining dominant scatterers of sound in mixed zooplankton populations. The Journal of the Acoustical Society of America, 122(6), 3304-26.

Levy, D., 1990. Reciprocal Diel Vertical Migration Behavior in Planktivores and Zooplankton in British Columbia Lakes. Canadian Journal of Fisheries and Aquatic Sciences, 47(9), 1755-1764.

Mackie, G. O., 1985 Midwater macroplankton of British Columbia studied by submersible PISCES IV. Journal of Plankton Research, 7, 753–777.

Mackie, Pugh, & Purcell., 1987. Siphonophore Biology. Advances in Marine Biology, 24(C), 97-262.

MacLennan, D., Fernandes, P. G., and Dalen, J., 2002. A consistent approach to definitions and symbols in fisheries acoustics. ICES Journal of Marine Science, 59: 365-369.
Marchal, E., & Lebourges, A. (1996). Acoustic evidence for unusual diel behaviour of a mesopelagic fish (Vinciguerria nimbaria) exploited by tuna. *ICES Journal of Marine Science*, *53*(2), 443-447.
Marshall, N. B., 1951. Bathypelagic fishes as sound scatterers in the ocean. Journal of Marine Research, 10, 1–17
Marshall, L. W., 1960. Swimbladder Structure of Deep-Sea Fishes in Relation to Their Systematic and Biology (Discovery Reports) (University Press, London, Cambridge), Vol. 31, pp. 1–122.
Mazhirina, G. P., 1988. Some information on the development of ovaries in Benthosema glaciale from different areas of the North Atlantic. NAFO Scientific Council Research Document 88(21), 1–11.
McCartney, B. S., 1976. Comparison of the acoustic and biological sampling of the sonic scattering layers: RRS 'Discovery' SOND Cruise, 1965. Journal of the Marine Biological Association of the United Kingdom 56, 16 1-1 78
McClatchie, S., Macaulay, G. J., and Coombs, R., 2003. "A requiem for the use of 20 $\log_{10}$ length for acoustic target strength with special reference to deep-sea fishes," ICES Journal of Marine Science, 60, 419–428.
Mianzan, H., Lasta, C., Acha, M., Guerrero, R., Macchi, G., and Bremec, C., 2001b. Rıo de la Plata estuary, Argentina–Uruguay.In Coastal Marine Ecosystems of Latin America, pp. 185–204. Ed. by U. Seeliger, and B. Kjerve. Springer, Heidelberg. pp. 144.
Mills, C. E., 1995. Medusae, siphonophores, and ctenophores as planktivorous predators in changing global ecosystems. ICES Journal of Marine Science, 52(3-4), 575-581.
Misund, O. A., Aglen, A., Johanessen, S. O., Skagen, D., & Totland, B., 1993. Assessing the reliability of fish density estimates by monitoring the swimming behaviour of fish schools during acoustic surveys. In ICES Jouran of Marine Sciens. symp (Vol. 196, pp. 202-206).
Mitson, R., & Wood, R., 1961. An Automatic Method of Counting Fish Echoes. ICES Journal of Marine Science, 26(3), 281-291.
MOZGOVOY, V. (1986). Determination of parameters and migration behavior of sound scattering layer fish by the spectra of scattered acoustic-signals. Okeanologiya, *26*(5),
Nakken, O., & Olsen, K. (1977). Target strength measurements of fish. ICES.
Neighbors, M. A., and Nafpaktitus, B. G., 1982. Lipid compositions, water content, swimbladder morphologies and buoyancies of 19 species of mid- water fishes (19 myctophids and 1 neoscopelid), Marine Biology. 66, 207–215.
Neilson, J. D., and Perry, R. I., 1990. Diel vertical migrations of marine fishes: an obligate or facultative process? Advances in Marine Biology, 26: 115–168.
Nero, R. W., Thompson, C. H., and Jech, J. M., 2004. In situ acoustic estimates of the swimbladder volume of Atlantic herring (Clupea harengus). ICES Journal of Marine Science, 61, 323–337
O'Driscoll, R. L., de Joux, P., Nelson, R., Macaulay, G. J., Dunford, A. J., Marriott, P. M., ... & Miller, B. S., 2012. Species identification in seamount fish aggregations using moored underwater video. ICES Journal of Marine Science, 69(4), 648-659.
Okiyama, M. 1971. Early life history of the gonostomatid fish, Maurolicus muelleri (Gmelin) in the Japan Sea. Bull. Japan Sea Regional Fish Research Labaratory, 23: 21-53.

Ona, E. (Ed)., 1999. Methodology for target strength measurements (with special reference to in situ techniques for fish and mikro-nekton. ICES Cooperative Research Report No. 235. 59 pp.
Ona, E., Mazauric, V., & Andersen, L., 2009. Calibration methods for two scientific multibeam systems. ICES Journal of Marine Science, 66(6), 1326-1334.
Ona, E., 2003. An expanded target-strength relationship for herring. ICES Journal of Marine Science. 60, 493–9.
Ona, E., & Korneliussen, R. J. (2000). Herring vessel avoidance; diving or density draining. In Proceedings of the Fifth European Conference on Underwater Acoustics, ECUA (Vol. 10, 1515-1520).
Ona E., Pedersen G., 2006. Calibrating split beam transducers at depth, Journal of the Acoustical Society of America, 120, 3017
Ona, E., Macaulay, G., and Kubilius, R., Pedersen R., (in preparation). Acoustic density estimation of mesopelagic fish layers; challenges and new solutions.
Page`s, F., and Kurbjeweit, F., 1994. Vertical-distribution and abundance of mesoplanktonic medusae and siphonophores from the Weddell Sea, Antarctica. Polar Biology 14, 243–251.
Pakhomov, E., & Yamamura, O., 2010 Report of the Advisory Panel on Micronekton Sampling Inter-calibration Experiment North Pacific Marine Science Organization (PICES).
Pavlov, D. S., Ben-Tuvia, A., & Dickson, W., 1969. The optomotor reaction of fishes.
Pugh, P. R., 1977. Some observations on the vertical migration and geographical distribution of siphonophores in the warm waters of the North Atlantic Ocean. Proceedings of the symposium on warm water zooplankton. National Institute of Oceanography, Goa, India, pp. 362–378.
Pugh, P. R., 1984. The diel migrations and distributions within a mesopelagic community in the North East Atlantic. 7. Siphonophores. Progress in Oceanography, 13(3-4), 461-489.
Pugh, P. R., 1999. A review of the genus Bargamannia Totton, 1954 (Siphonophorae, Physonecta, Pyrostephidae). Bulletin-Natural History Museum Zoology Series, 65, 51-72.
Purcell, J. E., 1981. Dietary composition and diel feeding patterns of epipelagic siphonophores. Marine Biology, 65, 83–90.
Proud, R., Cox, M. J., Handegard, N. O., Kloser, R. J., and Brierley, A. S., 2018. From siphonophores to deep scattering layers: an estimation of global mesopelagic fish biomass. ICES Journal of Marine science
Robison, B. H., Reisenbichler, K. R., Sherlock, R. E. et al., 1998. Seasonal abundance of the siphonophore, Nanomia bijuga, in Monterey Bay. Deep-Sea Research II, 45, 1741–1751.
Roe, HSJ., Badcock, J., 1984. The diel migrations and distributions within a mesopelagic community in the North East Atlantic. 5. Vertical migrations and feeding of fish. Progress in Oceanogrophy 13,389–424
Rosland, R., & Giske, J., 1997. A dynamic model for the life history of Maurolicus muelleri, a pelagic planktivorous fish. Fisheries Oceanography, 6(1), 19-34.
Salvanes, AGV., Kristoffersen, JB., 2001 Mesopelagic fishes. In: Steel J, Thorpe S, Turekian K, eds. Encyclopedia of Ocean Sciences. San Diego: Academic Press. pp 1711–1717
Sameoto, DD., 1988. Feeding of lantern fish Benthosema glaciale off the Nova Scotia Shelf. Marine Ecology Progress Series, 44,113–129

Sameoto, D., 1989. Feeding ecology of the lantern fish Benthosema glaciale in a subarctic region. Polar Biol 9:169–178

Scoulding, B., Chu, D., Ona, E., & Fernandes, P., 2015. Target strengths of two abundant mesopelagic fish species. The Journal of the Acoustical Society of America, 137(2), 989-1000.

Simmonds, E.J., Armstrong, F. and Copland, P.J., 1996. Species identification using wideband backscatter with neural network and discriminant analysis. ICES Journal of Marine Science, 53,189–96.

Simmonds, J., & MacLennan, D., 2005. Fisheries acoustics: Theory and practice (2nd ed., Vol. 10, Fish and aquatic resources series). Oxford: Blackwell Science.'

St John, M. A., Borja A., Chust, G., Heath, M., Grigorov, I., Mariani, P., Martin, A. P.et al., 2016. A dark hole in our understanding of marine ecosystems and their services: perspectives from the mesopelagic community. Frontiers in Marine Science, 3: 1–6

Staby, A., 2010. Seasonal Dynamics of the Vertical Migration Behaviour of Mesopelagic Fish.

Staby A, Aksnes DL., 2011. Follow the light—diurnal and seasonal variations in vertical distribution of the mesopelagic fish Maurolicus Muelleri. Marine Ecology Progress Series, 422, 265-273

Staby, A., Røstad, A., & Kaartvedt, S., 2011. Long-term acoustical observations of the mesopelagic fish Maurolicus muelleri reveal novel and varied vertical migration patterns. Marine Ecology Progress Series, 441, 241-255.

Stanton, T. K., Wiebe, P. H., Chu, D., & Goodman, L., 1994. Acoustic characterization and discrimination of marine zooplankton and turbulence. ICES Journal of Marine Science, 51(4), 469-479.

Stanton, T.K., Chu, D. and Wiebe, P.H., 1996 Acoustic scattering characteristics of several zooplankton groups. ICES Journal of Marine Science, 53, 289–302.

Stanton, T.K., Chu, D., Wiebe, P.H., Martin, L. and Eastwood, R.L., 1998a. Sound scattering by several zooplankton groups I: experimental determination of dominant scattering mechanisms. The Journal of the Acoustical Society of America, 103 (1), 225–35.

Stanton, T.K., Chu, D., 2000. Review and recommendations for the modelling of acoustic scattering by fluid-like elongated zooplankton: euphausiids and copepods ICES Journal of Marine Science, 57, 793-807

Stanton, T. K., Chu, D., Jech, J. M., & Irish, J. D., 2010. New broadband methods for resonance classification and high-resolution imagery of fish with swimbladders using a modified commercial broadband echosounder. ICES Journal of Marine Science, 67(2), 365-378.

Toyokawa, M., Inagaki, T., and Terazaki, M., 1997. Distribution Of Aurelia aurita (Linnaeus, 1758) in Tokyo Bay, observations with echosounder and plankton net. In Proceedings of the Sixth International Conference on Coelenterate Biology, 1995. pp. 483–490. Ed. by J. C. Den Hartog. National Naturhistorisch Museum, Leiden

Tont, S., 1976. Short-period climatic fluctuations: Effects on diatom biomass. Science (New York, N.Y.), 194(4268), 942-4.

Tréguer, P., Legendre, L., Rivkin, R. T., Ragueneau, O. & N, D., 2003. Ocean Biogeochemistry: The Role of Ocean Carbon Cycle in Global Change 145–156Springer

Yasuma, H., Sawada, K., Ohshima, T., Miyashita, K., and Aoki, I., 2003. Target strength of mesopelagic lanternfishes (family Myctophidae) based on swimbladder morphology, ICES Journal of Marine Science, 60, 584–591.

Yasuma, H., Sawada, K., Takao, Y., Miyashita, K., and Aoki, I., 2010. Swimbladder condition and target strength of myctophid fish in the tem- perate zone of the Northwest Pacific,ICES Journal of Marine Science, 67, 135–144.

Ye, Z., and Farmer, D.M., 1996 Acoustic scattering by fish in the forward direction. ICES Journal of Marine Science, 53, 249–52.

Youngbluth, M., Owen, G., Robison, B. et al., 1996. Estimates of diel predation rates by vertically migrating populations of the physonect siphonophore Nanomia cara in the Gulf of Maine. EOS, 76(Suppl. 3), OS180.

Williams, R., & Conway, D. V. P., 1981. Vertical distribution and seasonal abundance of Aglantha digitale (OF Müller)(Coelenterata: Trachymedusae) and other planktonic coelenterates in the northeast Atlantic Ocean. Journal of Plankton Research, 3(4), 633-643.

Wardle, C. S., 1984. Fish behaviour, trawl efficiency and energy saving strategies.

Wardle, C. S., 1986. Fish behaviour and fishing gear. In The behaviour of teleost fishes (pp. 463-495). Springer, Boston, MA

Warren, J. D., T. K. Stanton, M. C. Benfield, P. H. Wiebe, D. Chu, and M. Sutor., 2001. In Situ Measurements of Acoustic Target Strengths of Gas-bearing Siphonophores. 58.4 (2001): 740-49. Web.

www.marec.no, The “Large Scale Survey System” (L-triple-S) for marine stock assessment and research. http://www.marec.no/english/contactus.htm.

www.simrad.com, “Simrad ES38-18DK Split.” First Fishery Sonar with Selectable Beam Width - Simrad, www.simrad.com/www/01/nokbg0240.nsf/AllWeb/4E4C91CE1646F8DBC12581FA00488A9A?OpenDocument.

Appendix I. Echogram for each station, combined with category allocation for each acoustic class

November 25th, 2017 vessel data

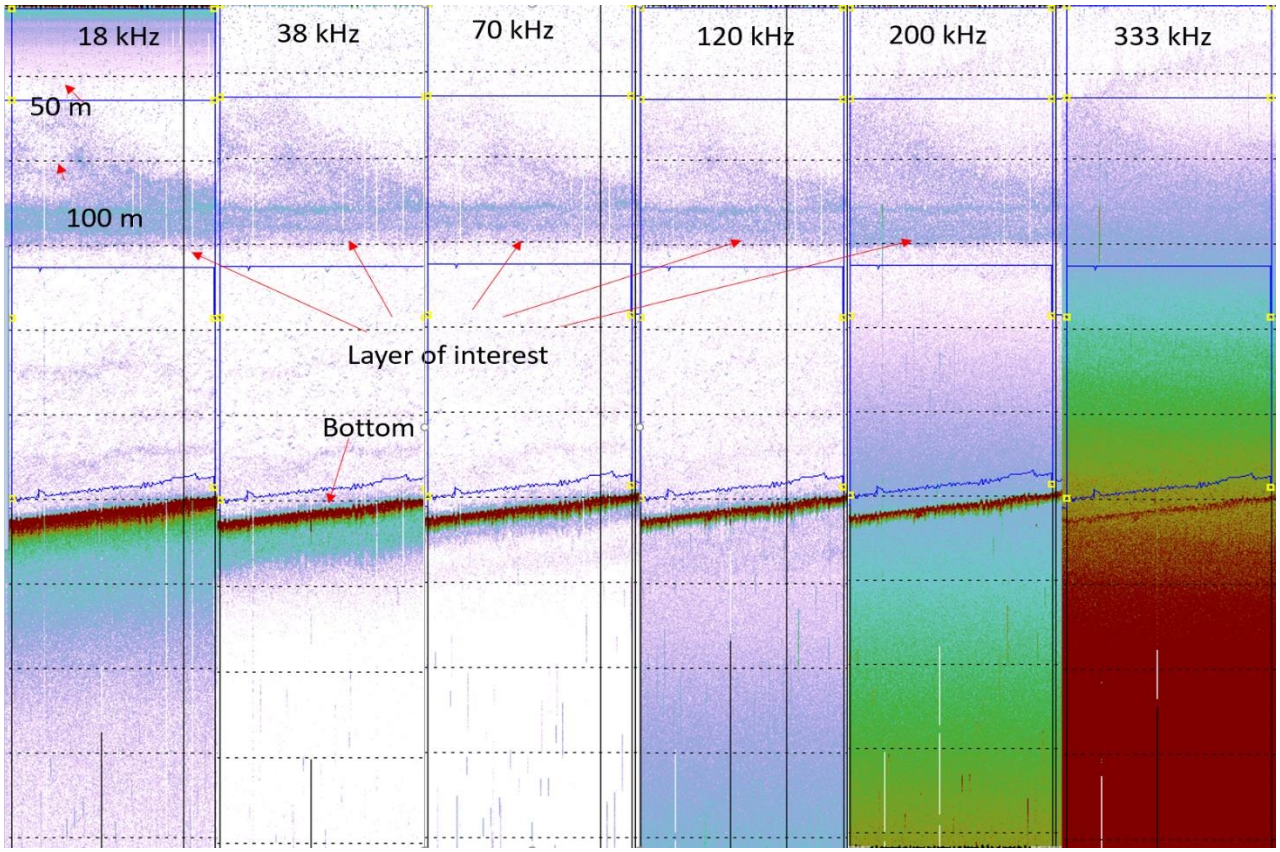

Depth (m)	S_v threshold (dB)	Category	s_A 18 kHz (m^2/ Nmi^{-2})	s_A 38 kHz (m^2/ Nmi^{-2})	s_A 70 kHz (m^2/ Nmi^{-2})	s_A 120 kHz (m^2/ Nmi^{-2})	s_A 200 kHz (m^2/ Nmi^{-2})
70-170	-70	Mesopelagic fish	347	115	67	73	120
70-170	-82	Plankton	69	76	63	74	106
70-170	Sum	All species	416	130	130	147	226

November 29th, 2017 vessel data, before probing

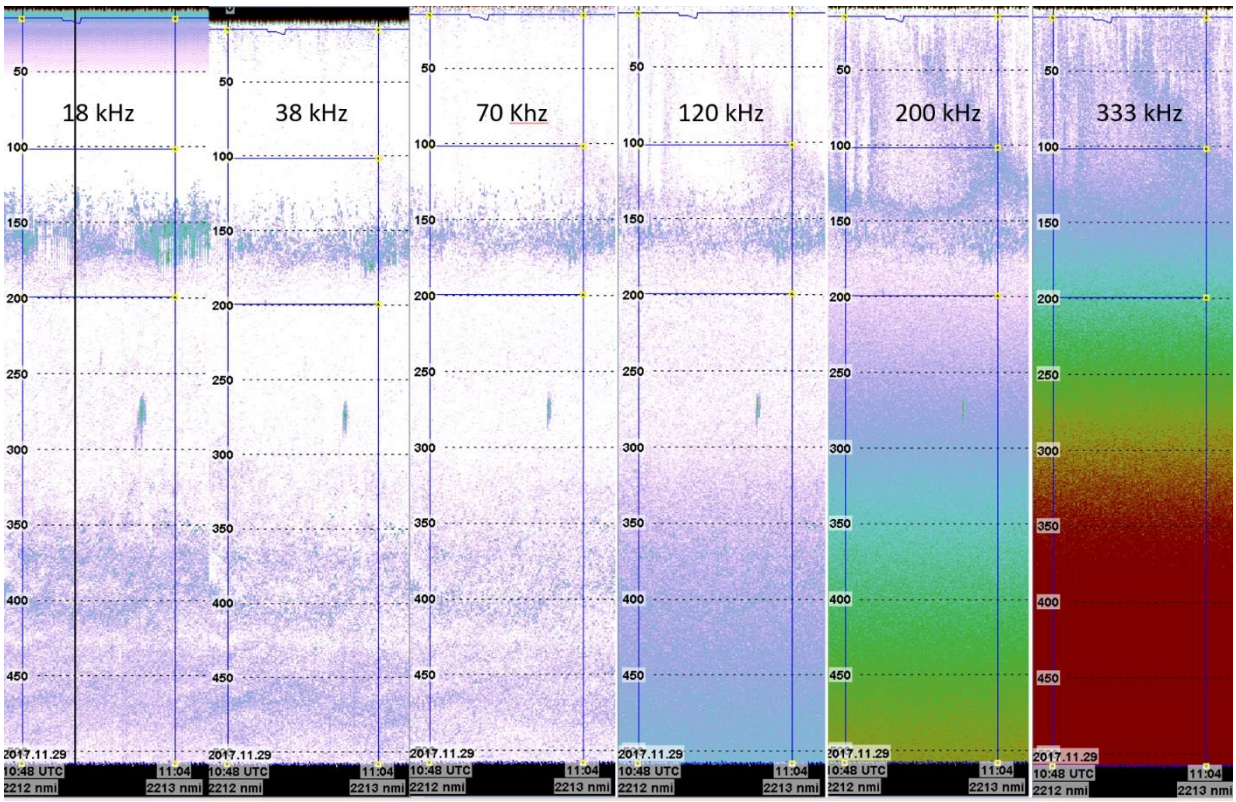

Depth (m)	S_v threshold (dB)	Category	s_A 18 kHz (m^2/ Nmi^{-2})	s_A 38 kHz (m^2/ Nmi^{-2})	s_A 70 kHz (m^2/ Nmi^{-2})	s_A 120 kHz (m^2/ Nmi^{-2})	s_A 200 kHz (m^2/ Nmi^{-2})
10-100	-70	Other	NA	5	1	0	42
10-100	-82	Plankton	NA	5	4	12	65
10-100	sum	All species	NA	10	5	12	107
100-200	-70	Mesopelagic fish	475	147	77	72	156
100-200	-82	Plankton	31	28	29	44	80
100-200	sum		506	175	106	116	236
200-500	-70	Mesopelagic fish	210	146	98	NA	NA
200-500	-82	plankton	191	157	33	NA	NA
200-500	sum		401	303	231	NA	NA

November 29th,2017 vessel data, after probing

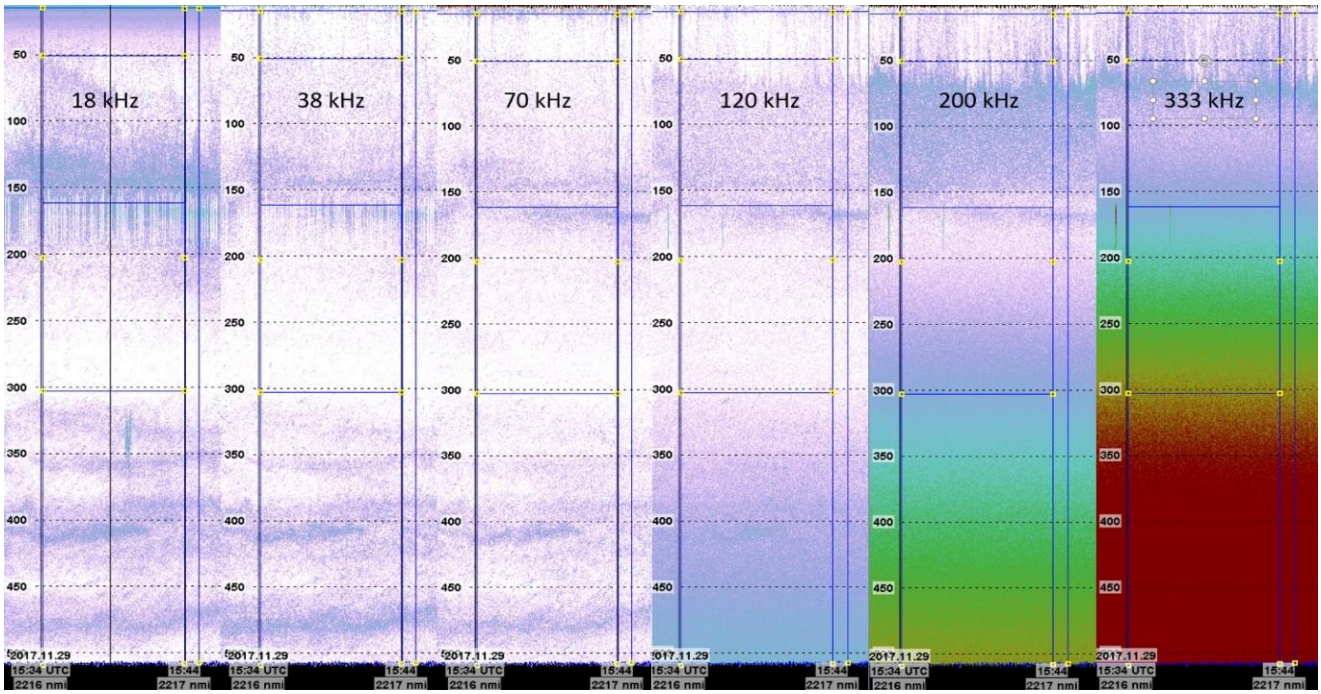

Depth (m)	S_v threshold (dB)	Category	s_A 18 kHz (m^2/ Nmi^{-2})	s_A 38 kHz (m^2/ Nmi^{-2})	s_A 70 kHz (m^2/ Nmi^{-2})	s_A 120 kHz (m^2/ Nmi^{-2})	s_A 200 kHz (m^2/ Nmi^{-2})
10-50	-70	other	NA	4.5	2.5	0.5	2.5
10-50	-70	Mesopelagic fish	NA	4.5	2.5	0.5	2.5
10-50	-82	plankton	NA	9	8	9	23
10-50	sum	All species	NA	18	13	10	28
50-157	-70	Mesopelagic fish	283	29	9	15	368
50-157	-82	Plankton	88	76	60	96	115
50-157	Sum	All categories	371	105	69	109	483
157-300	-70	Mesopelagic fish	104	16	9	6	NA
157-300	-82	Plankton	58	33	37	52	NA
157-300	Sum	All categories	12	49	46	58	NA
300-500	-70	Mesopelagic fish	138	148	64	NA	NA
300-500	-82	Plankton	153	113	114	NA	NA
300-500	Sum	all categories	291	261	178	NA	NA

November 30th, 2017

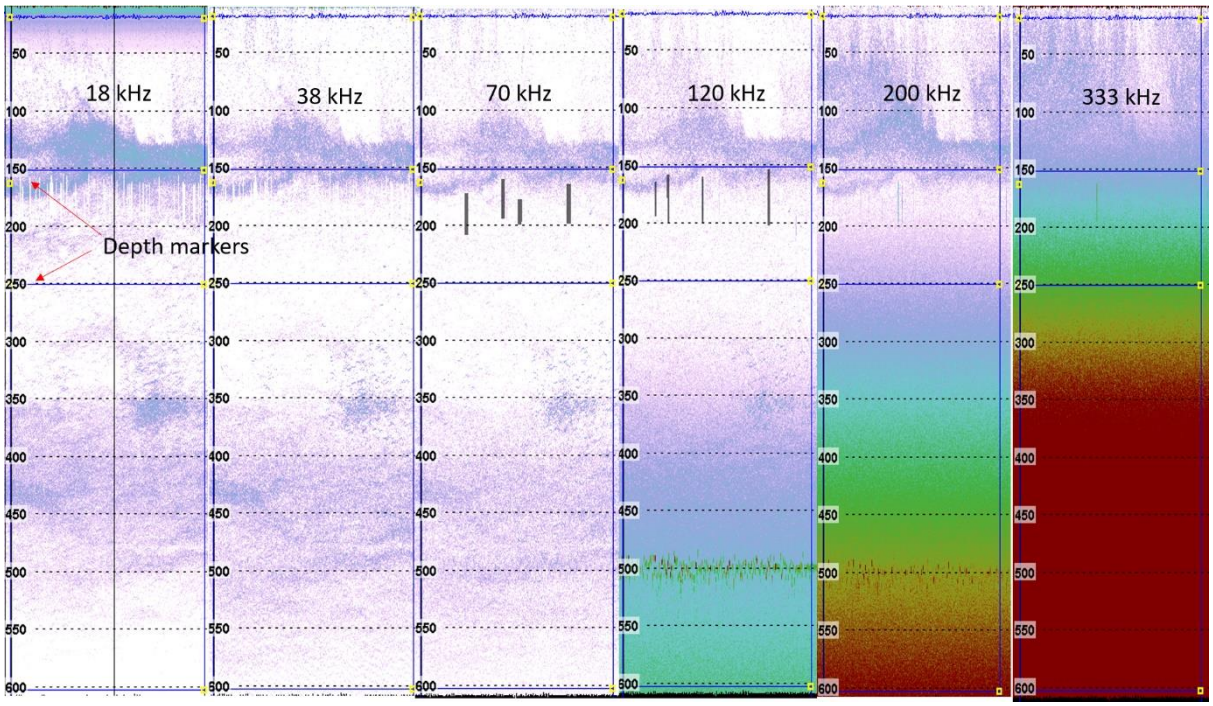

Depth (m)	S_v threshold (dB)	Categories	s_A 18 kHz (m^2/ Nmi^{-2})	s_A 38 kHz (m^2/ Nmi^{-2})	s_A 70 kHz (m^2/ Nmi^{-2})	s_A 120 kHz (m^2/ Nmi^{-2})	s_A 200 kHz (m^2/ Nmi^{-2})
10-150 (50-150 18 kHz)	-70	Mesopelagic fish	308	73	36	34	NA
10-150	-82	Plankton	52	57	52	68	NA
10-150	sum	All categories	360	130	88	102	
150-250	-70	Mesopelagic fish	109	28	15	11	NA
150-250	-82	Plankton	55	29	29	31	NA
150-250	sum	All categories	64	57	44	42	
250-600	-70	Mesopelagic fish	139	98	72	NA	NA
250-600	-82	Plankton	187	190	175	NA	NA
250-600	sum	All categories	326	288	247	NA	NA

Probing

November 25th, 2017

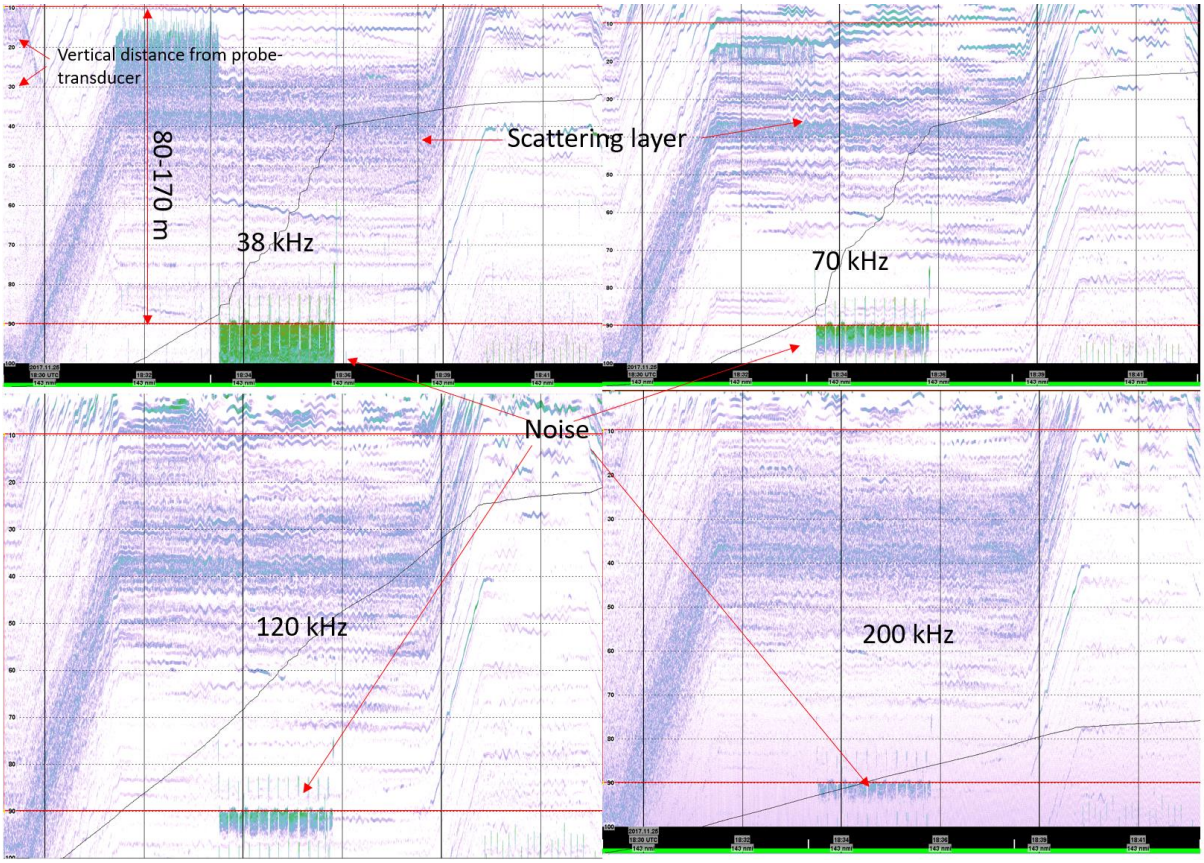

Depth (m)	S_v threshold (dB)	Categories	s_A 38 kHz (m^2/ Nmi^{-2})	s_A 70 kHz (m^2/ Nmi^{-2})	s_A 200 kHz (m^2/ Nmi^{-2})
80-160	-60 dB	Noise	3	NA	NA
80-160	-70 dB	Mesopelagic fish	38	72	33
80-160	-82 dB	Plankton	38	31	50
80-160	Sum	all categories	79	103	83

November 29th, 2017

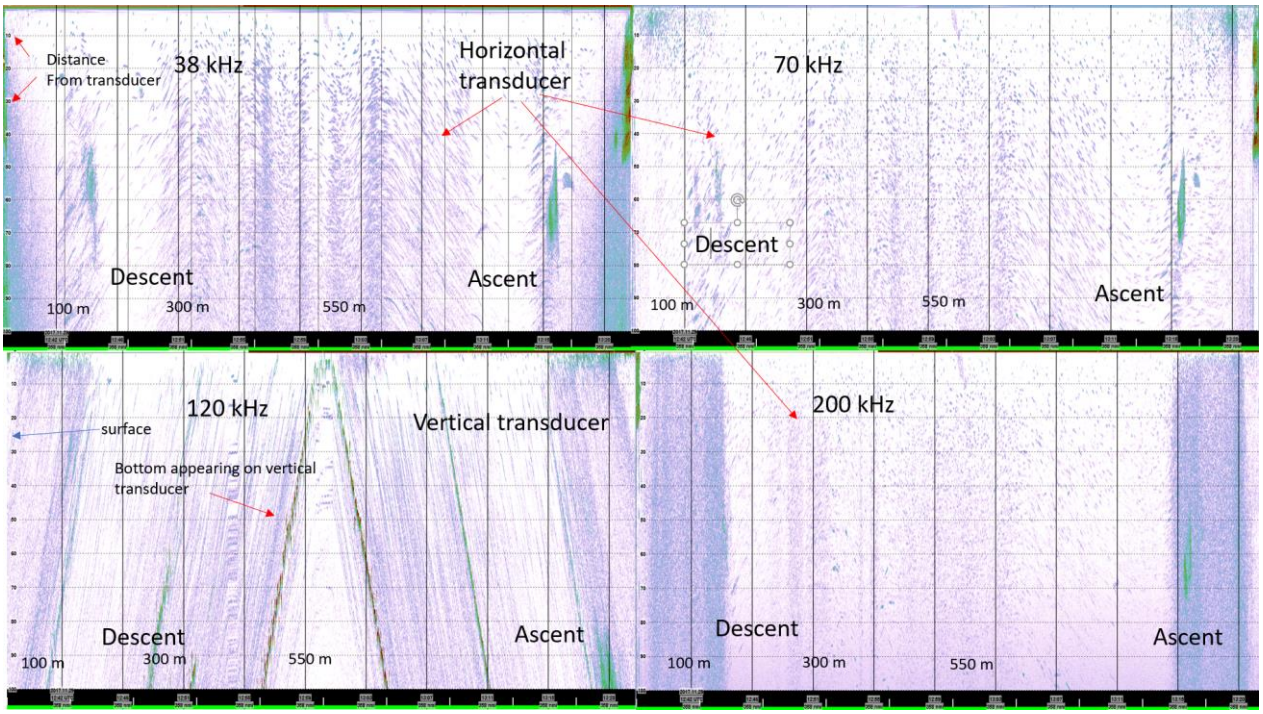

Depth (m)	S_v threshold (dB)	Categories	s_A 38 kHz (m^2/ Nmi^{-2})	s_A 70 kHz (m^2/ Nmi^{-2})
100-200	-70	Mesopelagic fish	5	13
100-200	-82	Plankton	2	4
100-200	Sum	All categories	7	17
200-550	-70	Mesopelagic fish	7	6
200-550	-82	Plankton	4	2
200-550	Sum	All categories	11	8

Zooplankton Measurement

Depth (m)	S_v threshold (dB)	Categories	s_A 200 kHz (m^2/ Nmi^{-2})
0-200	-60	Separable fish	1
0-200	-82	Plankton	36
0-200	Sum	All categories	37
200-550	-70	Separable fish	1
200-550	-82	Plankton	3
200-550	sum	All categories	4

November 30th 2017

First profiling

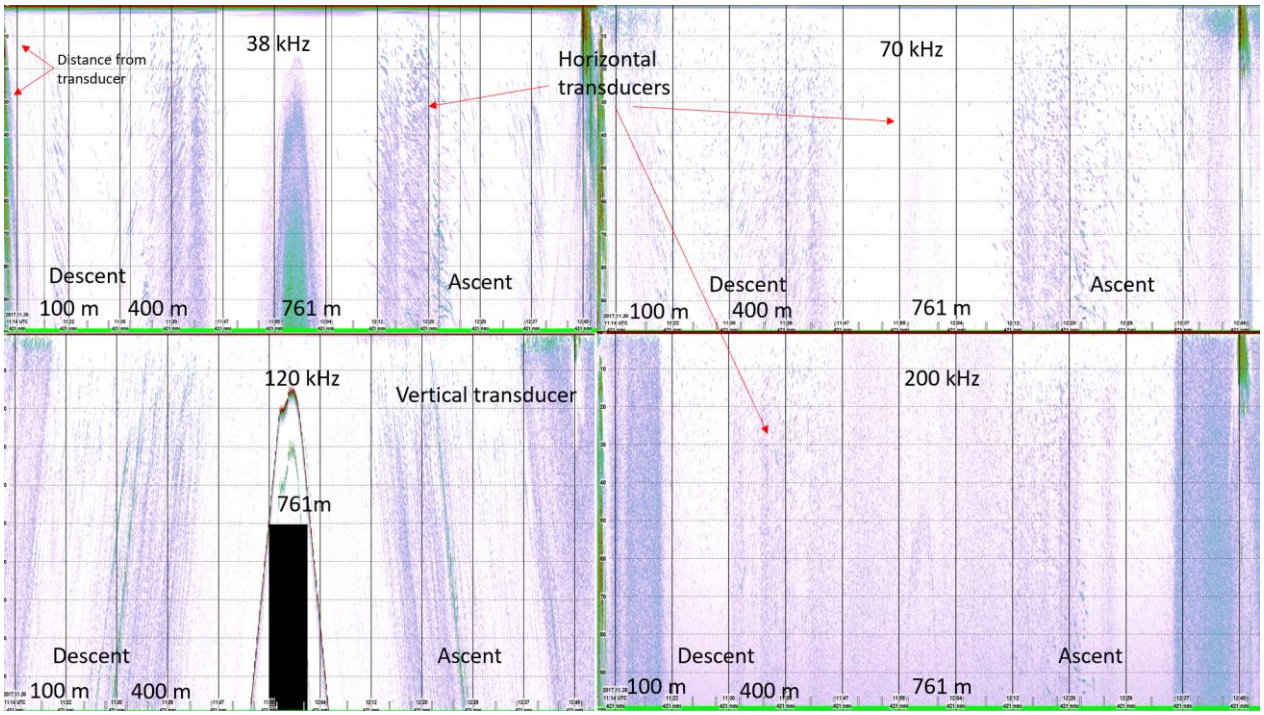

Depth	S_v threshold (dB)	Categories	s_A 38 kHz (m^2/ Nmi^2)	s_A 70 kHz (m^2/ Nmi^{-2})
100-700	-70	Mesopelagic fish	3	3
100-700	-82	Plankton	2	1
100-700	Sum	All categories	5	4

Zooplankton measurement

Depth (m)	S_v threshold (dB)	Categories	s_A 200 kHz (m^2/ Nmi^{-2})
0-200	-60	Separable fish	1
0-200	-82	Plankton	43
0-200	Sum	All categories	44
200-700	-70	Separable fish	2
200-700	-82	Plankton	4
200-700	Sum	All categories	6

Second profiling

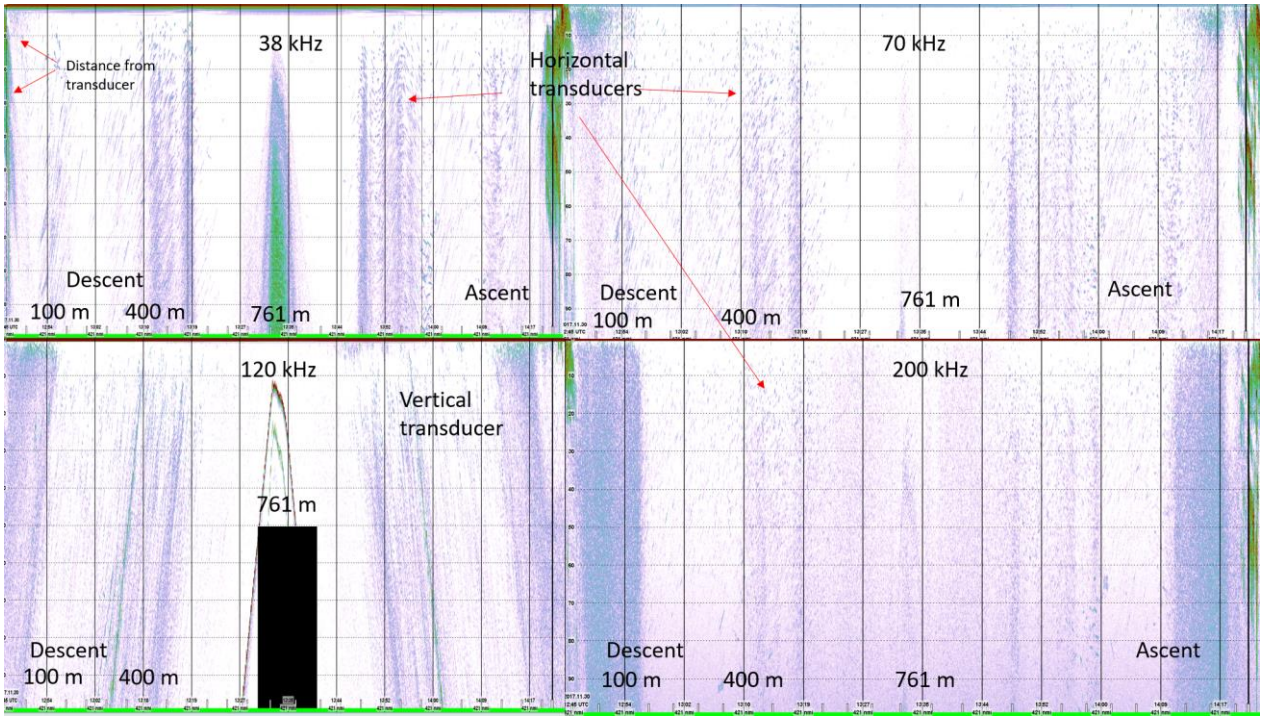

Depth (m)	S_v threshold (dB)	Categories	s_A 38 kHz (m^2/ Nmi^{-2})	s_A 70 kHz (m^2/ Nmi^{-2})
100-700	-70	Mesopelagic fish	5	4
100-700	-82	Plankton	3	2
100-700	Sum	All categories	8	6

Zooplankton measurement

Depth (m)	S_v threshold (dB)	Categories	s_A 200 kHz (m^2/ Nmi^{-2})
0-200	-60	Separable fish	1
0-200	-82	Plankton	87
0-200	Sum	All categories	88
200-700	-70	Separable fish	1
200-700	-82	Plankton	2
200-700	Sum	All categories	3

Third profiling

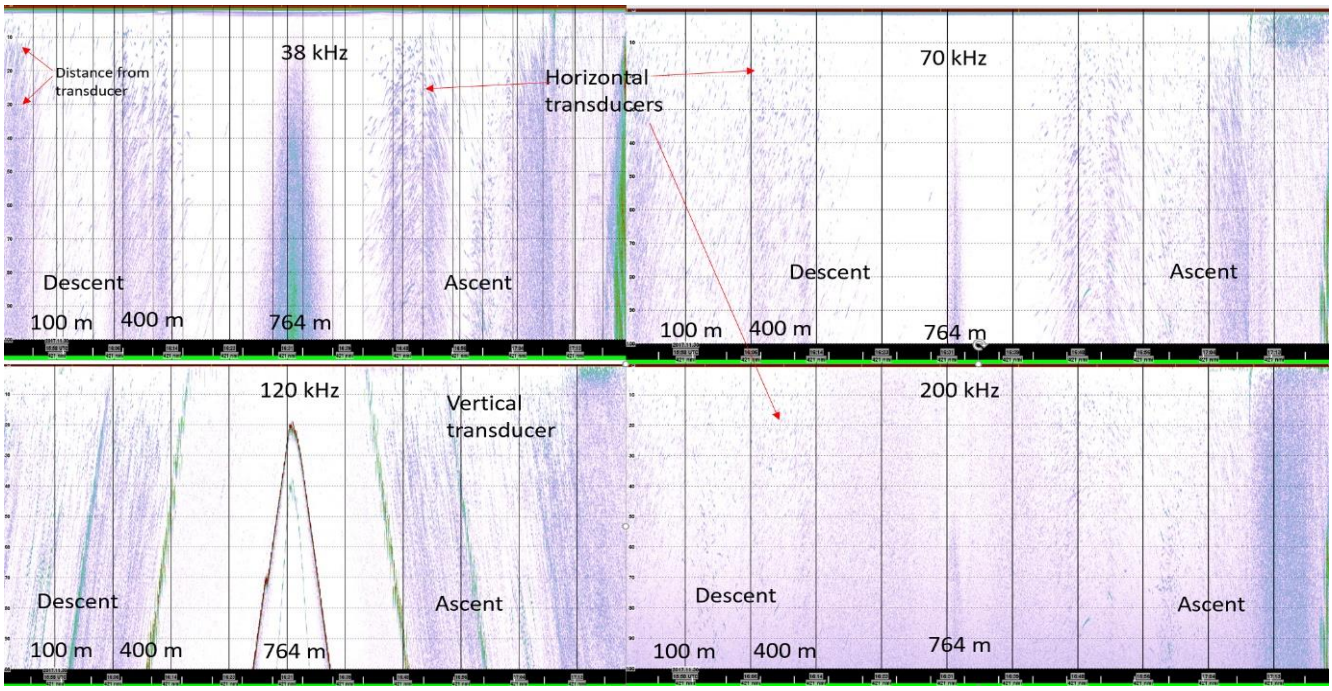

depth	S_v threshold (dB)	s_A 38 kHz (m^2/ Nmi^2)	s_A 70 kHz (m^2/ Nmi^{-2})
0-100	-70	1	7
0-100	-82	3	7
0-100	Sum	4	14
100-700	-70	5	6
100-700	-82	5	3
100-700	Sum	10	9

depth	S_v threshold (dB)	Categories	s_A 200 kHz (m^2/ Nmi^{-2})
0-200	-60	Separable fish	0
0-200	-82	Plankton	42
0-200	Sum	All catecories	43
200-700	-70 dB	Separable fish	1
200-700	-82	Plankton	2
0-200	Sum	All categories	3

Appendix II rank test results

November 25th, 2017

38 kHz

Wilcoxon Signed Ranks Test Results

Counts of Differences (row variable greater than column)

	SHIP_DATA	PROBE_DATA
SHIP_DATA	0.000	7.000
PROBE_DATA	1.000	0.000

Z = (Sum of signed ranks)/Square root(sum of squared ranks)

	SHIP_DATA	PROBE_DATA
SHIP_DATA	0.000	
PROBE_DATA	-2.380	0.000

Two-sided Probabilities using Normal Approximation

	SHIP_DATA	PROBE_DATA
SHIP_DATA	1.000	
PROBE_DATA	0.017	1.000

70 kHz

Wilcoxon Signed Ranks Test Results

Counts of Differences (row variable greater than column)

	SHIP_DATA_70KHZ	PROBE_DATA_70KH-Z
SHIP_DATA_70KHZ	0.000	5.000
PROBE_DATA_70KHZ	3.000	0.000

Z = (Sum of signed ranks)/Square root(sum of squared ranks)

	SHIP_DATA_70KHZ	PROBE_DATA_70KH-Z
SHIP_DATA_70KHZ	0.000	
PROBE_DATA_70KHZ	-0.980	0.000

Two-sided Probabilities using Normal Approximation

	SHIP_DATA_70KHZ	PROBE_DATA_70KH-Z
SHIP_DATA_70KHZ	1.000	
PROBE_DATA_70KHZ	0.327	1.000

120 kHz

Wilcoxon Signed Ranks Test Results

Counts of Differences (row variable greater than column)

	SHIP_DATA_120KH-Z	PROBE_DATA120KH-Z
SHIP_DATA_120KHZ	0.000	5.000
PROBE_DATA120KHZ	3.000	0.000

Z = (Sum of signed ranks)/Square root(sum of squared ranks)

	SHIP_DATA_120KH-Z	PROBE_DATA120KH-Z
SHIP_DATA_120KHZ	0.000	
PROBE_DATA120KHZ	-1.400	0.000

Two-sided Probabilities using Normal Approximation

	SHIP_DATA_120KH-Z	PROBE_DATA120KH-Z
SHIP_DATA_120KHZ	1.000	
PROBE_DATA120KHZ	0.161	1.000

November 29th, 2017

38 kHz before probing

	SHIPDATA_29_OCTOBER_38KHZ_BEFO-REPROBING	PROBE_DATA29NOV_38KHZ
SHIPDATA_29_OCTOBER_38KHZ_BEFOREPROBING	0.000	26.000
PROBE_DATA29NOV_38KHZ	17.000	0.000

Z = (Sum of signed ranks)/Square root(sum of squared ranks)

	SHIPDATA_29_OCTOBER_38KHZ_BEFO-REPROBING	PROBE_DATA29NOV_38KHZ
SHIPDATA_29_OCTOBER_38KHZ_BEFOREPROBING	0.000	
PROBE_DATA29NOV_38KHZ	-2.717	0.000

Two-sided Probabilities using Normal Approximation

	SHIPDATA_29_OCTOBER_38KHZ_BEFO-REPROBING	PROBE_DATA29NOV_38KHZ
SHIPDATA_29_OCTOBER_38KHZ_BEFOREPROBING	1.000	
PROBE_DATA29NOV_38KHZ	0.007	1.000

70 kHz before probing

Wilcoxon Signed Ranks Test Results

Counts of Differences (row variable greater than column)

	SHIPDATA_29_OCTOBER_70KHZ_BEFOREPROBING	PROBEDATA_29NOVEMBER_70KHZ
SHIPDATA_29_OCTOBER_70KHZ_BEFOREPROBING	0.000	19.000
PROBEDATA_29NOVEMBER_70KHZ	24.000	0.000

Z = (Sum of signed ranks)/Square root(sum of squared ranks)

	SHIPDATA_29_OCTOBER_70KHZ_BEFOREPROBING	PROBEDATA_29NOVEMBER_70KHZ
SHIPDATA_29_OCTOBER_70KHZ_BEFOREPROBING	0.000	
PROBEDATA_29NOVEMBER_70KHZ	0.688	0.000

Two-sided Probabilities using Normal Approximation

	SHIPDATA_29_OCTOBER_70KHZ_BEFOREPROBING	PROBEDATA_29NOVEMBER_70KHZ
SHIPDATA_29_OCTOBER_70KHZ_BEFOREPROBING	1.000	
PROBEDATA_29NOVEMBER_70KHZ	0.491	1.000

38 kHz after probing

Wilcoxon Signed Ranks Test Results

Counts of Differences (row variable greater than column)

	SHIP_AFTER_PROBING_70KHZ	PROBE_DATA38KHZ_29NOV
SHIP_AFTER_PROBING_70KHZ	0.000	36.000
PROBE_DATA38KHZ_29NOV	14.000	0.000

Z = (Sum of signed ranks)/Square root(sum of squared ranks)

	SHIP_AFTER_PROBING_70KHZ	PROBE_DATA38KHZ_29NOV
SHIP_AFTER_PROBING_70KHZ	0.000	
PROBE_DATA38KHZ_29NOV	-3.219	0.000

Two-sided Probabilities using Normal Approximation

	SHIP_AFTER_PROBING_70KHZ	PROBE_DATA38KHZ_29NOV
SHIP_AFTER_PROBING_70KHZ	1.000	
PROBE_DATA38KHZ_29NOV	0.001	1.000

After probing 70 kHz

Wilcoxon Signed Ranks Test Results

Counts of Differences (row variable greater than column)

	AFTER_PROBING70-KHZ_29NOV	PROBING_70KHZ_2-9NOV
AFTER_PROBING70KHZ_29NOV	0.000	25.000
PROBING_70KHZ_29NOV	25.000	0.000

Z = (Sum of signed ranks)/Square root(sum of squared ranks)

	AFTER_PROBING70-KHZ_29NOV	PROBING_70KHZ_2-9NOV
AFTER_PROBING70KHZ_29NOV	0.000	
PROBING_70KHZ_29NOV	0.150	0.000

Two-sided Probabilities using Normal Approximation

	AFTER_PROBING70-KHZ_29NOV	PROBING_70KHZ_2-9NOV
AFTER_PROBING70KHZ_29NOV	1.000	
PROBING_70KHZ_29NOV	0.881	1.000

November 30th,2017 1st profiling 38 kHz

Wilcoxon Signed Ranks Test Results

Counts of Differences (row variable greater than column)

	SHIPDATA_30TH_N-OVEMBER_38KHZ	PROBEDATA_1_38K-HZ
SHIPDATA_30TH_NOVEMBER_38KHZ	0.000	59.000
PROBEDATA_1_38KHZ	1.000	0.000

Z = (Sum of signed ranks)/Square root(sum of squared ranks)

	SHIPDATA_30TH_N-OVEMBER_38KHZ	PROBEDATA_1_38K-HZ
SHIPDATA_30TH_NOVEMBER_38KHZ	0.000	
PROBEDATA_1_38KHZ	-6.721	0.000

Two-sided Probabilities using Normal Approximation

	SHIPDATA_30TH_N-OVEMBER_38KHZ	PROBEDATA_1_38K-HZ
SHIPDATA_30TH_NOVEMBER_38KHZ	1.000	
PROBEDATA_1_38KHZ	0.000	1.000

1st profiling70 kHz

Wilcoxon Signed Ranks Test Results

Counts of Differences (row variable greater than column)

	SHIP_70	PROBE_70
SHIP_70	0.000	50.000
PROBE_70	10.000	0.000

Z = (Sum of signed ranks)/Square root(sum of squared ranks)

	SHIP_70	PROBE_70
SHIP_70	0.000	
PROBE_70	-5.455	0.000

Two-sided Probabilities using Normal Approximation

	SHIP_70	PROBE_70
SHIP_70	1.000	
PROBE_70	0.000	1.000

2nd profiling 38 kHz

Wilcoxon Signed Ranks Test Results

Counts of Differences (row variable greater than column)

	SHIPDATA_38	PROBE_38_SECOND-D
SHIPDATA_38	0.000	58.000
PROBE_38_SECONDD	2.000	0.000

Z = (Sum of signed ranks)/Square root(sum of squared ranks)

	SHIPDATA_38	PROBE_38_SECOND-D
SHIPDATA_38	0.000	
PROBE_38_SECONDD	-6.316	0.000

Two-sided Probabilities using Normal Approximation

	SHIPDATA_38	PROBE_38_SECOND-D
SHIPDATA_38	1.000	
PROBE_38_SECONDD	0.000	1.000

2nd profiling 70 kHz

Wilcoxon Signed Ranks Test Results

Counts of Differences (row variable greater than column)

	SHIP_70_2	PROBE_70_SECOND
SHIP_70_2	0.000	46.000
PROBE_70_SECOND	14.000	0.000

Z = (Sum of signed ranks)/Square root(sum of squared ranks)

	SHIP_70_2	PROBE_70_SECOND
SHIP_70_2	0.000	
PROBE_70_SECOND	-4.100	0.000

Two-sided Probabilities using Normal Approximation

	SHIP_70_2	PROBE_70_SECOND
SHIP_70_2	1.000	
PROBE_70_SECOND	0.000	1.000

Third profiling 38 kHz

Wilcoxon Signed Ranks Test Results

Counts of Differences (row variable greater than column)

	SHIP_38_3	PROBE_38_3
SHIP_38_3	0.000	51.000
PROBE_38_3	10.000	0.000

Z = (Sum of signed ranks)/Square root(sum of squared ranks)

	SHIP_38_3	PROBE_38_3
SHIP_38_3	0.000	
PROBE_38_3	-5.463	0.000

Two-sided Probabilities using Normal Approximation

	SHIP_38_3	PROBE_38_3
SHIP_38_3	1.000	
PROBE_38_3	0.000	1.000

Third profiling 70 kHz

Wilcoxon Signed Ranks Test Results

Counts of Differences (row variable greater than column)

	SHIP_70_3	PROBE_70_3
SHIP_70_3	0.000	32.000
PROBE_70_3	28.000	0.000

Z = (Sum of signed ranks)/Square root(sum of squared ranks)

	SHIP_70_3	PROBE_70_3
SHIP_70_3	0.000	
PROBE_70_3	0.744	0.000

Two-sided Probabilities using Normal Approximation

	SHIP_70_3	PROBE_70_3
SHIP_70_3	1.000	
PROBE_70_3	0.457	1.000

Appendix III Calculating grids for probing stations

November 25th vertical transducers

$$Time\ used\ investigating\ the\ layer\ 18{:}31{:}34 - 18{:}38{:}34 = \ 420\ seconds$$

$$Number\ of\ pings\ = \ 420 * 4 = 1680\ pings$$

For getting 10 measurements, horizontal grids were saved as 168 pings. The depth sensor was used to find the starting depth, and further the data were saved in pelagic depth channels in the same manner as with the vessel data.

Probe station 2 November 29th, 2017 horizontal transducers

Depth sensor present

$$\text{Ping rate} = 4 \text{ pings } s^{-1}$$

$$\text{Time used profiling 100 meters} \approx 225 \text{ seconds}$$

$$\text{Grid cell} = \frac{(4 * 225)}{10} = 90 \text{ pings}$$

Time (UTC)	Depth (m)
12:42:03	100
12:45:45	200
12:49:29	300
12:53:12	400
12:57:39	500
13:00:28	550

Probe station 3, November 30th 1st profiling depth sensor absent

$$Time\ used\ profiling\ the\ water\ column = 11{:}11{:}39 - 11{:}58{:}40$$

$$47{:}01\ min = 2821\ seconds$$

$$Lowering\ speed = \frac{751}{2821} = 0.267\ \mathrm{ms}^{-1}$$

$$\text{Seconds used profiling 10 meters} = \frac{10}{0.274} = 37.5\ \text{seconds}$$

$$\text{Ping rate} = 2\ \text{pings}\ s^{-1}$$

$$\text{Grid cell} = 75\ \text{pings}$$

Time (UTC)	Depth (m)
11:11:39	10
11:17:16	100
11:23:30	200
11:29:44	300
11:35:58	400
11:42:02	500
11:48:16	600
11:54:30	700
11:58:40	761

Probe station 2, November 30th 2nd profiling

$$Time\ used\ profiling\ the\ water\ column = 12{:}47{:}00 - 13{:}32{:}40$$

$$45{:}40\ min = 2740\ \ seconds$$

$$Lowering\ speed = \frac{751}{2740} = 0.274\ ms^{-1}$$

$$Seconds\ used\ profiling\ 10\ meters = \frac{10}{0.274}\ ms^{-1}\ =\ 36.5\ seconds$$

$$\text{Ping rate} =\ 2\ \text{pings}\ s^{-1}$$

$$\text{Grid cell} =\ 73\ \text{pings}$$

Time (UTC)	Depth (m)
12:47:00	10
12:52:28	100
12:58:32	200
13:04:36	300
13:10:40	400
13:16:46	500
13:22:50	600
13:28:54	700
1332:40	761

Probe station 2, November 30th 3rd profiling

$$Time\ used\ profiling\ the\ water\ column = 16{:}31{:}53 - 17{:}19{:}16$$

$$47{:}23 = 2843\ sesonds$$

$$Hieving\ speed = \frac{754}{2843} = 0.265\ ms^{-1}$$

$$Seconds\ used\ profiling\ 10\ meters = \frac{10}{0.265} = 37.7m$$

$$\text{Ping rate} = 4\ \text{pings} * s^{-1}$$

$$\text{Grid cell} = 150\ \text{pings}$$

Time (UTC)	Depth (m)
16:31:53	764
16:35:54	700
16:42:11	600
16:48:28	500
16:54:45	400
17:01:02	300
17:07:19	200
17:13:36	100
17:19:15	10

Appendix IV Siphonophore photos with corresponding depth

Station 1, November 25th, 2017

Siphonophore observed November 25th at 18:40 UTC at 120 meters depth.

Siphonophore observed November 25th at 18:40 UTC and 120 meters depth.

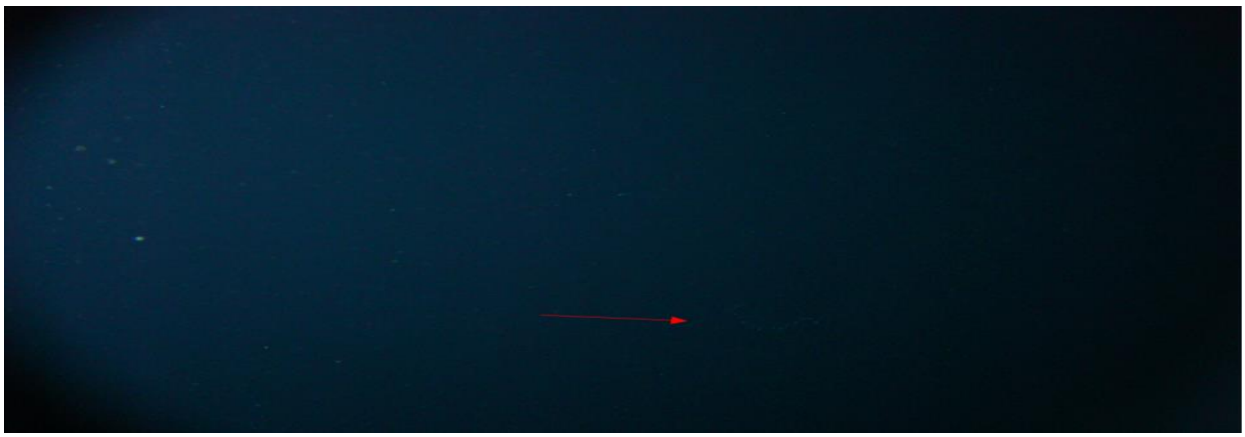

Siphonphore observed November 25th at 18:40 UTC at 120 meters depth.

November 29th, 2017

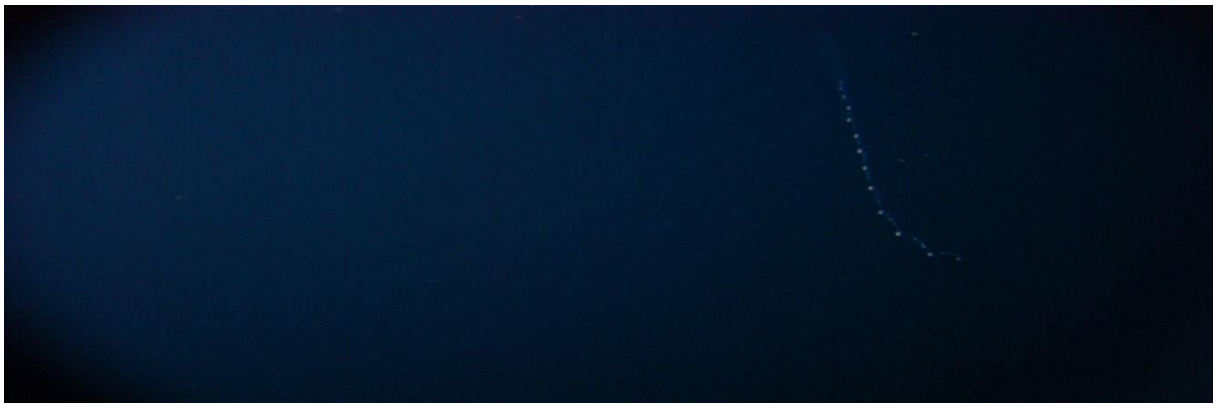

Siphonophore observed November 29th 12:40 UTC at 75 meters depth.

Two siphonophores observed November 29th 12:41 UTC at 75 meters depth.

Siphonophore observed November 29th 12:47 UTC at 233 meters depth.

Siphonophore observed November 29th 12:55 UTC at 432 meters depth.

November 30th 2017

Siphonophore observed November 30th 11:19 UTC at 127 meters depth.

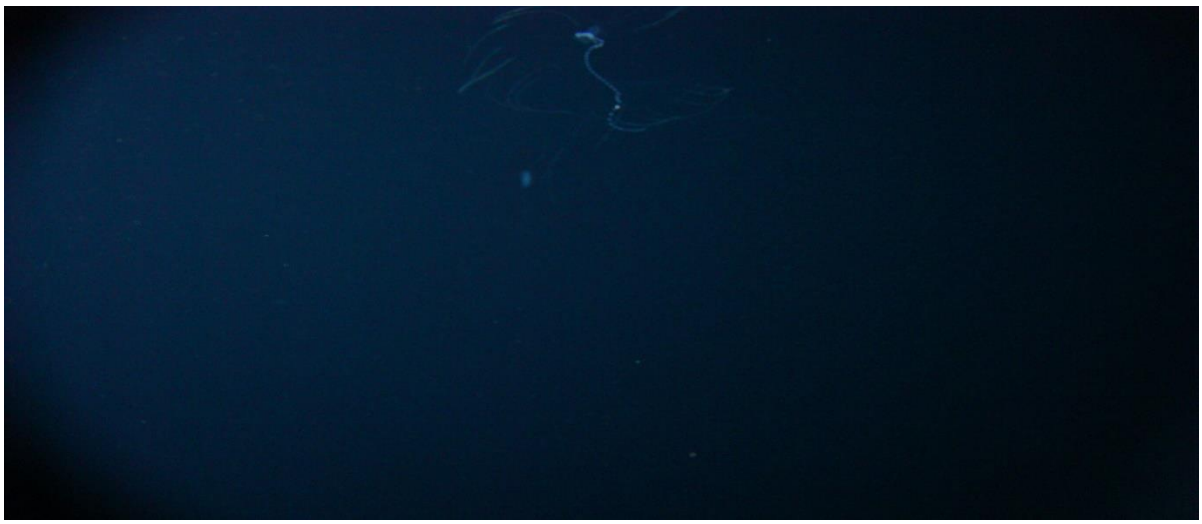

Siphonophore observed November 30th 11:26 UTC at 242 meters depth.

Siphonophore observed November 30th 11:40 at 464 meters depth.

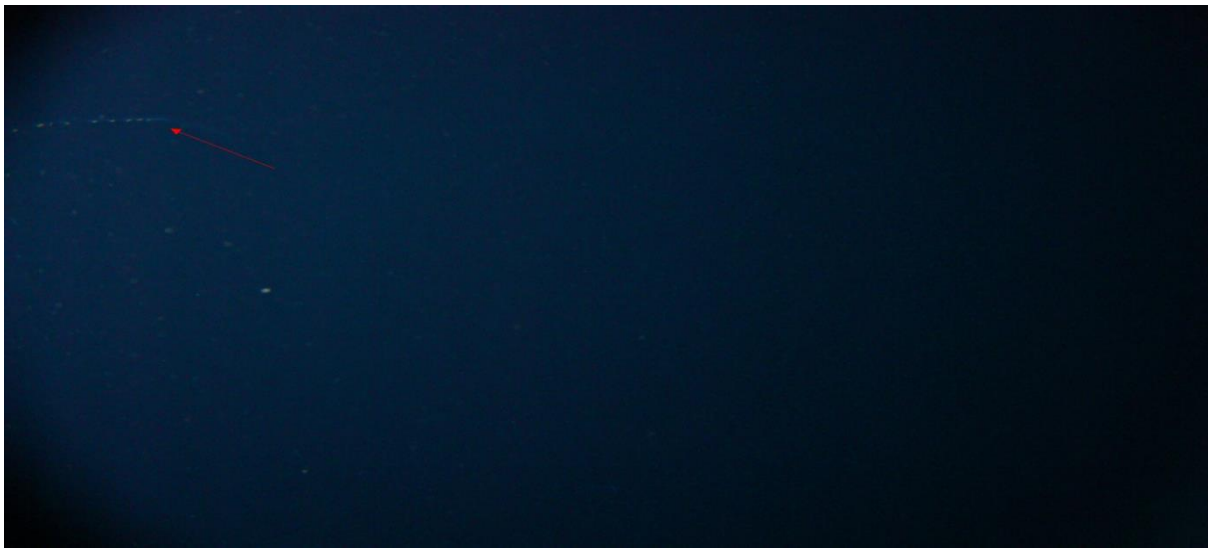

Siphonophore observed November 30th 15:59 at 164 meters depth.

Siphonophore observed November 30th 16:09 UTC at 389 meters depth.

Siphonophore observed November 30th 16:11 UTC at 473 meters depth.

Siphonophore observed November 30th 16:33 UTC at 731 meter depth.

Siphonophore observed November 30th 16:35 UTC at 713 meters depth.

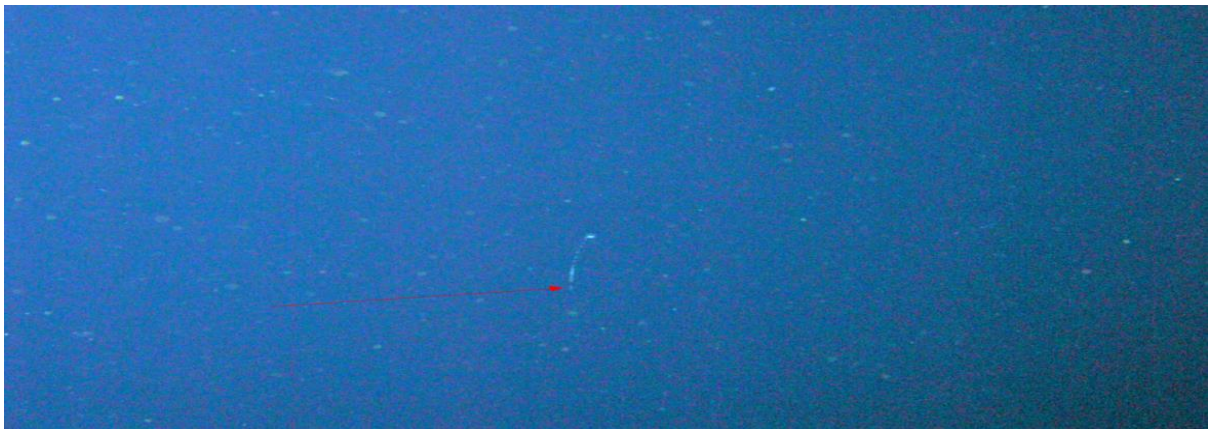

Siphonophore observed 16:51 UTC at 451 meters depth

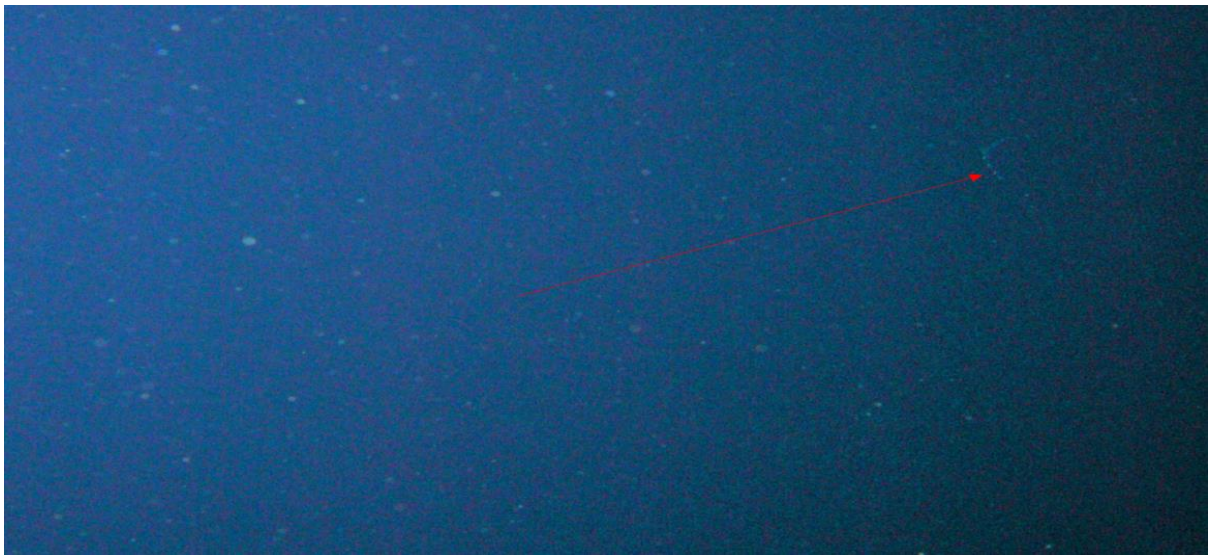

Siphonophore Observed at November 30th 16:52 UTC at 437 meters depth.

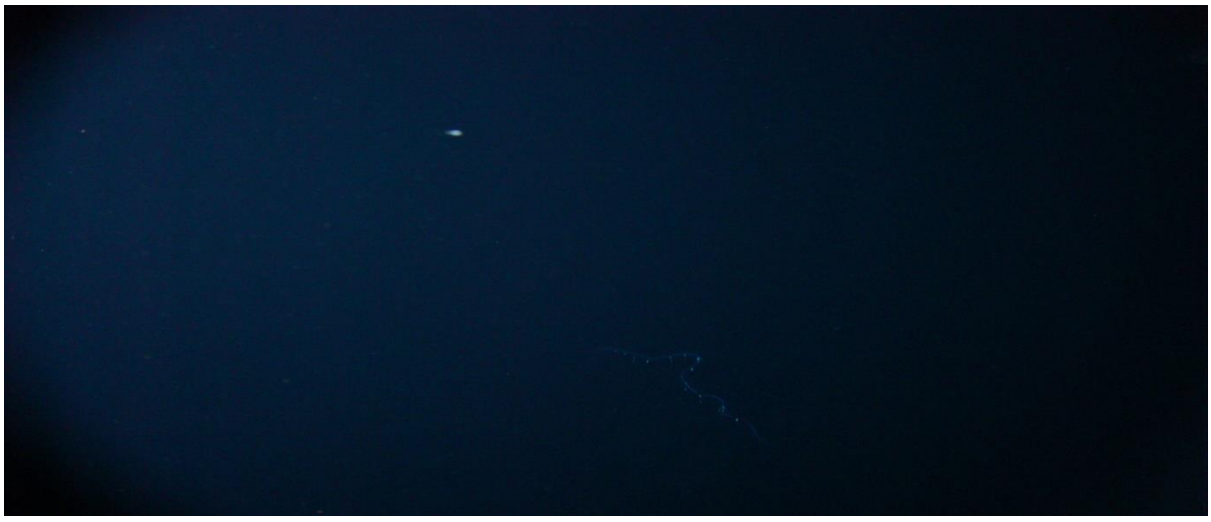

Siphonophore observed at November 30th 17:04 UTC at 296 meters depth.